

# A Bayesian prevalence-incidence mixture model for screening outcomes with misclassification\*

Thomas Klausch ([t.klausch@amsterdamumc.nl](mailto:t.klausch@amsterdamumc.nl))<sup>1</sup>, Birgit I. Lissenberg-Witte<sup>1</sup>, and Veerle M. Coupé<sup>1</sup>

<sup>1</sup>Amsterdam University Medical Centers, Department of Epidemiology and Data Science, Amsterdam, The Netherlands

December 23, 2024

## Abstract

We propose **BayesPIM**, a Bayesian prevalence-incidence mixture model for estimating time- and covariate-dependent disease incidence from screening and surveillance data. The method is particularly suited to settings where some individuals may have the disease at baseline, baseline tests may be missing or incomplete, and the screening test has imperfect sensitivity. Building on the existing **PIMixture** framework, which assumes perfect sensitivity, **BayesPIM** accommodates uncertain test accuracy by incorporating informative priors. By including covariates, the model can quantify heterogeneity in disease risk, thereby informing personalized screening strategies. We motivate the model using data from high-risk familial colorectal cancer (CRC) surveillance through colonoscopy, where adenomas—precursors of CRC—may already be present at baseline and remain undetected due to imperfect test sensitivity. We show that conditioning incidence and prevalence estimates on covariates explains substantial heterogeneity in adenoma risk. Using a Metropolis-within-Gibbs sampler and data augmentation, **BayesPIM** robustly recovers incidence times while handling latent prevalence. Informative priors on the test sensitivity stabilize estimation and mitigate non-convergence issues. Model fit can be assessed using information criteria and validated against a non-parametric estimator. In this way, **BayesPIM** enhances estimation accuracy and supports the development of more effective, patient-centered screening policies.

## 1 Introduction

Screening and surveillance programs aim to detect diseases, such as cancer, at an early stage to improve treatment outcomes. Electronic health records (EHR) from these programs provide valuable insights into disease progression and can optimize screening schedules, such as personalizing test frequency and timing. This study focuses on EHR from colorectal cancer (CRC) surveillance among individuals with elevated risk due to family history (section 2). These individuals undergo regular colonoscopies to detect and remove adenomas, which are precursors to CRC. Estimating adenoma incidence time is critical for this high-risk group, as they may develop adenomas more frequently and rapidly than the general population. Our objective is to estimate time to adenoma incidence.

To this end, we develop a modeling framework with an accompanying R package called **BayesPIM**. Our model is a type of so-called prevalence-incidence mixture model (PIM) with a Bayesian estimation back-end. The class of PIM was first suggested by [Cheung et al. \(2017\)](#) and [Hyun](#)

---

\*We gratefully acknowledge the FCRC research group for providing the familial risk CRC data used in the application section.

et al. (2017). The primary goal of their PIM was to model time to incidence when the disease status is ascertained at irregularly spaced discrete points in time and a part of the population can have the (pre-state) disease already at baseline (i.e., the point in time when an individual is first included in the study), which is called prevalence. This observation process is also present in the CRC EHR, because individuals may have had adenomas already at inclusion into study; see section 2.

Prevalence complicates the estimation of the interval-censored incidence model, in particular if the prevalence status is not observed (latent) for some or all individuals in the EHR. In the Cheung-Hyun PIM, the prevalence status is unobserved if no test is administered at baseline for at least a subset of the population and hence it is unknown for these individuals whether they have prevalent disease or not. Ignoring the issue of latent prevalence in standard interval-censored survival models, such as the Accelerated failure time model (AFT) or the Cox model, causes underestimation bias of the time to incidence, because latent prevalent cases can be discovered after baseline and are then treated as incident cases. The Cheung-Hyun PIM model solves this issue through jointly estimating the incidence and the prevalence model by an expectation maximization (EM) algorithm. The model has been implemented in the R package `PIMixture` (Cheung et al., 2023) and is currently suggested as a principal modeling approach for screening data on the US National Cancer Institute (NCI) website (National Cancer Institute, 2024).

Building on the PIM framework, our model `BayesPIM` extends the approach to account for imperfect test sensitivity (less than one), where sensitivity is the probability to find the (pre-state) disease when it is truly present. This enhancement is motivated by the CRC EHR, where colonoscopies can miss adenomas due to technical or human error at baseline or during follow-up. The test sensitivity of a colonoscopy for an adenoma varies depending on the study, with reports ranging between 0.65 and 0.95. As `PIMixture` and standard models for interval-censored survival data (Boruvka and Cook, 2015; Anderson-Bergman, 2017) have been developed under the assumption of perfect test sensitivity, their estimates are prone to bias. Importantly, with imperfect tests, latent prevalence due to misclassification at baseline may occur even when all subjects receive a baseline test while `PIMixture` assumes prevalence can only occur in subjects that do not receive a baseline test. `BayesPIM` handles latent prevalence regardless of whether its cause is an omitted baseline test or misclassification and can co-estimate the test sensitivity. As we show, including prior information on the sensitivity is an advantage of the Bayesian approach, as it stabilizes estimation and incorporates prior uncertainty. While the model accommodates imperfect sensitivity, we assume perfect specificity, a reasonable assumption in CRC screening, and cancer screening in general, where initial findings are usually confirmed via pathology. `BayesPIM` allows for parametric survival distributions and uses model selection criteria to identify the best fit. In addition, we propose a joint non-parametric estimator of the cumulative incidence function (CIF) and prevalence, based on Witte et al. (2017), which we use to validate model fit visually.

This article is structured as follows. Section 2 introduces the Dutch CRC EHR as the motivating case. Section 3 reviews related methods. Sections 4 and 5 describe the data-generating mechanism and estimation methodology, respectively. Section 6 evaluates `BayesPIM` through simulations, while section 7 presents an application to Dutch CRC EHR, including estimates and real-world simulations.

## 2 Motivating data example: Dutch CRC EHR

Our motivating case involves CRC surveillance through colonoscopy in individuals with an elevated CRC risk due to family history. Specifically, we analyze a merged dataset ( $n = 810$ ) of EHR from two sources (Table 1). The primary dataset comes from the Dutch Familial Colorectal Cancer Surveillance (FACTS) randomized controlled trial (Hennink et al., 2015), which experimentally compared two surveillance protocols in this high-risk group (three- vs. six-year intervals between colonoscopies). This was supplemented with observational EHR from a similar high-risk population undergoing CRC surveillance according to current guidelines. These additional data were collected through ongoing research at two Dutch hospitals, Radboudumc and Rijnstate. Eligible participants for this case study were those with at least one successful colonoscopy, with baseline defined as the time of the first colonoscopy. The primary objective was to estimate the time from baseline to the first adenoma. However, given the progressive nature of CRC, a cancer may occasionally be detected instead of an adenoma during surveillance. In this study, the number of cancers was negligible ( $n = 8$ , 1%).

**Table 1:** Baseline characteristics of the Dutch CRC EHR screening data (time is measured in years).

| Statistic                          | Total          | Event in follow up |                 |
|------------------------------------|----------------|--------------------|-----------------|
|                                    |                | Adenoma            | Right censored  |
| Sample size $n$                    | 810            | 330                | 480             |
| Known prevalent individuals (%)    | 20.4           | 50.0               | 0               |
| Baseline test unsuccessful (%)     | 6.5            | 6.7                | 6.5             |
| Censoring time (min/median/max)    | 1.2/6.0/30.1   | 1.2/6.3/22.1       | 1.4/6.0/30.1    |
| No. of screenings (min/median/max) | 1/1.5/7        | 1/1.5/7            | 1/2/7           |
| Interval length (min/median/max)   | 1.0/3.1/20.3   | 1/3.3/13.7         | 1/3.1/20.3      |
| Age at baseline (min/median/max)   | 24.3/53.2/86.3 | 27.6/54.7/86.3     | 24.26/52.3/73.5 |
| Gender is female (in %)            | 55.8           | 53.0               | 57.8            |

At baseline, 20.4% ( $n = 165$ ) of individuals were found to have an adenoma. Since any finding during colonoscopy is verified by pathology we assume that the combined test has perfect specificity (cf. Section 1). Hence, 20.4% of individuals have confirmed (i.e., known) prevalence (Table 1). However, in the remaining 79.6% ( $n = 645$ ), the prevalence status was unknown (latent) due to two possible reasons. First, in 6.5%, the baseline colonoscopy was not completed successfully, due to, for example, incomplete visualization of the colon. These test outcomes are categorized as missing. In the remaining cases, while the baseline colonoscopy was successfully performed and returned a negative result, it may have missed an adenoma due to misclassification. Thus, although the baseline non-completion rate was relatively low (6.5%), substantial uncertainty regarding baseline prevalence remains due to the potential for missed adenomas.

There were six types of surveillance visit patterns present in the CRC EHR that are processed by BayesPIM (Table 2). Table 2 gives an example data vector for all types using four screening moments (i.e., time points  $v_1$  to  $v_4$ ). For convenience, we always set  $v_1 = 0$  denoting baseline; whether a test is available at baseline is indicated by  $r_i$ , with  $r_i = 1$  if yes and  $r_i = 0$  if not. We address all resulting pattern types in turn. First, incident cases in the follow-up can occur after a successful baseline colonoscopy (type 1, 18%). The data example shows that incidence was found at  $v_3 = 6$  years. The adenoma thus surely occurred before 6 years, and, more specifically, it occurred in the  $(3.0, 6.0]$  interval if it was not missed at the colonoscopy at  $v_2 = 3$  years, or it occurred in  $(0, 3.0]$  if it was not missed at the  $v_1 = 0$  baseline colonoscopy. Whether the adenoma was missed at any test occasion is unknown. Second, right censoring (loss to

follow-up) can occur after a successful baseline colonoscopy (type 2, 47%). Here, we adopt the common notation that the last screening time is set to infinity in case of right censoring. The data example then suggests that right censoring occurred after the last colonoscopy had been performed at  $v_3 = 6.3$  years. Note that due to misclassification right censoring may have occurred even if an adenoma is present before  $v_3 = 6.3$  including the possibility of a latent prevalent adenoma at baseline. To the contrary, type 3 denotes prevalence found at baseline, as indicated by  $v_1 = 0$  without further screening moments (20.4%; cf. Table 1). It is important to distinguish the prevalent case from type 4 that denotes a negative baseline test with loss to follow up before the first surveillance moment in the regular follow-up, as indicated by  $(0, \infty)$  in the data example (8.9%). Again, type 4 also might denote a prevalent case with falsely negative baseline test. Furthermore, note that case types 3 and 4 do not provide information on incidence, but they do inform the estimation of the prevalence model. The final two types 5 (2.7%) and 6 (3.8%), concern cases without baseline test ( $r_i = 0$ ) and an event in the follow-up (until  $v_3 = 8.3$  years) or loss to follow-up (at  $v_2 = 5.9$  years), respectively. Finally, we note that the situations of  $v_1 = 0$  and  $(v_1 = 0, v_2 = \infty)$  cannot occur without baseline test ( $r_i = 0$ ), because we require that at least one test result is available.

**Table 2:** Typology of screening cases in the Dutch CRC EHR with observed proportion per type (n=810; note: the data example uses up to four visits for illustration, but the real CRC EHR contained up to seven visits, see Table 1).

| Type | Description                                   | Proportion (%) | Data example |          |          |          |       |
|------|---|----------------|--------------|----------|----------|----------|-------|
|      |   |                | $v_1$        | $v_2$    | $v_3$    | $v_4$    | $r_i$ |
| 1    | Incident in follow-up with baseline test      | 17.7           | 0            | 3.0      | 6.0      |          | 1     |
| 2    | Right censored with baseline test             | 46.5           | 0            | 2.9      | 6.3      | $\infty$ | 1     |
| 3    | Observed prevalent at baseline test           | 20.4           | 0            |          |          |          | 1     |
| 4    | Right censored with only a baseline test      | 8.9            | 0            | $\infty$ |          |          | 1     |
| 5    | Incident in follow-up without a baseline test | 2.7            | 0            | 6.2      | 8.3      |          | 0     |
| 6    | Right censored without a baseline test        | 3.8            | 0            | 5.9      | $\infty$ |          | 0     |

### 3 Related statistical modeling approaches

The primary approach for modeling the incidence time using the CRC EHR exhibited in Table 2 is PIMixture, introduced in section 1 (Cheung et al., 2017; Hyun et al., 2017; Cheung et al., 2023). The PIMixture methodology has been applied in numerous epidemiological studies. For example, studies of cervical cancer screening estimated time to CIN2/3 lesions with prevalence at baseline (Clarke et al., 2019; Saraiya et al., 2021). The model has also been recently extended to take competing events into account (Hyun et al., 2020). However, as discussed, PIMixture assumes that the screening test can always ascertain the (pre-state) disease without error.

PIM have well-known similarities to cure models; for a review of cure models, see Amico and Keilegom (2018). Specifically, the Cheung-Hyun PIM puts point probability mass on incidence at baseline (time zero), denoting effectively immediate transition for prevalent cases (Cheung et al., 2017). Cure models achieve the opposite by putting incidence probability mass on infinity, hence allowing a proportion of the population to never progress.

A relevant question is whether a fully non-parametric estimator of incidence can be constructed using EHR with prevalence and misclassification which could then be used to assess model fit. In the standard interval-censored setting, the non-parametric maximum likelihood estimator (NPMLE) is applied to obtain an estimate of the population-averaged (i.e., marginal) cumulative incidence function, CIF (Turnbull, 1976). The NPMLE can also be applied to

prevalence-incidence EHR without misclassification, after a recoding step described by [Cheung et al. \(2017\)](#) has been performed on the EHR. In section 5.4, we suggest a similar adaptation to a non-parametric estimator developed by [Witte et al. \(2017\)](#) for the setting with misclassified test outcomes but without prevalence.

Misclassification and prevalence have also been discussed in the context of multi-state models. Specifically, continuous-time hidden Markov models (HMM) allow modeling transition processes between multiple (disease) states, while specifying a probability distribution relating the observed states to underlying true states which may be used to account for imperfect test sensitivity ([Jackson et al., 2003](#); [Jackson, 2011](#)). Bayesian HMM have been suggested that can additionally deal with prevalence ([Luo et al., 2021](#); [Raffa and Dubin, 2015](#)). These models rely on the Markov assumption, meaning that the transition probability to a state does not depend on the time spent in the state which is akin to assuming an exponential transition time distribution (constant hazard function). We believe that this is too restrictive for many cancer screening settings, where hazards of (pre-state) disease events may change across time. Semi-Markov models have been suggested to account for the time-dependence of transition rates ([Aastveit et al., 2023](#); [Barone and Tancredi, 2022](#)). AFT models, applied in the present approach, are very similar to semi-Markov models in this regard; for example, a Weibull AFT specification allows for non-constant hazards of transition. Recently, [Klausch et al. \(2023\)](#) used AFT models for three-state screening data demonstrating the robustness of Bayesian estimation when using regularization priors, similar as in BayesPIM (section 4.3). However, these models do not take prevalence and misclassification into account. An exception is a continuous-time HMM approach by [Lange and Minin \(2013\)](#) used to approximate semi-Markov transitions with misclassification and latent prevalence using phase-type distributions ([Lange et al., 2015](#)).

## 4 BayesPIM: data generating mechanism

In this section, we define the data generating mechanism (DGM) of the BayesPIM model with three components: a latent variable PIM (section 4.1), the generation of the observed screening times via a censoring mechanism (section 4.2), and the prior assumptions (section 4.3).

### 4.1 Prevalence-incidence model

We assume that the latent random transition time variable  $x_i$  follows an AFT model

$$\log x_i = \mathbf{z}'_{xi} \boldsymbol{\beta}_x + \sigma \epsilon_i, \quad i = 1, \dots, n \quad (1)$$

where  $\mathbf{z}_{xi}$  is a  $p_x \times 1$  vector of covariates,  $\boldsymbol{\beta}_x$  a  $p_x \times 1$  vector of regression coefficients, and  $\sigma$  a scaling parameter. Residuals  $\epsilon_i$  have density  $q_\epsilon(\epsilon_i)$ . The specific distribution chosen for  $\epsilon_i$  induces the distribution of  $x_i$ , by a change of variables. For example, if  $\epsilon_i$  is standard extreme value, logistically, or normally distributed,  $x_i$  is, respectively, Weibull, loglogistically or lognormally distributed. An exponential (Markov-type) transition time model is obtained by choosing a Weibull distribution and constraining  $\sigma = 1$ . We denote the density of  $x_i$  as  $f_x$  and the cumulative distribution function, also called the cumulative incidence function (CIF), as  $F_x$ .

Furthermore, we assume that the population is stratified into a non-prevalent and a prevalent group, as indicated by random variable  $g_i$  with  $g_i = 0$  in case of non-prevalence and  $g_i = 1$  in case of prevalence. To link  $g_i$  to the covariates and  $x_i$ , we specify a probit model for  $g_i$ . For this, we introduce the latent random variable  $w_i$  with linear model

$$w_i = \mathbf{z}'_{wi} \boldsymbol{\beta}_w + \psi_i, \quad \psi_i \sim \phi(\psi_i|0, 1) \quad (2)$$

where  $\phi(\psi_i|0, 1)$  is the density of the standard normal distribution. The latent model for  $w_i$  is linked to  $g_i$  by the relation

$$g_i = \mathbb{1}_{\{w_i > 0\}}. \quad (3)$$

This model uses the  $p_w \times 1$  covariate vector  $\mathbf{z}_{wi}$  with coefficients  $\boldsymbol{\beta}_w$ . The joint distribution of the residuals of  $\log x_i$  and  $w_i$  is assumed to factorize  $q_{\epsilon, \psi}(\epsilon_i, \psi_i) = q_\epsilon(\epsilon_i)\phi(\psi_i|0, 1)$ . Thus,  $x_i$  is independent of  $g_i$  conditional on the covariates  $\mathbf{z} = \mathbf{z}_{wi} \cup \mathbf{z}_{xi}$ . This assumption is akin to the missing at random (MAR) assumption (Little and Rubin, 2002).

The CIF of  $x_i$  given non-prevalence at baseline is given by  $F_x(x_i|g_i = 0, \boldsymbol{\beta}_x, \sigma, \mathbf{z}_i)$  which is interpreted as the cumulative risk of disease for healthy individuals at baseline. Furthermore, to describe the CIF of the mixture of prevalent and non-prevalent cases we need to set the event time of prevalent cases to a value, where zero is the obvious choice, i.e.

$$x_i^* := (1 - g_i)x_i. \quad (4)$$

Subsequently, we estimate

$$\begin{aligned} F_{x^*}(x_i^*|\boldsymbol{\beta}, \sigma, \mathbf{z}_i) &= \Pr(g_i = 1|\boldsymbol{\beta}_w, \mathbf{z}_i) + \Pr(g_i = 0|\boldsymbol{\beta}_w, \mathbf{z}_i)F_x(x_i|g_i = 0, \boldsymbol{\beta}_x, \sigma, \mathbf{z}_i) \\ &= \Phi(\mathbf{z}'_{wi}\boldsymbol{\beta}_w) + (1 - \Phi(\mathbf{z}'_{wi}\boldsymbol{\beta}_w))F_x(x_i|g_i = 0, \boldsymbol{\beta}_x, \sigma, \mathbf{z}_i), \end{aligned}$$

where  $\Phi$  is the CDF of the standard normal distribution function. This CIF is similar to the CIF defined by Cheung et al. (2017) who also put point probability mass at zero for prevalent cases. Section 5.3 gives further details on CIF estimation and also discusses marginalization over the empirical covariate distribution to obtain population (marginal) CIF.

## 4.2 Censoring mechanism

Every unit has an observed vector of ordered screening times  $\mathbf{v}_i = (v_{i1}, v_{i2}, \dots, v_{ic_i})$ , with  $v_{i1} < v_{i2} < \dots < v_{ic_i}$ , where we set  $v_{i1} = 0$  to denote baseline (Table 2). Here, we define the mechanism that leads to the observed  $\mathbf{v}_i$ . For any  $i$ , this process has two components; first, the generation of a new screening time  $v_{ij}$  and, second, a decision whether the  $j$ -th screening moment is the last one (either due to an event or right censoring).

First, the screening times may be either fixed before screening commences or generated randomly, in which case we assume that the times are independent of  $x_i$  and  $w_i$  conditional on  $\mathbf{z}_i$ , so that the censoring mechanism is uninformative. Let  $q$  denote the density of a generic distribution. Then, we assume that the screening times are generated by a non-Markov process

$$\begin{aligned} v_{i1} &= 0 \\ v_{i2} &\sim q(v_{i2}|\mathbf{z}) \\ v_{i3} &\sim q(v_{i3}|v_{i2}, \mathbf{z}) \\ &\dots \\ v_{ij} &\sim q(v_{ij}|\bar{v}_{ij}, \mathbf{z}), \end{aligned} \quad (5)$$

where  $\bar{v}_{ij} = (v_{i2}, \dots, v_{ij-1})$  is the screening times history before  $v_{ij}$ .

Second, it is also evaluated at every  $v_{ij}$  whether screening is stopped. This happens precisely when a screening test is positive or right censoring occurs. Specifically, disease testing is administered at every screening time after baseline. At baseline ( $v_{i1}$ ), the disease status may be either tested or not tested, as indicated by  $r_i = 1$  (test administered at baseline) or  $r_i = 0$  (test not administered). We assume  $r_i$  is generated according to  $\Pr(r_i = 1|\mathbf{z}_i)$  so that  $r_i$  is conditionally



independent of  $x_i$  and  $w_i$ . In addition, we allow for the boundary cases  $r_i = 0 \forall i$  and  $r_i = 1 \forall i$ , in which case  $r_i$  is not random. Let  $\kappa$  denote the test sensitivity. Then screening is stopped at any occasion  $j$  with probability

$$s(g_i, x_i, r_i, v_{ij}) = \begin{cases} 0 & \text{if } g_i = 0 \cap v_{ij} < x_i \\ \kappa & \text{if } g_i = 0 \cap v_{ij} \geq x_i \\ 0 & \text{if } g_i = 1 \cap r_i = 0 \cap j = 1 \\ \kappa & \text{if } g_i = 1 \cap r_i = 0 \cap j \geq 2 \\ \kappa & \text{if } g_i = 1 \cap r_i = 1. \end{cases} \quad (6)$$

The resulting screening times are  $\mathbf{v}_i = (v_{i1}, v_{i2}, \dots, v_{ic_i})$  where  $v_{ic_i} = v_{ij}$  is the moment of the positive test (stopping); we set  $\mathbf{v}_i = v_{i1}$  if the test is positive at baseline (cf. Table 2). In addition, right censoring may occur and stops the screening process; specifically let  $v_{ir} \sim q(v_{ir} | \mathbf{z}_i)$  denote the latent exact time of right censoring. Hence, when  $v_{ij+1} > v_{ir}$  right censoring occurs at  $v_{ij}$ . Time  $v_{ir}$  may depend on covariates  $\mathbf{z}_i$  and is conditionally independent of  $x_i$  and  $w_i$ , so that the right censoring mechanism is uninformative. With right censoring, the resulting screening times are  $\mathbf{v}_i = (v_{i1}, v_{i2}, \dots, v_{ij}, v_{ic_i})$  where  $v_{ic_i}$  is set to infinity ( $v_{ic_i} = \infty$ ) to indicate right censoring.

### 4.3 Prior assumptions

We assume that the model parameters  $(\boldsymbol{\beta}_x, \boldsymbol{\beta}_w, \sigma, \kappa)$  are random variables with independent prior distributions

$$\pi(\boldsymbol{\beta}_x, \boldsymbol{\beta}_w, \sigma, \kappa | \tau_x, \tau_w, \lambda, \boldsymbol{\alpha}) = \left[ \prod_{j=1}^{p_x} \pi(\beta_{x,j} | \tau_x) \right] \left[ \prod_{k=1}^{p_w} \pi(\beta_{w,k} | \tau_w) \right] \pi(\sigma | \lambda) \pi(\kappa | \boldsymbol{\alpha}).$$

Specifically, we choose zero-centered normal priors for  $\beta_{x,j}$  and  $\beta_{w,j}$  with standard deviation 1. Furthermore, we specify a half normal prior with standard deviation  $\sqrt{10}$  for  $\sigma$ . These prior choices are called weakly informative, as they do not provide strong information on the location of the parameters, but do regularize parameter estimation. Regularization facilitates parameter estimation in sparse data settings that result from the interval and right censored observation process, the fact that in cancer screening there are typically few events, latent prevalence. Finally, for the sensitivity parameter  $\kappa$  a Beta prior with shape parameters  $(\alpha_1, \alpha_2)$  is applied which can be chosen informatively. For an example, see the application, section 7.

## 5 Model estimation

Let  $\mathbb{V} = \{\mathbf{v}_1, \dots, \mathbf{v}_n\}$  denote the set of all observed screening time vectors,  $\mathbf{c} = (c_1, \dots, c_n)$  the associated lengths of the screening vectors in  $\mathbb{V}$ ,  $\mathbf{r} = (r_1, \dots, r_n)$  the baseline testing indicators, and  $\mathbf{Z}$  the  $n \times p$  matrix of stacked covariate vectors  $\mathbf{z}_i'$ . Furthermore, we wrap all parameters in vector  $\boldsymbol{\theta} = (\boldsymbol{\beta}_x', \boldsymbol{\beta}_w', \sigma, \kappa)$  and the data in  $\mathcal{D} = \{\mathbf{c}, \mathbf{r}, \mathbb{V}, \mathbf{Z}\}$ . We note that  $\mathbf{c}$  is encoded in  $\mathbb{V}$ , but an explicit notation for  $\mathbf{c}$  is useful as will be clear from the following.

### 5.1 Observed data likelihood

The observed data likelihood can be written as

$$\mathcal{L}(\boldsymbol{\theta} | \mathcal{D}) = \prod_{i=1}^n q(c_i, r_i, \mathbf{v}_i | \boldsymbol{\theta}, \mathbf{z}_i).$$

where

$$\begin{aligned} q(c_i, r_i, \mathbf{v}_i | \boldsymbol{\theta}, \mathbf{z}_i) &= \sum_{k=0}^1 \int_0^\infty \int_{-\infty}^\infty q(g_i = k, w_i, x_i, \boldsymbol{\theta}, r_i, \mathbf{v}_i | \mathbf{z}_i) \pi(\boldsymbol{\theta})^{-1} dw_i dx_i \\ &= \sum_{k=0}^1 \left[ \int_{-\infty}^\infty \Pr(g_i = k | w_i) q(w_i | \boldsymbol{\beta}_w, \mathbf{z}_{wi}) dw_i \right. \\ &\quad \left. \times \int_0^\infty q(c_i, \mathbf{v}_i | g_i = k, x_i, \kappa, r_i, \mathbf{z}_i) f_x(x_i | \boldsymbol{\beta}_x, \sigma, \mathbf{z}_{xi}) dx_i \right] \Pr(r_i = 1 | \mathbf{z}_i). \end{aligned}$$

From screening process (5), the stopping probability (6) with sensitivity  $\kappa$  as well as right censoring, defined in section 4.2, we have in the non-prevalent group ( $g_i = 0$ )

$$\begin{aligned} q(c_i, \mathbf{v}_i | g_i = 0, x_i, \kappa, r_i) &= \prod_{j=1}^{c_i} q(v_{ij} | \bar{v}_{ij}, \mathbf{z}_i) \kappa^{\mathbb{1}_{\{v_{ic_i} < \infty\}} \mathbb{1}_{\{j=c_i\}}} (1 - \kappa)^{\mathbb{1}_{\{x_i \leq v_{ij}\}} \mathbb{1}_{\{j < c_i\}}} \\ &= \left[ \prod_{j=1}^{c_i} q(v_{ij} | \bar{v}_{ij}, \mathbf{z}_i) \right] \kappa^{\rho_i} (1 - \kappa)^{l_i} \\ &= q(\mathbf{v}_i | \mathbf{z}_i) \Pr(\tilde{c}_i = c_i | g_i = 0, x_i, \kappa, r_i, \mathbf{v}_i). \end{aligned} \quad (7)$$

Here,  $\rho_i = \mathbb{1}_{\{v_{ic_i} < \infty\}}$  indicates that the series is not right censored at  $v_{ic_i}$  and  $l_i = [\sum_{j=1}^{c_i} \mathbb{1}_{\{x_i \leq v_{ij}\}}] - 1$  denotes the number of falsely negative tests conducted before the  $c_i$ -th screening moment. Likelihood component  $q(c_i, \mathbf{v}_i | g_i, x_i, \kappa, r_i)$  thus factorizes into a component emerging from the screening times generation (5),  $q(\mathbf{v}_i | \mathbf{z}_i)$ , and the probability to stop screening at screening occasion  $\tilde{c}_i = c_i$  as opposed to one of the previous  $\tilde{c}_i = 1, \dots, c_i - 1$  occasions, given by

$$\Pr(\tilde{c}_i = m | g_i = 0, x_i, \kappa, r_i, \mathbf{v}_i) = \begin{cases} 0 & \text{if } x_i > v_{im} \\ \kappa^{\rho_i} (1 - \kappa)^{l_i} & \text{if } x_i \leq v_{im}. \end{cases} \quad (8)$$

Since  $l_i$  can also be determined by finding  $\{j : v_{im-j} < x_i \leq v_{im-j+1}\}$  and setting  $l_i := j - 1$ , we may rewrite (8) as

$$\Pr(\tilde{c}_i = m | g_i = 0, x_i, \kappa, r_i, \mathbf{v}_i) = \begin{cases} 0 & \text{if } m_i = 1 \\ \sum_{j=1}^{m-1} \kappa^{\rho_i} (1 - \kappa)^{j-1} \mathbb{1}_{\{v_{im-j} < x_i \leq v_{im-j+1}\}} & \text{if } m_i > 1, \end{cases} \quad (9)$$

showing that the stopping probability at screening time  $v_{im}$  depends on a discretized space of  $x_i$ . Probability (9) evaluates to 0 if  $\tilde{c}_i = 1$ , because, for non-prevalent patients, screening cannot stop at baseline, as the specificity is one; see section 1. To the contrary, in the prevalent group we have

$$\Pr(\tilde{c}_i = m | g_i = 1, x_i, \kappa, r_i, \mathbf{v}_i) = \begin{cases} \kappa^{\rho_i} (1 - \kappa)^{m-2} \mathbb{1}_{\{m > 1\}} & \text{if } r_i = 0 \\ \kappa^{\rho_i} (1 - \kappa)^{m-1} & \text{if } r_i = 1, \end{cases} \quad (10)$$

allowing to stop screening at baseline if there is a test ( $r_i = 1$ ). We strongly leverage expressions (9) and (10) in the derivation of the Gibbs sampler (section 5.2) and the observed data likelihood (see Supplemental Material, section A.1), given by

$$\begin{aligned} \mathcal{L}(\boldsymbol{\theta} | \mathcal{D}) &= \left[ \prod_{i:c_i > 1} (1 - \Phi(\mathbf{z}'_{wi} \boldsymbol{\beta}_w)) \right] \left[ \sum_{j=1}^{c_i-1} \kappa^{\rho_i} (1 - \kappa)^{j-1} (F_x(v_{ic_i-j+1} | \mathbf{z}_x, \beta_x, \sigma) - F_x(v_{ic_i-j} | \mathbf{z}_x, \beta_x, \sigma)) \right] \\ &\quad \times \left[ \Phi(\mathbf{z}'_{wi} \boldsymbol{\beta}_w) \kappa^{\rho_i} (1 - \kappa)^{c_i-2+r_i} \right] \times \prod_{i:c_i=1} \Phi(\mathbf{z}'_{wi} \boldsymbol{\beta}_w) \kappa. \end{aligned} \quad (11)$$



## 5.2 Gibbs sampler

Our primary motivation to develop the Gibbs sampler is that maximizing the likelihood (11) or simultaneous sampling of all parameters from the observed data posterior, i.e.

$$q(\boldsymbol{\theta} | \mathcal{D}) \propto \mathcal{L}(\boldsymbol{\theta} | \mathcal{D})\pi(\boldsymbol{\theta} | \tau_x, \tau_w, \lambda, \boldsymbol{\alpha}),$$

is challenging due to the mixture structure of the likelihood. The Gibbs sampler suggests a series of data augmentation steps (12-14) of the latent random variables (Albert and Chib, 1993) and subsequent parameter updating steps (15-17) from the full conditional distributions.

$$x_i^{(t+1)} \sim q(x_i | g_i^{(t)}, w_i^{(t)}, \boldsymbol{\theta}^{(t)}, \mathcal{D}), \quad i = 1, \dots, n \quad (12)$$

$$g_i^{mis, (t+1)} \sim q(g_i | \boldsymbol{\theta}^{(t)}, \mathcal{D}), \quad i = 1, \dots, n \quad (13)$$

$$w_i^{(t+1)} \sim q(w_i | g_i^{(t+1)}, x_i^{(t+1)}, \boldsymbol{\theta}^{(t)}, \mathcal{D}), \quad i = 1, \dots, n \quad (14)$$

$$(\boldsymbol{\beta}_x, \sigma)^{(t+1)} \sim q(\boldsymbol{\beta}_x, \sigma | \mathbf{g}^{(t+1)}, \mathbf{w}^{(t+1)}, \mathbf{x}^{(t+1)}, \boldsymbol{\beta}_w^{(t)}, \kappa^{(t)}, \mathcal{D}) \quad (15)$$

$$\boldsymbol{\beta}_w^{(t+1)} \sim q(\boldsymbol{\beta}_w | \mathbf{g}^{(t+1)}, \mathbf{w}^{(t+1)}, \mathbf{x}^{(t+1)}, \boldsymbol{\beta}_x^{(t+1)}, \sigma^{(t+1)}, \kappa^{(t)}, \mathcal{D}) \quad (16)$$

$$\kappa^{(t+1)} \sim q(\kappa | \mathbf{g}^{(t+1)}, \mathbf{w}^{(t+1)}, \mathbf{x}^{(t+1)}, \boldsymbol{\beta}_x^{(t+1)}, \sigma^{(t+1)}, \boldsymbol{\beta}_w^{(t+1)}, \mathcal{D}) \quad (17)$$

Index  $t$  denotes the iterations of the sampler and  $\mathbf{x} = (x_1, \dots, x_n)$ ,  $\mathbf{g} = (g_1, \dots, g_n)$ , and  $\mathbf{w} = (w_1, \dots, w_n)$ . Vectors  $\mathbf{x}$  and  $\mathbf{w}$  are fully latent, whereas  $\mathbf{g}$  consists of a mix of observed and missing (latent) elements. We refer to missing  $g_i$  by  $g_i^{mis}$  and to observed  $g_i$  by  $g_i^{obs}$ . Whether  $g_i$  is observed is determined by the condition  $\mathbb{1}_{\{c_i=1\}}$ , which reflects that the prevalence status is observed if a baseline test was done and it was positive. Hence  $g_i^{obs} = 1$  without exception. If  $g_i$  is missing (if  $c_i > 1$ ), no baseline test was administered ( $r_i = 0$ ) or the baseline test was administered but possibly falsely negative ( $r_i = 1$ ,  $\kappa < 1$ ), so that the prevalence status is missing (latent). Consequently, Gibbs sampler step (13) only needs to augment  $g_i^{mis}$ . In augmenting  $g_i^{mis}$  we note that step (13) integrates out  $w_i$  and  $x_i$ , i.e. it is 'collapsed' (Liu, 1994); for a motivation see section 5.2.2.

### 5.2.1 Augmenting the transition time

We first consider data augmentation of  $x_i$  in step (12). The full conditional distribution of  $x_i$  in the non-prevalent case ( $g_i = 0$ ) is a finite mixture of truncated distributions of  $x_i$

$$q(x_i | g_i = 0, w_i, \boldsymbol{\theta}, \mathcal{D}) = \sum_{j=1}^{c_i-1} \omega_{ij} f_x(x_i | v_{ic_i-j} < x_i \leq v_{ic_i-j+1}, \boldsymbol{\beta}_x, \sigma, \mathbf{z}_{xi}) \quad \forall i : c_i > 1, \quad (18)$$

where

$$\omega_{ij} = \frac{\tilde{w}_{ij}}{\sum_{j=1}^{c_i-1} \tilde{w}_{ij}} \quad (19)$$

and

$$\tilde{w}_{ij} = \kappa^{\rho_i} (1 - \kappa)^{j-1} [F_x(v_{ic_i-j+1} | \boldsymbol{\beta}_x, \sigma, \mathbf{z}_{xi}) - F_x(v_{ic_i-j} | \boldsymbol{\beta}_x, \sigma, \mathbf{z}_{xi})],$$

see the Supplemental Material, section A.2 for a proof. It is interesting to observe that the mixture components of (18) are non-overlapping, because the truncation bounds are equal to the screening times. With perfect test sensitivity,  $\kappa = 1$ , the augmentation simplifies to sampling from the truncated distribution  $f_x(x_i | v_{ic_i-j} < x_i \leq v_{ic_i-j+1}, \boldsymbol{\beta}_x, \sigma, \mathbf{z}_{xi})$  where  $v_{ic_i-j} < x_i \leq v_{ic_i-j+1}$  is known to bound  $x_i$ . For  $\kappa < 1$ , the relative importance of a mixture component is determined by two factors. First, it decreases geometrically in the number of tests conducted since the most recent moment  $c_i$ , and, second, it increases with the

probability mass of  $x_i$  corresponding to the truncation interval. In general, more recent intervals are thus given higher weight, which is plausible. Sampling from (18) is straight-forward when viewed as a two-stage sampling procedure for mixture distributions, i.e., first, sample  $J \sim \text{categorical}(\omega_{i1}, \dots, \omega_{ic_i-1})$ , and, second, use the associated interval bounds of  $J$  as truncation bounds for  $x_i$ , i.e. sample  $x_i \sim f_x(x_i | v_{ic-J} < x_i \leq v_{ic-J+1}, \boldsymbol{\beta}_x, \sigma, \mathbf{z}_{xi})$ . The draws of  $J$  may also be viewed as a posterior prediction of the interval in which  $x_i$  occurred.

In the prevalent case ( $g_i = 1$ ), the observed screening series contains no information on  $x_i$ , and hence

$$q(x_i | g_i = 1, w_i, \boldsymbol{\theta}, \mathcal{D}) = f_x(x_i | \boldsymbol{\beta}_x, \sigma, \mathbf{z}_{xi}), \quad (20)$$

so that  $x_i$  is updated uninformatively.

### 5.2.2 Augmenting the prevalence status

Augmenting the unknown prevalence status consists of two steps; first update the group membership  $g_i^{mis}$  by (13), and, second, update the latent propensity  $w_i$  by (14). As defined in (3), variables  $g_i$  and  $w_i$  have the deterministic relationship  $\Pr(g_i = 1 | w_i) = \mathbb{1}_{\{w_i > 0\}}$ . As a consequence, the full conditional distribution of  $g_i$  is also deterministic in  $w_i$  and does not depend on the observed screening times and the full conditional distribution of  $g_i^{mis}$  yields uninformative updates (see the Supplemental Material, section A.3, for a proof). Therefore, we apply a collapsed Gibbs sampler that treats the distribution of  $w_i$  as a prior of  $g_i$  which is integrated out. The result is a 'collapsed' Gibbs sampler which preserves the convergence property of fully conditional Gibbs but offers the benefits of a reduction in MCMC auto-correlation when data augmentation is used (Liu, 1994). We first consider doing so by deriving  $\Pr(g_i^{mis} = 1 | x_i, \boldsymbol{\theta}, \mathcal{D})$  as

$$\frac{\Phi(\mathbf{z}'_{wi} \boldsymbol{\beta}_w) \Pr(\tilde{c}_i = c_i | g_i^{mis} = 1, x_i, \kappa, r_i, \mathbf{v}_i)}{(1 - \Phi(\mathbf{z}'_{wi} \boldsymbol{\beta}_w)) \Pr(\tilde{c}_i = c_i | g_i^{mis} = 0, x_i, \kappa, r_i, \mathbf{v}_i) + \Phi(\mathbf{z}'_{wi} \boldsymbol{\beta}_w) \Pr(\tilde{c}_i = c_i | g_i^{mis} = 1, x_i, \kappa, r_i, \mathbf{v}_i)}, \quad (21)$$

see the Supplemental Material for a proof. However, we note that a boundary case can occur across the iterations of Gibbs sampler steps (12-13) if (21) is used instead of (13) that additionally marginalizes over  $x_i$ . Specifically, if  $g_i^{mis,(t)} = 1$ , an uninformative update of  $x_i$  according to (20) is done so that  $x_i^{(t+1)} > v_{ic_i}$  may occur. Then we have that  $\Pr(\tilde{c}_i = c_i | g_i = 0, x_i^{(t+1)}, \kappa, r_i, \mathbf{v}_i) = 0$  due to (9) and thus  $g_i^{mis,(t+1)} = 1$  with probability one due to (21). Therefore,  $g_i^{mis}$  is updated deterministically to one unless in a future draw  $t' > t$  we have  $x_i^{(t')} \leq v_{ic_i}$  which occurs with probability  $F_x(v_{ic_i} | \boldsymbol{\beta}_x^{(t')}, \sigma^{(t')})$ , see (20). We conjecture that this dependency may hamper efficient exploration of the posterior space. Hence, marginalizing (21) additionally over  $x_i$  is attractive as it eliminates this dependence and guarantees stochastic updates, i.e.

$$q(g_i^{mis} = 1 | \boldsymbol{\theta}, \mathcal{D}) = \frac{\Phi(\mathbf{z}'_{wi} \boldsymbol{\beta}_w) \sum_{j=1}^{c_i-1} \omega_{ij}}{(1 - \Phi(\mathbf{z}'_{wi} \boldsymbol{\beta}_w)) \kappa^{\rho_i} (1 - \kappa)^{c_i-2+r_i} + \Phi(\mathbf{z}'_{wi} \boldsymbol{\beta}_w) \sum_{j=1}^{c_i-1} \omega_{ij}}, \quad (22)$$

with  $\omega_{ij}$  defined in (19); see the Supplemental Material for a proof. Similar to (21), ratio (22) yields a weighted comparison of the probability that stopping probability (10) as opposed to (9) generated the observed screening times series. Repeated draws from (22), furthermore, may be interpreted as posterior evidence for the risk of prevalence at baseline. When testing the Gibbs algorithm during development, we found that using (21) instead of (22) indeed can cause non-convergence and biased estimates. All results in sections 6 and 7 are based on (22).

After updating  $g_i$ , we update the latent propensity  $w_i$  by drawing according to (14), that is

$$q(w_i|g_i, x_i, \boldsymbol{\theta}, \mathcal{D}) = \begin{cases} \phi(w_i|0 < w_i \leq \infty, \mathbf{z}'_{w_i} \boldsymbol{\beta}_w, 1) & \text{if } g_i = 1 \\ \phi(w_i|-\infty < w_i \leq 0, \mathbf{z}'_{w_i} \boldsymbol{\beta}_w, 1) & \text{if } g_i = 0 \end{cases}$$

where  $\phi(w_i|\mathbf{z}'_{w_i} \boldsymbol{\beta}_w, 1)$  is the normal density with mean  $\mathbf{z}'_{w_i} \boldsymbol{\beta}_w$  and variance one. This updating step is equivalent to standard data augmentation in Gibbs estimation of a probit model (Albert and Chib, 1993).

### 5.2.3 Updating the model parameters

Conditional on the transition times  $x_i$  and the latent propensity  $w_i$ , the model parameters are sampled from their complete data posterior distributions. The results in this section are standard in Bayesian inference and merely summarized. They also partly emerge due to our specific choice in conjugate priors for  $\boldsymbol{\beta}_w$  which offers computational efficiency. First, concerning the full conditional of  $\boldsymbol{\beta}_w$  we have that, due to prior conjugacy, (16) evaluates to

$$\begin{aligned} q(\boldsymbol{\beta}_w | \mathbf{g}, \mathbf{w}, \mathbf{x}, \boldsymbol{\theta}, \mathcal{D}) &\propto \left[ \prod_{i=1}^n \phi(w_i | \mathbf{z}'_{w_i} \boldsymbol{\beta}_w, 1) \right] \phi(\boldsymbol{\beta}_w | 0, \tau_w) \\ &\propto \phi(\boldsymbol{\beta} | \hat{\boldsymbol{\beta}}_w(\tau_w), (\mathbf{Z}'_w \mathbf{Z}_w + \tau_w^{-1} I_{p_w})^{-1}), \end{aligned}$$

where  $\hat{\boldsymbol{\beta}}_w(\tau_w) = (\mathbf{Z}'_w \mathbf{Z}_w + \tau_w^{-1} I_{p_w})^{-1} \mathbf{Z}'_w \mathbf{w}$ . Second, concerning the parameters of  $x_i$ , (15) evaluates to

$$q(\boldsymbol{\beta}_x, \sigma | \mathbf{g}, \mathbf{w}, \mathbf{x}, \boldsymbol{\theta}, \mathcal{D}) \propto \left[ \prod_{i=1}^n f_x(x_i | \boldsymbol{\beta}_x, \sigma, \mathbf{z}_{xi}) \right] \phi(\boldsymbol{\beta}_x | 0, \tau_x) \pi(\sigma | \lambda). \quad (23)$$

The specific posterior follows from the distributional assumptions on the transition times, that is, the distribution of the AFT residuals  $\epsilon_i$  in model (1). Here, we give the example of a Weibull model. Then the residuals are extreme value distributed with  $q_\epsilon(\epsilon_i) = \exp(\epsilon_i - \exp(\epsilon_i))$  so that, by a change of variable, it follows that  $x_i$  has density  $f_x(x_i | \boldsymbol{\beta}, \sigma, \mathbf{z}_{xi}) = \frac{\eta}{\gamma_i} (\frac{x_i}{\gamma_i})^{\eta-1} \exp(-(\frac{x_i}{\gamma_i})^\eta)$ , where  $\eta = \sigma^{-1}$  and  $\gamma_i = \exp(\mathbf{z}'_{xi} \boldsymbol{\beta}_x)$ . The log of the posterior (23) is then proportional to

$$n \log(\eta) + \sum_{i=1}^n \left[ (\eta - 1) \log(x_i) - \eta \log(\gamma_i) - \left(\frac{x_i}{\gamma_i}\right)^\eta \right] - \frac{1}{2} \left[ \left(\sum_{j=1}^{p_x} \frac{\beta_j^2}{\tau_x}\right) + \frac{\sigma^2}{\lambda} \right].$$

In general, (23) does not follow a known distribution and, therefore, we use a Metropolis sampler that applies a multivariate normal proposal (jumping) distribution that is mean-centered at the previous draw  $(\boldsymbol{\beta}_x^{(t)}, \sigma^{(t)})$  and has variance-covariance matrix  $\Sigma$  chosen by the user.

### 5.2.4 Updating the test sensitivity parameter

The sensitivity  $\kappa$  is the parameter of the stopping probability (9-10) and therefore, conditionally on  $\mathbf{x}$  and  $\mathbf{g}$ , its full conditional distribution depends on the observed screening series as follows

$$\begin{aligned} q(\kappa | \mathbf{g}, \mathbf{w}, \mathbf{x}, \boldsymbol{\beta}_x, \sigma, \boldsymbol{\beta}_w, \mathcal{D}) &\propto \left[ \prod_{i: g_i=0} \kappa^{\rho_i} (1 - \kappa)^{l_i} \right] \left[ \prod_{i: g_i=1} \kappa^{\rho_i} (1 - \kappa)^{c_i - 2 + r_i} \right] \text{Beta}(\kappa | \boldsymbol{\alpha}) \\ &\propto \text{Beta}(\kappa | \tilde{\rho} + \alpha_1, L_0 + C_1 - 2N_1 + \alpha_2), \end{aligned}$$

where  $\tilde{\rho} = \sum_{i=1}^n \rho_i$ ,  $L_0 = \sum_{i: g_i=0} l_i$ ,  $C_1 = \sum_{i: g_i=1} c_i + r_i$ ,  $N_1 = \sum_{i=1}^n g_i$ , and  $\text{Beta}(\kappa | \boldsymbol{\alpha})$  the density function of the Beta distribution with parameters  $\boldsymbol{\alpha} = (\alpha_1, \alpha_2)$ . The question whether  $\kappa$  can be estimated unbiased and consistent was given substantial attention in our simulations; see sections 6 and 7.2.

### 5.3 Posterior predictive cumulative incidence functions

We draw inference on the conditional CIF of  $x_i$  in the non-prevalent population stratum,  $F_x(x_i|g_i = 0, \beta_x, \sigma, \mathbf{z}_i)$ . To do so after observing the data, we calculate the posterior predictive probability that a newly sampled observation has an event on or before time  $x$  given new covariates  $\tilde{\mathbf{z}}$ ,

$$\Pr(\tilde{x} \leq x | \tilde{g} = 0, \tilde{\mathbf{z}}, \mathcal{D}) = F_x(\tilde{x} | \tilde{g} = 0, \tilde{\mathbf{z}}, \mathcal{D}) = \int_0^\infty \int_{\Theta_x} F_x(\tilde{x} | \tilde{g} = 0, \beta_x, \sigma_x, \tilde{\mathbf{z}}) q(\beta_x, \sigma_x | \mathcal{D}) d\beta_x d\sigma, \quad (24)$$

where  $\Theta_x = \{\beta_x \in \mathbb{R}^{p_x}\}$ . This is the posterior predictive CIF, conditional on  $\tilde{\mathbf{z}}$ . To sample from (24) we use the MCMC samples  $\theta^{(t)}$  generated by the Gibbs sampler (12)-(17); for details see the Supplemental Material (section A.4). Furthermore, we consider the case where we partially or fully marginalize over the empirical distribution of the covariates  $q_{\mathbf{z}}(\mathbf{z})$  to draw inference on  $F_x(x_i|g_i = 0, \beta_x, \sigma)$ . The marginal posterior predictive CIF is

$$\begin{aligned} \Pr(\tilde{x} \leq x | \tilde{g} = 0, \mathcal{D}) &= F_x(\tilde{x} | \tilde{g} = 0, \mathcal{D}) \\ &= \int_{\Theta_z} \int_0^\infty \int_{\Theta_x} F_x(\tilde{x} | \tilde{g} = 0, \beta_x, \sigma, \mathbf{z}) q(\beta_x, \sigma | \mathcal{D}) q_{\mathbf{z}}(\mathbf{z}) d\beta_x d\sigma d\mathbf{z}, \end{aligned} \quad (25)$$

where  $\Theta_z$  denotes the support of the covariate space. We use empirical Monte Carlo integration for the integration over  $\mathbf{z}$ ; for details see again the Supplemental Material. In addition, we want to estimate the conditional and marginal CIF of the mixture distribution implied by  $x^*$  defined in (4), i.e.  $F_{x^*}(x^* | \beta, \sigma, \tilde{\mathbf{z}})$  and  $F_{x^*}(x^* | \beta, \sigma)$ . The posterior predictive conditional mixture CIF is

$$\begin{aligned} F_{\tilde{x}^*}(\tilde{x}^* | \tilde{\mathbf{z}}, \mathcal{D}) &= \int_{\Theta_w} \int_0^\infty \int_{\Theta_x} F_{\tilde{x}^*}(\tilde{x}^* | \beta, \sigma, \tilde{\mathbf{z}}, \mathcal{D}) q(\beta, \sigma | \mathcal{D}) d\beta d\sigma d\beta_w \\ &= \int_{\Theta_w} \left[ \Phi(\tilde{\mathbf{z}}' \beta_w) + (1 - \Phi(\tilde{\mathbf{z}}' \beta_w)) F_x(\tilde{x} | \tilde{g} = 0, \tilde{\mathbf{z}}, \mathcal{D}) \right] q(\beta_w | \mathcal{D}) d\beta_w, \end{aligned} \quad (26)$$

where  $\Theta_w = \{\beta_w \in \mathbb{R}^{p_w}\}$ , and the marginal posterior predictive mixture CIF is

$$F_{\tilde{x}^*}(\tilde{x}^* | \mathcal{D}) = \int_{\Theta_z} F_{\tilde{x}^*}(\tilde{x}^* | \tilde{\mathbf{z}}, \mathcal{D}) q_{\mathbf{z}}(\mathbf{z}) d\mathbf{z}. \quad (27)$$

For details on sampling these distributions, see again the Supplemental Material.

### 5.4 Model fit and non-parametric estimator of the marginal CIF

To choose the best model specification in terms of the distribution of  $x_i$  we use the widely applicable information criterion (WAIC) given by

$$-2 \left( 2 \mathbb{E}_{\theta | \mathcal{D}} [\log \mathcal{L}(\theta | \mathcal{D})] - \log \mathbb{E}_{\theta | \mathcal{D}} [\mathcal{L}(\theta | \mathcal{D})] \right)$$

where the expectations are estimated by Monte Carlo integration over the posterior samples of  $\theta$  that are generated by the Gibbs sampler (Gelman et al., 2014). While WAIC offers a relative measure of fit to be used in selecting the best models among a number of candidate models, we additionally suggest a non-parametric estimator of the marginal CIF  $F_{\tilde{x}^*}(\tilde{x}^* | \mathcal{D})$ . This estimate can then be compared against the parametric BayesPIM estimate as a visual inspection of absolute goodness of fit. Specifically, Witte et al. (2017) developed a non-parametric estimator of  $F_{\tilde{x}}(\tilde{x} | \mathcal{D})$  implemented in a function `em_mixed` which is used in settings with interval censoring and misclassification from imperfect screening tests. However, their estimator does not handle

baseline prevalence. Our approach is to apply a recoding step that is similar to pre-processing suggested by [Cheung et al. \(2017\)](#) to use the Turnbull estimator ([Turnbull, 1976](#)) for estimating  $F_{\tilde{x}^*}(\tilde{x}^* | \mathcal{D})$  (27) from interval censored data when the sensitivity is one. To do so, we recode  $\mathbf{v}_i$  as follows. If  $r_i = 1$ ,  $v_{i1} = 0$  is set to  $\min[v_{12}, \dots, v_{n2}] \times 0.01$  for all  $i$ . If  $r_i = 0$ ,  $v_{i1} = 0$  has to be omitted, so that  $v_{i2}$  is the first screening time. Hence, if  $r_i = 0$  for all  $i$ , the estimator is not expected to perform well, since the anchoring to  $\min[v_{12}, \dots, v_{n2}] \times 0.01$  cannot be performed for any  $i$ . An R function implementing adapted `em_mixed` is included in the Supplemental Material.

## 6 Simulation study

We conducted two Monte Carlo simulations for evaluating the performance of `BayesPIM` compared to `PIMixture` and the non-parametric `em_mixed` estimator. In simulation 1, discussed in this section, we generated synthetic data sets under different conditions repeatedly and evaluated the performance of the estimators. The primary purpose of these experiments was to evaluate the implementation of `BayesPIM` in a controlled setting. Simulation 2, discussed in section 7.2, to the contrary, was designed to generate data sets that resemble the real data example using the CRC EHR.

### 6.1 Set-up of simulation 1

The incidence and prevalence models were parameterized as follows:

$$\log x_i = 5 + 0.2z_{1i} + 0.2z_{2i} + 0.2\epsilon_i,$$

where  $\epsilon_i$  was extreme value distributed with  $q_\epsilon(\epsilon_i) = \exp(\epsilon_i - \exp(\epsilon_i))$ , so that  $x_i | \mathbf{z}_i$  was Weibull distributed. Furthermore, the prevalence model was

$$w_i = \theta + 0.2z_{1i} + 0.2z_{2i} + \psi_i,$$

where  $\psi_i \sim N(0, 1)$ , so that  $g_i = \mathbb{1}_{\{w_i > 0\}}$  followed a probit model.

Our simulation set-up examined estimator performance in a wide range of scenarios:

- Sample size:  $n \in \{1000, 2000\}$
- Sensitivity:  $\kappa \in \{0.4, 0.8\}$
- Baseline prevalence  $\theta \in \{0.11, 0.22\}$  yielding  $\Pr(g_i = 1) \approx .13$  and  $\Pr(g_i = 1) \approx .26$
- Proportion of tests:  $\Pr(r_i = 1) \in \{0, 1\}$
- Type of prior on the sensitivity parameter: uninformative, informative, point (known  $\kappa$ )

Specifically, the sensitivity parameter  $\kappa$  was set to a high level, similar to the sensitivity of a colonoscopy for detection of an adenoma ( $\kappa = 0.8$ ) or to a lower level ( $\kappa = 0.4$ ). The intercept parameter  $\theta$ , furthermore, was employed to control the prevalence rates, where  $\theta \in \{0.11, 0.22\}$  lead to the marginal probabilities of prevalence  $\Pr(g_i = 1) \approx .13$  and  $\Pr(g_i = 1) \approx .26$ , with the higher prevalence resembling that estimated for the CRC EHR application (section 7.1). Moreover, we compared the situations where each individual receives a test at baseline ( $\Pr(r_i = 1) = 1$ ), again similar to the CRC EHR application (Table 1), to the other extreme when nobody receives a baseline test ( $\Pr(r_i = 1) = 0$ ). The latter setting was expected to be more challenging in estimation as it lead to fully latent prevalence status (i.e.  $g_i$ , missing for all  $i$ ). Finally, we also expected the estimator performance to depend on the degree of information that is available on the true test sensitivity. In particular, we were interested whether

BayesPIM is able to estimate the test sensitivity  $\kappa$  when there is no prior information available on the test. The latter is an extreme scenario, since, in cancer screening, there is usually some information available on test sensitivity. Hence, we compared a fully uninformative prior  $q(\kappa|\boldsymbol{\alpha}) = \text{uniform}(0, 1)$ , an informative prior  $q(\kappa|\boldsymbol{\alpha}) = \text{Beta}(\kappa|\boldsymbol{\alpha})$  where  $\boldsymbol{\alpha}$  was chosen such that the prior distribution was mean-centered at the true sensitivity with a standard deviation of 0.05, and a point-prior fixed at the true sensitivity (i.e.,  $\kappa$  is treated as known).

By a full factorial design we thus obtained  $2 \times 2 \times 2 \times 2 \times 3 = 48$  simulation conditions. We generated 200 Monte Carlo data sets for each condition and ran, on each data set, Gibbs sampler (12)-(17) until convergence using 4 randomly initiated MCMC chains. The sampler was implemented in package `BayesPIM`, available in the Supplementary Material. Convergence was assumed to be given when the Gellman-Rubin convergence statistic  $\hat{R}$  was below 1.1 for all model parameters and the effective sample size was at least 40 for each parameter, while discarding half of all posterior draws as burn-in (warm-up). We evaluated convergence every 20,000 draws.

## 6.2 Generation of screening times and right censoring

As defined in section 4.2, the latent transition times  $x_i$  and the prevalence status  $g_i$  yield observed  $\mathbf{v}_i$ . We iteratively generate  $v_{ij}$  from a  $q(v_{ij}|\bar{v}_{ij}, \mathbf{z}_i)$  defined below and stop generating new  $v_{ij}$  with probability (6) or after right censoring. Specifically, the screening times process after baseline (set to  $v_{i1} = 0$ ) was, for each  $j > 1$ ,

$$v_{ij} \sim \text{uniform}(v_{ij-1} + 20, v_{ij-1} + 30).$$

Furthermore, the time of right censoring was distributed as

$$v_{ir} = v_{i2} + \tilde{v}_{ir}, \quad \tilde{v}_{ir} \sim \text{exponential}(80^{-1}).$$

These choices allowed us to study BayesPIM with substantial follow-up on many units  $i$  and also assured that BayesPIM converged in acceptable time for most simulated data sets. In simulation 2, section 7.2, we examine a real-world setting with less frequent screening and stronger right censoring adopted from the CRC EHR application.

## 6.3 Results from simulation 1

The Gibbs sampler typically converged within  $2 \times 10^5$  iterations (Supplemental Figure B.1). However, convergence times varied substantially across conditions, with faster convergence observed for high sensitivity ( $\kappa = 0.8$ ) and slower convergence for lower sensitivity ( $\kappa = 0.4$ ). Prior information on  $\kappa$  reduced convergence time, whereas higher prevalence ( $\Pr(g_i = 1) = 0.26$ ) and the absence of baseline tests ( $\Pr(r_i = 1) = 0$ ) increased it. Runs were interrupted if convergence was not achieved after  $5 \times 10^5$  iterations, and non-converged runs were replaced by additional converged runs. Non-convergence was rare but occurred in three specific conditions with an uninformative prior on  $\kappa$ , high prevalence ( $\Pr(g_i = 1) = 0.26$ ), and no baseline testing ( $\Pr(r_i = 1) = 0$ ; Supplemental Figure B.2). Visual inspection of MCMC chains for exemplary datasets revealed that multi-modality of the posterior distribution was the primary cause of non-convergence; for an example see Supplemental Figure B.3. Crucially, non-convergence did not occur when an informative or point prior on  $\kappa$  was used instead of an uninformative prior.

We evaluated the Monte Carlo error of all parameter estimates, defined as  $\hat{\phi} - \phi$ , where  $\hat{\phi}$  is the posterior median estimate and  $\phi$  is the true value (Supplemental Figures B.4 to B.7). All parameters of the incidence and prevalence models (1) and (2) were approximately unbiased under all conditions. Parameters in the incidence model were estimated with greater precision



than those in the prevalence model. Lower true test sensitivity (0.4 vs. 0.8), absence of a baseline test ( $\Pr(r_i = 1) = 0$  vs.  $\Pr(r_i = 1) = 1$ ), and higher baseline prevalence probability (0.26 vs. 0.13) increased estimator variance for all parameters. Variance decreased with larger sample sizes ( $n = 2000$  vs.  $n = 1000$ ) and with the use of informative or point priors. These findings are illustrated by the Monte Carlo error of the marginal baseline prevalence probability  $\Pr(g_i = 1)$  (Figure 1). Estimated using the posterior median of the marginal mixture CIF (27) at  $\tilde{x}^* = 0$ ,  $\Pr(g_i = 1)$  depends on  $\beta_w$  and hence Figure 1 summarizes the aforementioned results on the separate parameters well. Furthermore, posterior median estimates of the test sensitivity  $\kappa$  are also shown in this figure and were approximately unbiased (Figure 1). Estimation was reliable for  $\kappa = 0.8$ , even with uninformative priors, but variance was high for  $\kappa = 0.4$  when uninformative priors were used. In this case, informative priors decreased variance. Supplemental Figure B.11 shows the approximate frequentist coverage probabilities of the 95% posterior credible intervals for all parameters. Coverage probabilities closely matched the nominal level across all conditions for all parameters, including test sensitivity.

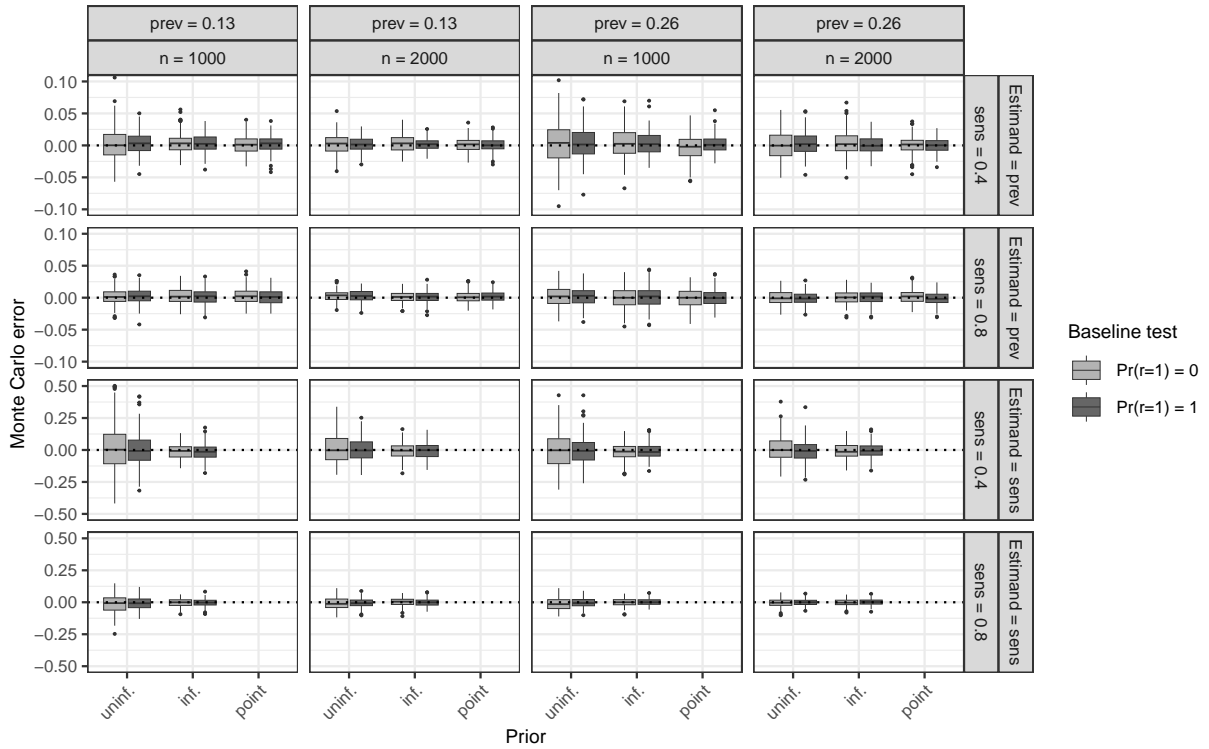


**Figure 1:** Monte Carlo error of the marginal prevalence probability (prev, i.e.  $\Pr(g_i = 1)$ ) and the test sensitivity (sens, i.e.  $\kappa$ ) estimands. The first two rows give errors for the prevalence and the second two rows for the sensitivity. The priors on the test sensitivity  $\kappa$  are either uninformative (uninf.), informative (inf.) or fixed at the true value (point).

To further compare model performance across conditions, we utilized posterior predictive mixture CIFs (27), which depend jointly on all model parameters and thus serve as summary statistics (Figure 2 illustrates results for  $\Pr(r_i = 1) = 1$ ; for  $\Pr(r_i = 1) = 0$ , see Supplemental Figure B.8). These CIFs visualize prevalence  $\Pr(g_i = 1) = 1$  as a point probability at time zero and enable comparisons between BayesPIM, PIMixture, and the adapted non-parametric CIF estimator `em_mixed` (section 5.4). For PIMixture, we specified a Weibull model for  $x_i$ , including all covariates as predictors of  $x_i$  and  $g_i$ , with logistic regression for  $g_i$ , which is similar to the probit model (2)-(3) applied by BayesPIM. The CIF estimates from BayesPIM were approximately unbiased, consistent with the results for individual model parameters discussed earlier. Estimator variance was slightly higher when an uninformative prior was used and true  $\kappa = 0.4$ ,

compared to  $\kappa = 0.8$ . Notably, the considerable uncertainty in  $\kappa$  estimation for  $\kappa = 0.4$  (Figure 1) did not result in significantly elevated uncertainty in CIF estimation, suggesting that posterior median CIF estimates are robust to posterior uncertainty in test sensitivity. In contrast, `PIMixture`, which assumes  $\kappa = 1$ , produced biased CIF estimates, with greater bias observed when true  $\kappa = 0.4$  due to the larger deviation from the assumption of perfect sensitivity. The non-parametric estimator `em_mixed` yielded approximately unbiased estimates, provided that sensitivity  $\kappa$  was correctly specified. However, `em_mixed` performed poorly, as expected (cf. section 5.4), when  $\Pr(r_i = 1) = 0$  (Figure B.8). In particular baseline prevalence estimates then were biased. Additional simulations showed that this bias decreases as more baseline tests become available and was negligible for a moderate proportion of tests done (e.g.  $\Pr(r_i = 1) = 0.5$ ; Figure B.12).

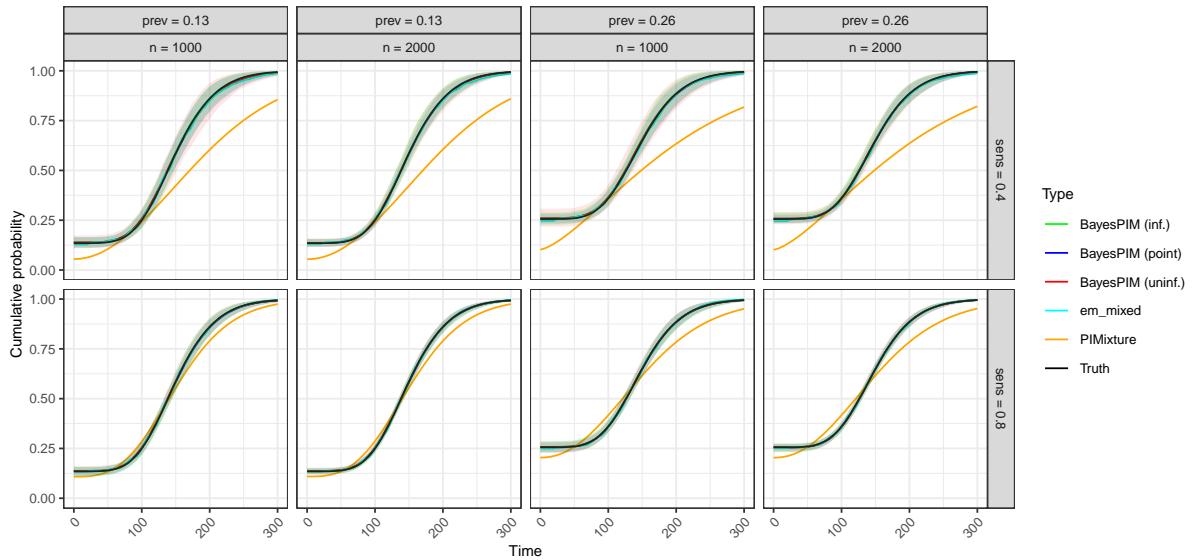


**Figure 2:** Posterior median marginal mixture CIFs (27), point-wise averaged over 200 Monte Carlo simulation runs with 95% quantiles shown as shaded regions. The condition  $\Pr(r_i = 1) = 1$  is shown (for  $\Pr(r_i = 1) = 0$  see the Supplemental Material, section B, Figure). For `em_mixed`,  $\kappa$  was set to its true value.

## 7 Application to the CRC EHR

We apply `BayesPIM`, `PIMixture`, and `em_mixed` to the CRC EHR introduced in section 2. In doing so, we specify `BayesPIM` models with Weibull, loglogistically, lognormally, and exponentially distributed transition times  $x_i$  (model (1)). To obtain the exponential model, we use a Weibull specification and constrain  $\sigma = 1$ . This model is equivalent to a Markov model due to its constant hazard property and it is primarily included for comparison with the less restrictive models. We included subjects' gender and age as covariates in, both, the incidence and the prevalence models (models (1) and (2)). We used priors as specified in section 4.3. For the sensitivity  $\kappa$ , we compared an uninformative prior that sets  $\alpha = (1, 1)$  to an informative prior that we based on a range of test sensitivities published in the literature (section 1). Specifically, test sensitivities for colonoscopy detection of adenomas ranged between 0.65 and 0.95. Hence, we centered the Beta prior for  $\kappa$  at 0.8 with standard error 0.05; using numerical root-finding we determined  $\alpha = (50.4, 12.6)$ , such that  $\Pr(\kappa \in (0.696, 0.890)) \approx 0.95$ . In addition, we added the setting of perfect test sensitivity by constraining  $\kappa = 1$ .

We ran Gibbs sampler steps (12)-(17) until convergence, where step (17) is omitted in the setting that constrains  $\kappa$  to one. Convergence was embraced when the upper confidence bound of the Gelman-Rubin convergence diagnostic  $\hat{R}$  calculated over the most recent half of all iterations first came under the value of 1.1 for all model parameters and the effective sample size of all MCMC samples was at least  $10^3$  for each parameter. We ran four randomly initialized MCMC chains in parallel and assessed convergence every  $5 \times 10^4$  draws.

## 7.1 Results

WAIC slightly favoured a Weibull model over the alternative distributions (Table 3). Furthermore, an informative prior gave slightly better WAIC than an uninformative prior. The models with perfect sensitivity ( $\kappa = 1$ ) had worse fit than the models allowing  $\kappa < 1$ , indicating that relaxing the assumption of perfect sensitivity made by PIMixture improved model fit.

**Table 3:** Model WAIC and number of draws per chain ( $\times 10^5$ ) after convergence. The prior for the test sensitivity  $\kappa$  is either chosen informative (Inf.), uninformative (Uninf.) or  $\kappa$  is constrained to one ( $\kappa = 1$ ).

| model       | WAIC   |        |              | Draws per chain ( $\times 10^5$ ) |        |              |
|-------------|--------|--------|--------------|-----------------------------------|--------|--------------|
|             | Inf.   | Uninf. | $\kappa = 1$ | Inf.                              | Uninf. | $\kappa = 1$ |
| exponential | 1598.0 | 1600.4 | 1599.5       | 1.5                               | 2.0    | 1.0          |
| Weibull     | 1595.4 | 1598.4 | 1597.0       | 4.0                               | 6.0    | 2.5          |
| loglogistic | 1596.1 | 1599.7 | 1599.1       | 2.0                               | 4.0    | 1.0          |
| lognormal   | 1596.8 | 1600.2 | 1601.0       | 2.5                               | 5.5    | 1.5          |

Estimates for the test sensitivity  $\kappa$  differed (.79 vs .70) between informative and uninformative priors but the uninformative prior model had a wide credible interval ([0.44, 0.94]), suggesting that  $\kappa$  was only weakly identified in this data set. This conclusion is supported by the fact that the credible interval of  $\kappa$  in the model with informative  $\kappa$  prior had similar length ([0.69, 0.88]) as the 2.5 to 97.5 quantile range of the Beta prior specified for  $\kappa$ ; see above. However, the added certainty of  $\kappa$  encoded in the informative Beta prior decreased the credible interval lengths of all other model parameters as compared to the model without informative  $\kappa$  prior. Having said this, the regression coefficient estimates were similar across models, including the exponential model, suggesting robustness of inference on risk factors to the model assumptions on  $\kappa$  and the distribution of  $x_i$ .

The sign and size of the coefficient estimates (Table 4) suggested that higher age increased incidence probability of an adenoma, while sex did not have a clear effect on incidence. Specifically, individuals who had an age of one standard deviation (7.71 years) above the sample mean of 52.9 years at baseline were expected to have transition time to an adenoma reduced by the factor  $\exp(-0.175) = 0.839$  (16.1% faster transition). Both sex and age were predictors of prevalence status at baseline, with female sex decreasing and older age increasing the probability of prevalence. These estimates are in line with epidemiological expectations suggesting that older subjects and men are at a higher risk of developing adenomas and CRC.

Figure 3 gives the marginal mixture CIF, (27), and the conditional CIF for different age groups, (26), for the Weibull and the exponential models. The CIF obtained from a fit by PIMixture is added. For this, we used a PIMixture model that assumes the same Weibull incidence model (1) as BayesPIM. Furthermore, we added the non-parametric estimator `em_mixed` of  $F_{x^*}(x^*|\beta, \sigma)$  (see section 5.4) which allows a visual inspection of goodness of fit of the marginal CIF. We set the sensitivity  $\kappa$  to 0.80 in `em_mixed`. See the Supplementary Material, section C, Figure C.2

**Table 4:** Posterior median estimates with 95% credible interval for the coefficients from the Weibull BayesPIM models for different prior settings on the test sensitivity  $\kappa$ .

|                                    | Weibull (inf.)       | Weibull (uninf.)     | Exponential (Inf.)   |
|------------------------------------|----------------------|----------------------|----------------------|
| <i>Model for <math>x_i</math>:</i> |                      |                      |                      |
| $\beta_{x0}$                       | 2.79 [2.50, 3.21]    | 2.78 [2.43, 3.31]    | 3.07 [2.77, 3.42]    |
| female                             | -0.11 [-0.44, 0.20]  | -0.13 [-0.61, 0.22]  | -0.11 [-0.52, 0.27]  |
| age*                               | -0.17 [-0.32, -0.03] | -0.16 [-0.33, 0.04]  | -0.17 [-0.36, 0.02]  |
| $\sigma$                           | 0.74 [0.55, 1.02]    | 0.72 [0.48, 1.04]    | 1.00 [1.00, 1.00]    |
| <i>Model for <math>w_i</math>:</i> |                      |                      |                      |
| $\beta_{w0}$                       | -0.51 [-0.69, -0.31] | -0.41 [-0.70, 0.09]  | -0.52 [-0.70, -0.32] |
| female                             | -0.24 [-0.46, -0.02] | -0.25 [-0.49, -0.01] | -0.24 [-0.46, -0.02] |
| age*                               | 0.33 [0.21, 0.45]    | 0.34 [0.21, 0.49]    | 0.34 [0.22, 0.46]    |
| <i>Sensitivity:</i>                |                      |                      |                      |
| $\kappa$                           | 0.79 [0.69, 0.88]    | 0.70 [0.44, 0.94]    | 0.79 [0.69, 0.88]    |

\* age was z-standardized (before standardization: mean = 52.9 years with sd = 7.71 years).

for an equivalent plot for the non-prevalent population, i.e. CIFs (25) and (24).

The mixture CIFs depict the sum of prevalence and follow-up incidence probability until a given point in time. The prevalence probability can be read at the intercept and is interpreted as the proportion of the population that has an adenoma at the point of inclusion in the surveillance program ( $\Pr(g_i = 1)$ ). Specifically, the models with informative and uninformative prior estimated this proportion at 0.274 [0.222, 0.333] and 0.307 [0.217, 0.475], respectively; the exponential (inf.) model at 0.269 [0.219, 0.330]. Again we note the wider credible interval of the Weibull (uninf.) model as a consequence of the uninformative  $\kappa$  prior. In addition, the prevalence estimate was higher, relating to the fact the Weibull (uninf.) model estimated  $\kappa$  lower (Table 4). The observed prevalence was 0.204 (Table 1), suggesting that an estimated 34% (0.07 points) of prevalence was unobserved (latent). The non-parametric estimator `em_mixed` estimated the prevalence probability at 0.271, which is very close to the Weibull (inf.) and exponential model estimates and reassured us about model fit of the best model according to WAIC. To the contrary, `PIMixture` estimated the prevalence lower at 0.228, owing to the assumption of  $\kappa = 1$ . The `PIMixture` prevalence estimate was similar to that of the BayesPIM model that assumed  $\kappa = 1$  (.217; not shown in Figure 3).

While there were pronounced differences in prevalence estimates between models, the incidence model estimates were similar (Table 4). The marginal CIF of Weibull (inf.), Weibull (uninf.), and `PIMixture` had an almost parallel trajectory (Figure 3, left side). The marginal CIF of the exponential model had different curvature, however, owing to its constraint of  $\sigma = 1$ , which lead in particular in the time after 10 years to different predicted probabilities as compared to the Weibull models. It is important to note that, in this data set, most censoring occurs before the time of 10 years, and the last adenoma event occurred at 22.5 years (Table 1). Hence, the uncertainty of the estimates increases after 10 years, as indicated by wider credible interval bounds shown for the Weibull (inf.) model. The non-parametric fit of `em_mixed` can be used as a visual inspection of incidence model fit. In this case, the Weibull (inf.) which has highest WAIC indeed had similar fit to `em_mixed`, but the exponential model fits similarly well in this visual inspection. Both models fit notably better to `em_mixed` than the `PIMixture` model.

The right panel of Figure 3 shows the conditional mixture CIF (26) for selected age groups. The higher risk of prevalence for older individuals was reflected by the increasing ordinate intercepts

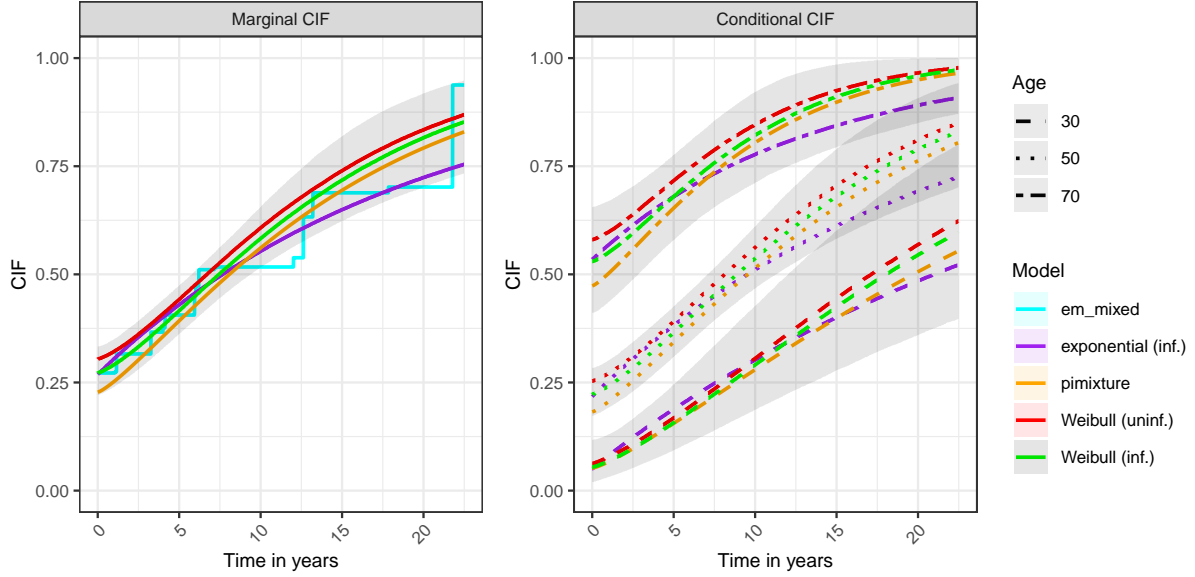


**Figure 3:** Marginal and conditional mixture cumulative incidence functions (CIF), (27) and (26), for Weibull BayesPIM with uninformative (uninf.) prior and informative (inf.) priors. For comparison, CIF from the Weibull PIMixture model, the exponential BayesPIM model (inf.), and `em_mixed` are given. The lines represent posterior median estimates and the shaded regions indicate the 95% credible interval of the Weibull (inf.) models (for overlaid intervals from the Weibull (uninf.) model see the Supplemental Material C, Figure C.1).

across groups. Furthermore, in the 30 and 70 year groups which were further from the sample mean of 52.9 years than the 50 year group, some pronounced differences between models were found. This suggests that model selection, in this case, was more important for the estimation of conditional risk than for estimation of marginal risk.

## 7.2 Simulation based on the CRC EHR

To evaluate BayesPIM in a realistic setting we conducted a Monte Carlo simulation in which we generated data that strongly resembled the CRC EHR (simulation 2).

### 7.2.1 Set-up of simulation 2

We simulated 200 data sets per condition and applied BayesPIM, PIMixture and `em_mixed`, as in simulation 1. Specifically, we considered  $3 \times 2 \times 2 = 12$  simulation conditions:

- Sample size  $n \in \{810, 1620, 3240\}$
- Test sensitivity  $\kappa \in \{0.4, 0.8\}$
- Observed right censoring vs. extended right censoring process (10 years)

The probability of a baseline test was set to its estimate of  $\Pr(r_i = 1) = 0.93$  (Table 1). Thus, the condition with  $n = 810$ ,  $\kappa = 0.8$  was similar to the real CRC EHR, while  $n \in \{1620, 3240\}$  and  $\kappa = 0.4$  represented conditions with larger sample sizes and lower test sensitivity, respectively. We generated covariate and screening times distributions similar to those observed in the CRC EHR by resampling from the empirical distributions of  $\mathbf{z}_i$  and the screening times  $v_{ij}$ , denoted  $\hat{q}(\mathbf{z})$  and  $\hat{q}(v_{ij}|\bar{v}_{ij}, \mathbf{z}_i)$ . In doing so, we limited the set of covariates to sex and age. In addition, we added a condition with an extended right censoring process where the time of right censoring

was simulated to occur ten years later than in the CRC EHR; see the Supplemental Material (section D.2). Specifically, we generated  $n$  new data points  $(\tilde{x}_k, \tilde{w}_k, \tilde{g}_k, \tilde{\mathbf{v}}_k, \tilde{\mathbf{z}}_k)$ ,  $k=1, \dots, n$ , per data set. For each new unit  $k$ , we randomly selected one  $i$  with replacement from  $i = 1, \dots, n$  and set  $\mathbf{z}_k$  to the associated covariates ( $\tilde{\mathbf{z}}_k := \mathbf{z}_i$ ). Subsequently, we generated  $x_k$ ,  $w_k$ , and  $g_k$  according to models (1)-(3) with the true model parameters  $\beta_x$ ,  $\sigma$ , and  $\beta_w$  fixed at the posterior median estimates (Table 4). The transition time  $x_i$  was Weibull distributed. Then, iterative for  $j = 1, 2, \dots$  screening moments we

1. Proposed a new  $\tilde{v}_{kj} \sim \hat{q}(v_{ij} | \bar{v}_{ij}, \mathbf{z}_i)$
2. Evaluated stopping  $\tilde{s}_{kj}$  with probability (6)

In step 1, to generate new screening times from  $\hat{q}(v_{ij} | \bar{v}_{ij}, \mathbf{z}_i)$ , the observed screening times vector  $\mathbf{v}_i = (v_{i1}, \dots, v_{ic_i})$  was used as donor (i.e.,  $v_{k1} := v_{i1}, v_{k2} := v_{i2}, \dots$ ), where  $i$  was identical to the index of the  $\mathbf{z}_i$  sampled before. The details of this procedure were more involved; see the Supplemental Material (sections D.1 and D.2). Supplemental Figure D.2 compares the sampling distributions of various statistics calculated on repeated samples of the screening times  $(\tilde{v}_1, \dots, \tilde{v}_n)$  to the observed statistics in the CRC EHR (e.g., mean and standard deviation of the event/censoring time; mean number of test occasions), demonstrating that the generated and observed screening times were similar.

### 7.2.2 Results

With informative or point (fixed) priors on test sensitivity, the Gibbs sampler reliably converged within  $5 \times 10^5$  draws (see Supplemental Figures E.1 and E.2). However, with uninformative priors, non-convergence was observed in the condition  $n = 810$ ,  $\kappa = 0.4$ , and observed right censoring. The impact of uninformative priors was also particularly evident in explaining variations in Monte Carlo errors across conditions. Pronounced bias was observed in the intercepts  $\beta_{x0}$  and  $\beta_{w0}$  of the incidence (1) and prevalence models (2) under the  $\kappa = 0.4$  condition (Supplemental Figures E.3 and E.4). This bias diminished with larger sample sizes, higher test sensitivity ( $\kappa = 0.8$ ), or extended follow-up. When informative or point priors (fixed at the true  $\kappa$ ) were employed, no bias was observed, and estimation was more efficient compared to the uninformative prior case. We also studied the frequentist coverage probability of the 95% posterior intervals for all parameters (Supplemental Figure E.7), demonstrating that coverage was approximately nominal in those conditions where the intercept and  $\kappa$  parameters did not suffer substantial bias (when uninformative priors were used).

These results are summarized in Figure 4, which shows the Monte Carlo errors for the marginal prevalence probability  $\Pr(g_i = 1)$  which depends on the prevalence model parameters  $\beta_w$ . Figure 4 also highlights that estimation precision for  $\kappa$  likely explained the observed biases. Specifically, under uninformative priors for  $\kappa$ , the estimation of  $\kappa$  was inaccurate in, both, the  $\kappa = 0.4$  and  $\kappa = 0.8$  conditions. Although estimation appeared consistent—bias decreased with larger sample sizes or extended follow-up—substantially larger samples (beyond  $n = 3240$ ) or longer follow-up would have been required to eliminate the bias in the  $\kappa$  estimates. A direct relationship was evident between inaccuracies in sensitivity estimates and biases in the incidence and prevalence model parameters. Even with informative priors correctly centered on the true  $\kappa$ , a small bias was observed in the  $\kappa = 0.4$  condition. This suggests that estimating test sensitivity was challenging given the CRC EHR screening time process.

A key question was how the Monte Carlo errors of the model parameters affected the estimates of the marginal mixture CIFs (27) (Figure 5; for marginal CIFs of the non-prevalent population (25), see Supplemental Figure E.5). As in Simulation 1 (Section 6), these CIFs facilitated comparisons with PIMixture and em\_mixed. When BayesPIM used an uninformative  $\kappa$  prior,



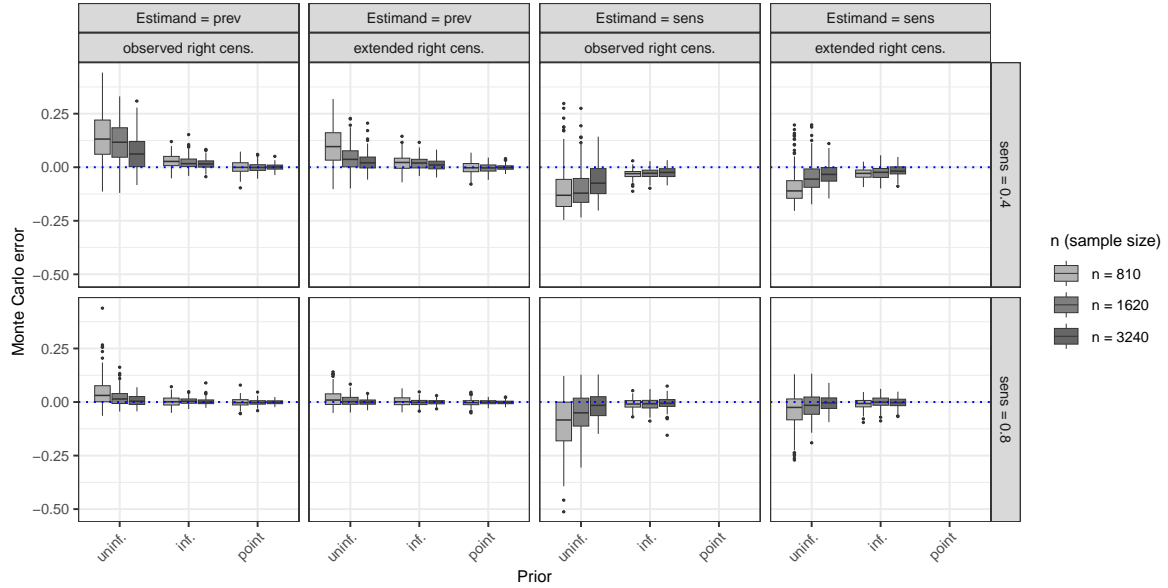


**Figure 4:** Monte Carlo error of the marginal prevalence probability (prev, i.e.  $\Pr(g_i = 1)$ ) and the test sensitivity (sens, i.e.  $\kappa$ ) estimands. The first two columns give errors for the prevalence and the second two columns for the sensitivity. The priors on the test sensitivity  $\kappa$  are either uninformative (uninf.), informative (inf.) or fixed at the true value (point).

the resulting bias was evident in the CIFs, though the bias was smaller in the  $\kappa = 0.8$  conditions. In contrast, BayesPIM with  $\kappa$  fixed at its true value (point prior) provided the most precise estimates, even in the most challenging condition ( $n = 810$ ,  $\kappa = 0.4$ ). The non-parametric `em_mixed` estimator was generally accurate but exhibited some bias beyond ten years when  $\kappa = 0.4$ . This bias disappeared with longer follow-up (extended right censoring). Given that most cases in the observed right-censoring process were censored after approximately ten years (Supplemental Figure D.1), it is evident that the non-parametric estimator lacked sufficient data to produce accurate incidence estimates beyond this time. This limitation also resulted in larger variance, which is not shown in Figure 5 but can be seen in Supplemental Figure E.6. In contrast, BayesPIM leveraged model-based extrapolation, providing better estimates in these sparse-data settings. For the comparison model PIMixture, the results were consistent with Simulation 1. Specifically, under  $\kappa = 0.4$ , PIMixture exhibited greater bias compared to  $\kappa = 0.8$ , due to its stronger deviation from the assumption of perfect sensitivity.

## 8 Discussion

We introduced BayesPIM, a modeling framework for estimating time- and covariate-dependent incidence probabilities from screening and surveillance data. The model is used when the disease may be prevalent at baseline, tests at baseline are fully or partially missing, and the test for disease has imperfect sensitivity. In this regard, we extend the available prevalence-incidence mixture model PIMixture, which assumes perfect sensitivity (Cheung et al., 2017; Hyun et al., 2017). We applied the model to data from high familial risk CRC EHR surveillance by colonoscopy, demonstrating that conditioning incidence and prevalence estimates on covariates explains substantial heterogeneity in adenoma risk (cf. Figure 3). These estimates can serve as valuable input for targeted screening strategies, such as higher intensity for older individuals with familial risk cancer and recognizing that older individuals have a high probability of having adenomas at baseline. More generally, BayesPIM is readily applicable to other

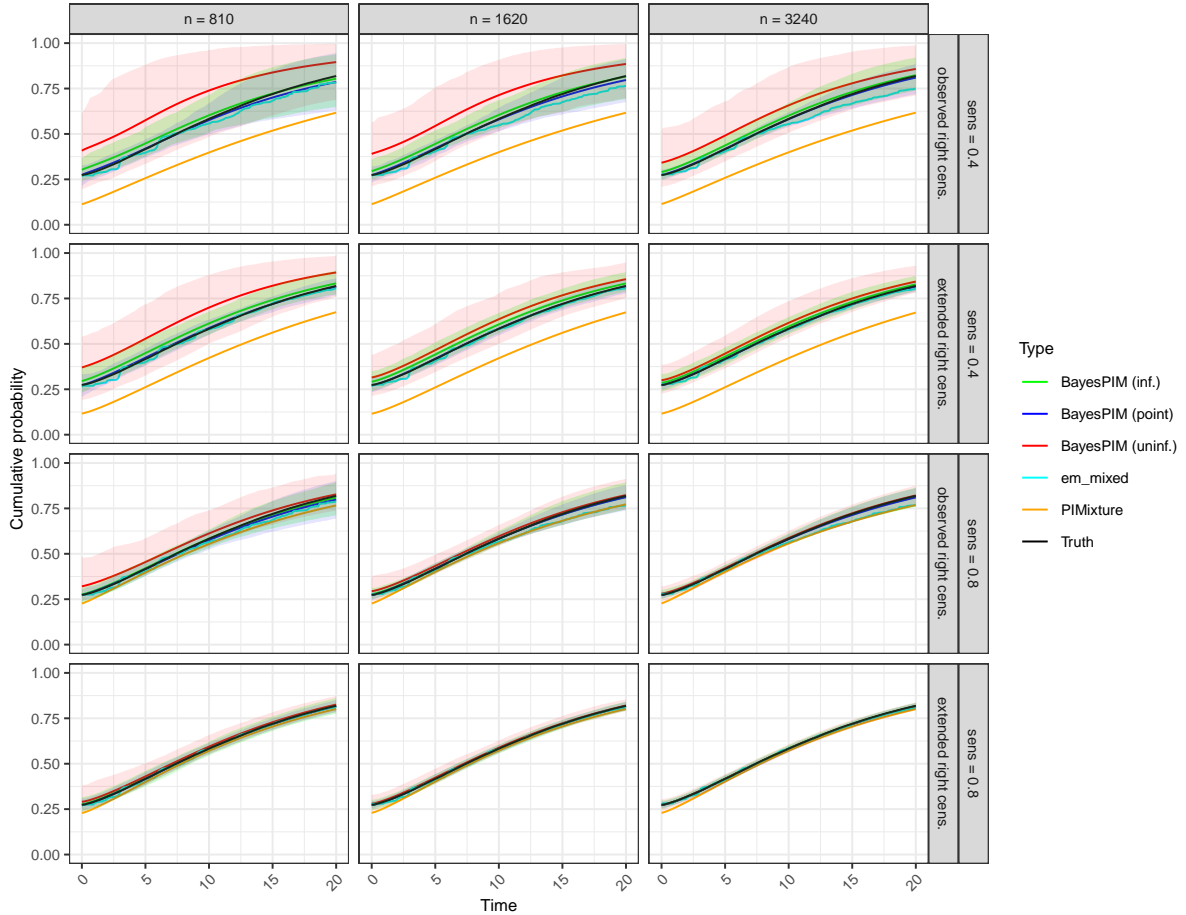


**Figure 5:** Marginal mixture CDFs (27), point-wise averaged over 200 Monte Carlo simulation runs with 95% quantiles shown as shaded regions (for clarity these bounds have been omitted for PIMixture and `em_mixed`). For BayesPIM the posterior median of the posterior predictive CDF (27) is used. For PIMixture and `em_mixed` the corresponding maximum likelihood estimates are used.

screening data that often have a similar structure (section 2).

In estimation, we leveraged a Bayesian Metropolis-within-Gibbs sampler with data augmentation for the latent transition times and the latent prevalence status. Our Bayesian approach facilitates the inclusion of prior information on the model parameters. We have found that weakly informative priors on the incidence and prevalence model parameters (cf. section 4.3) provide effective regularization without biasing the parameter estimates. Arguably, the prior information on  $\beta_x$ , model (1), and  $\beta_w$ , model (2), is scarce in practice, making a weakly informative prior choice an attractive default. Furthermore, we studied the role of the prior on the test sensitivity  $\kappa$  in substantial detail. When a Beta prior is used, updating  $\kappa$  is conjugate (see (17)) and hence fast. However, through simulations we demonstrated that a fully uninformative prior, chosen uniform in  $(0,1)$ , can lead to estimation problems, such as non-convergence, multimodality of the posterior, and bias in  $\kappa$  and other model parameters. Adding some information on  $\kappa$  through a mean-centered prior on the most likely value yielded reliably converging Markov chains and approximately zero bias in the BayesPIM parameter estimates. This included more challenging settings than the one actually observed in the CRC EHR, such as low sensitivity  $\kappa = 0.4$  or the absence of a baseline test ( $\Pr(r_i = 1) = 0$ ). We, therefore, advise the use of informative priors in practice, which is facilitated by the fact that test sensitivity is usually roughly known in cancer screening, as demonstrated for the CRC EHR (section 7). Alterna-

tively, several analyses may be run with a range of fixed  $\kappa$  values, and the model with the highest WAIC given preference. Clearly, if  $\kappa$  is known with high certainty, fixing  $\kappa$  at this value is the best option. These measures are particularly important in small samples or when there is only short follow-up, as in the EHR CRC (Table 1, Supplemental Figure D.1).

Model fit evaluation is an important aspect of modeling with BayesPIM, and we proposed the WAIC as a means to select the best transition times ( $x_i$ ) distribution. In the application, WAIC only slightly favored a Weibull model over the alternative models (lognormal, loglogistic, and exponential). In addition, we adapted the non-parametric estimator `em_mixed`, initially proposed by Witte et al. (2017) for screening data without baseline prevalence but imperfect test sensitivity, to our setting with prevalence. In simulations, `em_mixed` had excellent performance, provided baseline tests were available for a moderate to high proportion of the sample. Hence, the estimator serves as an additional fit assessment in these settings. In the application, the visual comparison of the `em_mixed` CIF to that of BayesPIM was indeed reassuring on model fit. In future work, `em_mixed` might be extended to work well in settings with only a few or no baseline tests.

A strong aspect of our study of the CRC EHR is that we assessed the performance of BayesPIM under the observed screening times and right censoring process (section 7.2). Our results indicated that BayesPIM can reliably estimate the model parameters under that condition ( $n = 810$ ,  $\kappa = 0.8$ , observed right censoring), and also provided good performance in the more challenging setting with  $\kappa = 0.4$ , provided that an informative  $\kappa$  prior was used. Here, we found a small bias in the  $\kappa$  and prevalence estimates, unless  $\kappa$  was set to its true value through a point prior. This finding illustrates the importance of evaluating estimation performance in real-world settings as a supplementary analysis to the data analysis. To this end, Supplemental Material sections D.1 and D.2 explain how to generate screening times from observed screening EHR. This approach could be adopted and refined in future work.

Limitations of BayesPIM currently include the focus on two-parameter survival distributions, the assumption of perfect specificity, and uninformative screening time generation from  $q(v_{ij}|\bar{v}_{ij}, \mathbf{z}_i)$ . Specifically, if transition times strongly deviate from the considered distributions, BayesPIM estimates may be biased. Semi-parametric extensions (e.g., Cox-type transitions) may be considered in the future to make BayesPIM more flexible, but they may require large samples. As noted, the assumption of perfect specificity is plausible for the CRC EHR because colonoscopy is validated by pathology; similar confirmatory tests are common in cancer screening. The assumption of uninformative censoring is also plausible for the CRC EHR, since adenomas are not symptomatic. For pre-state diseases or diseases causing patient-initiated screenings, however, methods need to be developed that address informative censoring (Lange et al., 2015).

In summary, BayesPIM brings a flexible, Bayesian approach to handling latent prevalence and imperfect test sensitivity in screening and surveillance data. By incorporating informative priors, assessing model fit through both parametric and non-parametric approaches, and demonstrating robust performance under realistic conditions, BayesPIM enables more accurate, data-driven, and ultimately patient-centered screening strategies.

## References

- Aastveit, M. E., Cunen, C., and Hjort, N. L. (2023). A new framework for semi-Markovian parametric multi-state models with interval censoring. *Statistical Methods in Medical Research*, 32(6):1100–1123. Publisher: SAGE Publications Ltd STM.
- Albert, J. H. and Chib, S. (1993). Bayesian Analysis of Binary and Polychotomous Response Data. *Journal of the American Statistical Association*, 88(422):669–679.
- Amico, M. and Keilegom, I. V. (2018). Cure Models in Survival Analysis. *Annual Review of Statistics and Its Application*, 5(Volume 5, 2018):311–342. Publisher: Annual Reviews.
- Anderson-Bergman, C. (2017). icenReg: Regression Models for Interval Censored Data in R. *Journal of Statistical Software*, 81:1–23.
- Barone, R. and Tancredi, A. (2022). Bayesian inference for discretely observed continuous time multi-state models. *Statistics in Medicine*, 41(19):3789–3803.
- Boruvka, A. and Cook, R. J. (2015). A Cox-Aalen Model for Interval-censored Data. *Scandinavian Journal of Statistics*, 42(2):414–426.
- Cheung, L. C., Hyun, N., Xiong, X., Pan, Q., and Katki, H. A. (2023). *Package PIMixture*. <https://dceg.cancer.gov/tools/analysis/pimixture/pimixture.pdf>.
- Cheung, L. C., Pan, Q., Hyun, N., Schiffman, M., Fetterman, B., Castle, P. E., Lorey, T., and Katki, H. A. (2017). Mixture models for undiagnosed prevalent disease and interval-censored incident disease: applications to a cohort assembled from electronic health records. *Statistics in Medicine*, 36(22):3583–3595.
- Clarke, M. A., Cheung, L. C., Castle, P. E., Schiffman, M., Tokugawa, D., Poitras, N., Lorey, T., Kinney, W., and Wentzensen, N. (2019). Five-Year Risk of Cervical Precancer Following p16/Ki-67 Dual-Stain Triage of HPV-Positive Women. *JAMA Oncology*, 5(2):181–186.
- Gelman, A., Hwang, J., and Vehtari, A. (2014). Understanding predictive information criteria for Bayesian models. *Statistics and Computing*, 24(6):997–1016.
- Hennink, S. D., van der Meulen-de Jong, A. E., Wolterbeek, R., Crobach, A. S. L., Becx, M. C., Crobach, W. F., van Haastert, M., ten Hove, W. R., Kleibeuker, J. H., Meijssen, M. A., Nagengast, F. M., Rijk, M. C., Salemans, J. M., Stronkhorst, A., Tuynman, H. A., Vecht, J., Verhulst, M.-L., de Vos tot Nederveen Cappel, W. H., Walinga, H., Weinhardt, O. K., Westerveld, D., Witte, A. M., Wolters, H. J., Cats, A., Veenendaal, R. A., Morreau, H., and Vasen, H. F. (2015). Randomized Comparison of Surveillance Intervals in Familial Colorectal Cancer. *Journal of Clinical Oncology*, 33(35):4188–4193.
- Hyun, N., Cheung, L. C., Pan, Q., Schiffman, M., and Katki, H. A. (2017). Flexible risk prediction models for left or interval-censored data from electronic health records. *The Annals of Applied Statistics*, 11(2):1063–1084.
- Hyun, N., Katki, H. A., and Graubard, B. I. (2020). Sample-weighted semiparametric estimation of cause-specific cumulative risk and incidence using left- or interval-censored data from electronic health records. *Statistics in Medicine*, 39(18):2387–2402.
- Jackson, C. (2011). Multi-State Models for Panel Data: The msm Package for R. *Journal of Statistical Software*, 038(i08).

- Jackson, C. H., Sharples, L. D., Thompson, S. G., Duffy, S. W., and Couto, E. (2003). Multistate Markov models for disease progression with classification error. *Journal of the Royal Statistical Society: Series D (The Statistician)*, 52(2):193–209.
- Klausch, T., Akwiwu, E. U., Wiel, M. A. v. d., Coupé, V. M. H., and Berkhof, J. (2023). A Bayesian accelerated failure time model for interval censored three-state screening outcomes. *The Annals of Applied Statistics*, 17(2):1285–1306.
- Lange, J. M., Hubbard, R. A., Inoue, L. Y. T., and Minin, V. N. (2015). A joint model for multistate disease processes and random informative observation times, with applications to electronic medical records data. *Biometrics*, 71(1):90–101.
- Lange, J. M. and Minin, V. N. (2013). Fitting and interpreting continuous-time latent Markov models for panel data. *Statistics in Medicine*, 32(26):4581–4595.
- Little, R. J. A. and Rubin, D. B. (2002). *Statistical analysis with missing data*. Wiley, Hoboken, 2 edition.
- Liu, J. S. (1994). The Collapsed Gibbs Sampler in Bayesian Computations with Applications to a Gene Regulation Problem. *Journal of the American Statistical Association*, 89(427):958–966.
- Luo, Y., Stephens, D. A., Verma, A., and Buckeridge, D. L. (2021). Bayesian latent multi-state modeling for nonequidistant longitudinal electronic health records. *Biometrics*, 77(1):78–90.
- National Cancer Institute (2024). *Prevalence Incidence Mixture Models*. National Cancer Institute. <https://dceg.cancer.gov/tools/analysis/pimixture>.
- Raffa, J. D. and Dubin, J. A. (2015). Multivariate longitudinal data analysis with mixed effects hidden Markov models. *Biometrics*, 71(3):821–831.
- Saraiya, M., Cheung, L. C., Soman, A., Mix, J., Kenney, K., Chen, X., Perkins, R. B., Schiffman, M., Wentzensen, N., and Miller, J. (2021). Risk of cervical precancer and cancer among uninsured and underserved women from 2009 to 2017. *American Journal of Obstetrics and Gynecology*, 224(4):366.e1–366.e32.
- Turnbull, B. W. (1976). The Empirical Distribution Function with Arbitrarily Grouped, Censored and Truncated Data. *Journal of the Royal Statistical Society: Series B (Methodological)*, 38(3):290–295.
- Witte, B. I., Berkhof, J., and Jonker, M. A. (2017). An EM algorithm for nonparametric estimation of the cumulative incidence function from repeated imperfect test results. *Statistics in Medicine*, 36(21):3412–3421.

**Supplemental Material to**  
**”A Bayesian prevalence-incidence mixture model**  
**for screening outcomes with misclassification”**

by Thomas Klausch & Veerle Coupé



## A Proofs

### A.1 Observed data likelihood

To derive the observed data likelihood (11) we note that the data are comprised by the set  $\mathcal{D} = \{\mathbf{c}, \mathbf{r}, \mathbb{V}, \mathbf{Z}\}$ . Treating the covariates  $\mathbf{Z}$  as fixed, the observed data likelihood can be written as

$$\mathcal{L}(\boldsymbol{\theta} | \mathcal{D}) = \prod_{i=1}^n q(c_i, r_i, \mathbf{v}_i | \boldsymbol{\theta}, \mathbf{z}_i).$$

Hence we need to derive  $q(c_i, r_i, \mathbf{v}_i | \boldsymbol{\theta}, \mathbf{z}_i)$ , i.e.

$$\begin{aligned} q(c_i, r_i, \mathbf{v}_i | \boldsymbol{\theta}, \mathbf{z}_i) &= \sum_{k=0}^1 \int_0^\infty \int_{-\infty}^\infty q(g_i = k, w_i, x_i, \boldsymbol{\theta}, c_i, r_i, \mathbf{v}_i | \mathbf{z}_i) \pi(\boldsymbol{\theta})^{-1} dw_i dx_i \\ &= \sum_{k=0}^1 \left[ \int_{-\infty}^\infty \Pr(g_i = k | w_i) q(w_i | \boldsymbol{\beta}_w, \mathbf{z}_{wi}) dw_i \right. \\ &\quad \left. \times \int_0^\infty q(\mathbf{v}_i, c_i | g_i, x_i, \kappa, r_i) f_x(x_i | \boldsymbol{\beta}_x, \sigma, \mathbf{z}_{xi}) dx_i \right] \Pr(r_i = 1 | \mathbf{z}_i) \\ &= \sum_{k=0}^1 \left[ \int_{-\infty}^\infty \Pr(g_i = k | w_i) q(w_i | \boldsymbol{\beta}_w, \mathbf{z}_{wi}) dw_i \right. \\ &\quad \left. \times \int_0^\infty \Pr(\tilde{c}_i = c_i | g_i, x_i, \kappa, r_i, \mathbf{v}_i) f_x(x_i | \boldsymbol{\beta}_x, \sigma, \mathbf{z}_{xi}) dx_i \right] q(\mathbf{v}_i | \mathbf{z}_i) \Pr(r_i = 1 | \mathbf{z}_i) \\ &\propto \sum_{k=0}^1 \left[ \int_{-\infty}^\infty \Pr(g_i = k | w_i) q(w_i | \boldsymbol{\beta}_w, \mathbf{z}_{wi}) dw_i \right. \\ &\quad \left. \times \int_0^\infty \Pr(\tilde{c}_i = c_i | g_i = k, x_i, \kappa, r_i, \mathbf{v}_i) f_x(x_i | \boldsymbol{\beta}_x, \sigma, \mathbf{z}_{xi}) dx_i \right] \end{aligned} \quad (\text{S-1})$$

where  $q(\mathbf{v}_i | \mathbf{z}_i)$  and  $\Pr(\tilde{c}_i = c_i | g_i = k, x_i, \kappa, r_i, \mathbf{v}_i)$  are defined in (7), (9), and (10). Since the likelihood is proportional to  $q(\mathbf{v}_i | \mathbf{z}_i) \Pr(r_i | \mathbf{z}_i)$ , we do not need to parameterize these terms. The first factor in the last equation of (S-1) simplifies as

$$\begin{aligned} \int_{-\infty}^\infty \Pr(g_i = k | w_i) q(w_i | \boldsymbol{\beta}_w, \mathbf{z}_{wi}) dw_i &= \begin{cases} \int_{-\infty}^\infty \mathbb{1}_{\{w_i > 0\}} \phi(w_i | \mathbf{z}'_{wi} \boldsymbol{\beta}_w, 1) dw_i & \text{if } k = 1 \\ \int_{-\infty}^\infty \mathbb{1}_{\{w_i \leq 0\}} \phi(w_i | \mathbf{z}'_{wi} \boldsymbol{\beta}_w, 1) dw_i & \text{if } k = 0 \end{cases} \\ &= \Phi(\mathbf{z}'_{wi} \boldsymbol{\beta}_w)^k (1 - \Phi(\mathbf{z}'_{wi} \boldsymbol{\beta}_w))^{(1-k)}, \end{aligned}$$

where  $\phi(w_i | \mu, 1)$  denotes the normal density function with mean  $\mu$  and variance one, and  $\Phi$  denotes the standard normal distribution function. Furthermore, the second factor, if  $g_i = 0$  and  $c_i > 1$ , evaluates to

$$\begin{aligned} &\int_0^\infty \Pr(\tilde{c}_i = c_i | g_i = 0, x_i, \kappa, r_i, \mathbf{v}_i) f_x(x_i | \boldsymbol{\beta}_x, \sigma, \mathbf{z}_{xi}) dx_i \\ &= \int_0^\infty \sum_{j=1}^{c_i-1} \kappa^{\rho_i} (1 - \kappa)^{j-1} \mathbb{1}_{\{v_{ic_i-j} < x_i \leq v_{ic_i-j+1}\}} f_x(x_i | \boldsymbol{\beta}_x, \sigma, \mathbf{z}_{xi}) dx_i \\ &= \sum_{j=1}^{c_i-1} \kappa^{\rho_i} (1 - \kappa)^{j-1} \int_{v_{ic_i-j}}^{v_{ic_i-j+1}} f_x(x_i | \boldsymbol{\beta}_x, \sigma, \mathbf{z}_{xi}) dx_i \\ &= \sum_{j=1}^{c_i-1} \kappa^{\rho_i} (1 - \kappa)^{j-1} [F_x(v_{ic_i-j+1} | \boldsymbol{\beta}_x, \sigma, \mathbf{z}_{xi}) - F_x(v_{ic_i-j} | \boldsymbol{\beta}_x, \sigma, \mathbf{z}_{xi})], \end{aligned}$$

and it evaluates to 0 if  $c_i = 1$  instead.

Similarly, if  $g_i = 1$ ,

$$\begin{aligned} & \int_0^\infty \Pr(\tilde{c}_i = c_i | g_i = 1, x_i, \kappa, r_i, \mathbf{v}_i) f_x(x_i | \boldsymbol{\beta}_x, \sigma, \mathbf{z}_{xi}) dx_i \\ &= \begin{cases} \int_0^\infty \kappa^{\rho_i} (1 - \kappa)^{c_i - 2} \mathbf{1}_{\{c_i > 1\}} f_x(x_i | \boldsymbol{\beta}_x, \sigma, \mathbf{z}_{xi}) dx_i & \text{if } r_i = 0 \\ \int_0^\infty \kappa^{\rho_i} (1 - \kappa)^{c_i - 1} f_x(x_i | \boldsymbol{\beta}_x, \sigma, \mathbf{z}_{xi}) dx_i & \text{if } r_i = 1, \end{cases} \\ &= \kappa^{\rho_i} (1 - \kappa)^{c_i - 2 + r_i}. \end{aligned}$$

The last equation follows because  $x_i$  integrates out and  $c_i = 1$  cannot occur when  $r_i = 0$  due to the censoring mechanism defined in (10). Bringing the above elements together we have

$$\begin{aligned} q(c_i, r_i, \mathbf{v}_i | \boldsymbol{\theta}, \mathbf{z}_i) &\propto \left[ (1 - \Phi(\mathbf{z}'_{wi} \boldsymbol{\beta}_w)) \left[ \sum_{j=1}^{c_i - 1} \kappa^{\rho_i} (1 - \kappa)^{j-1} (F_x(v_{ic_i - j + 1} | \mathbf{z}_x, \beta_x, \sigma) - F_x(v_{ic_i - j} | \mathbf{z}_x, \beta_x, \sigma)) \right] \right. \\ &\quad \left. + \Phi(\mathbf{z}'_{wi} \boldsymbol{\beta}_w) \kappa^{\rho_i} (1 - \kappa)^{c_i - 2 + r_i} \right] \quad \text{if } c_i > 1 \end{aligned}$$

and

$$q(c_i, r_i, \mathbf{v}_i | \boldsymbol{\theta}, \mathbf{z}_i) \propto \Phi(\mathbf{z}'_{wi} \boldsymbol{\beta}_w) \kappa^{\rho_i} \quad \text{if } c_i = 1,$$

so that the likelihood is

$$\begin{aligned} \mathcal{L}(\boldsymbol{\theta} | \mathcal{D}) &\propto \left[ \prod_{i:c_i > 1} (1 - \Phi(\mathbf{z}'_{wi} \boldsymbol{\beta}_w)) \left[ \sum_{j=1}^{c_i - 1} \kappa^{\rho_i} (1 - \kappa)^{j-1} (F_x(v_{ic_i - j + 1} | \mathbf{z}_x, \beta_x, \sigma) - F_x(v_{ic_i - j} | \mathbf{z}_x, \beta_x, \sigma)) \right] \right. \\ &\quad \left. + \Phi(\mathbf{z}'_{wi} \boldsymbol{\beta}_w) \kappa^{\rho_i} (1 - \kappa)^{c_i - 2 + r_i} \right] + \prod_{i:c_i = 1} \Phi(\mathbf{z}'_{wi} \boldsymbol{\beta}_w) \kappa^{\rho_i}. \end{aligned}$$

## A.2 Full conditional distribution of $x_i$

Here we derive the full conditional distribution of  $x_i$ . We first consider the non-prevalent case ( $g_i = 0$ ) in (12), i.e. if  $c_i > 1$ ,

$$\begin{aligned} q(x_i | g_i = 0, w_i, \boldsymbol{\theta}, \mathcal{D}) &\propto \Pr(\tilde{c}_i = c_i | g_i = 0, x_i, \kappa, r_i, \mathbf{v}_i) f_x(x_i | \boldsymbol{\beta}_x, \sigma, \mathbf{z}_{xi}) \Pr(g_i = 0 | w_i) q(w_i | \boldsymbol{\beta}_w, \mathbf{z}_{wi}) \\ &\quad \times q(\mathbf{v}_i | \mathbf{z}_i) \Pr(r_i = 1 | \mathbf{z}_i) \pi(\boldsymbol{\theta}) \\ &\propto \Pr(\tilde{c}_i = c_i | g_i = 0, x_i, \kappa, r_i, \mathbf{v}_i) f_x(x_i | \boldsymbol{\beta}_x, \sigma, \mathbf{z}_{xi}) \\ &= \sum_{j=1}^{c_i - 1} \kappa^{\rho_i} (1 - \kappa)^{j-1} \mathbf{1}_{\{v_{ic_i - j} < x_i \leq v_{ic_i - j + 1}\}} f_x(x_i | \boldsymbol{\beta}_x, \sigma, \mathbf{z}_{xi}) \\ &= \sum_{j=1}^{c_i - 1} f_x(x_i | v_{ic_i - j} < x_i \leq v_{ic_i - j + 1}, \boldsymbol{\beta}_x, \sigma, \mathbf{z}_{xi}) \\ &\quad \times [F_x(v_{ic_i - j + 1} | \boldsymbol{\beta}_x, \sigma, \mathbf{z}_{xi}) - F_x(v_{ic_i - j} | \boldsymbol{\beta}_x, \sigma, \mathbf{z}_{xi})] \kappa^{\rho_i} (1 - \kappa)^{j-1} \\ &= \sum_{j=1}^{c_i - 1} \omega_{ij} f_x(x_i | v_{ic_i - j} < x_i \leq v_{ic_i - j + 1}, \boldsymbol{\beta}_x, \sigma, \mathbf{z}_{xi}). \end{aligned}$$

The first equation follows from the factorization of the joint likelihood into the data generating densities and by applying the result in (7). The second equation follows due to independence of various terms from  $x_i$ . The third equation applies definition 9. The fourth equation uses the fact

that  $\mathbb{1}_{\{v_{ic_i-j} < x_i \leq v_{ic_i-j+1}\}} f_x(x_i | \boldsymbol{\beta}_x, \sigma, \mathbf{z}_{xi})$  is an unnormalized truncated distribution. The last three terms can then be recognized as the weights of an unnormalized mixture distribution of  $x_i$ , as shown by the fifth equation. After normalizing the weights, the result in (12) is obtained. Finally, in the prevalent case, when  $g_i = 1$ , we have

$$q(x_i | g_i = 0, w_i, \boldsymbol{\theta}, \mathcal{D}) \propto f_x(x_i | \boldsymbol{\beta}_x, \sigma, \mathbf{z}_{xi}) \kappa^{\rho_i} (1 - \kappa)^{c_i - 2 + r_i} \propto f_x(x_i | \boldsymbol{\beta}_x, \sigma, \mathbf{z}_{xi}),$$

irrespective of  $r_i = 0$  or  $r_i = 1$ .

### A.3 Compound conditional distribution of $g_i$

We start by noting that the full conditional distribution of  $g_i$  is degenerate. We have

$$\begin{aligned} \Pr(g_i | w_i, x_i, \boldsymbol{\theta}, \mathcal{D}) &\propto \Pr(\tilde{c}_i = c_i | g_i = 0, x_i, \kappa, r_i, \mathbf{v}_i) f_x(x_i | \boldsymbol{\beta}_x, \sigma, \mathbf{z}_{xi}) \Pr(g_i = 0 | w_i) q(w_i | \boldsymbol{\beta}_w, \mathbf{z}_{wi}) \\ &\quad \times q(\mathbf{v}_i | \mathbf{z}_i) \Pr(r_i = 1 | \mathbf{z}_i) \pi(\boldsymbol{\theta}) \\ &\propto \Pr(\tilde{c}_i = c_i | g_i, x_i, \kappa, r_i, \mathbf{v}_i) \Pr(g_i | w_i). \end{aligned}$$

It follows, after normalization, that

$$\begin{aligned} \Pr(g_i = 1 | w_i, x_i, \boldsymbol{\theta}, \mathcal{D}) &= \frac{\Pr(\tilde{c}_i = c_i | g_i = 1, x_i, \kappa, r_i, \mathbf{v}_i) \mathbb{1}_{\{w_i > 0\}}}{\Pr(\tilde{c}_i = c_i | x_i, g_i = 0, \kappa, r_i, \mathbf{v}_i) \mathbb{1}_{\{w_i \leq 0\}} + \Pr(\tilde{c}_i = c_i | g_i = 1, x_i, \kappa, r_i, \mathbf{v}_i) \mathbb{1}_{\{w_i > 0\}}} \\ &= \begin{cases} 1 & \text{if } w_i > 0 \\ 0 & \text{if } w_i \leq 0. \end{cases} \end{aligned}$$

Clearly, the full conditional distribution is independent of the data, so that a Gibbs sampler using a fully conditional updating step does not converge. Therefore, we apply a collapsed updating step. First, we integrate over the latent propensities  $w_i$  to obtain (21). Specifically,

$$\begin{aligned} \Pr(g_i | x_i, \boldsymbol{\theta}, \mathcal{D}) &\propto \int_{-\infty}^{\infty} \Pr(\tilde{c}_i = c_i | g_i = 0, x_i, \kappa, r_i, \mathbf{v}_i) f_x(x_i | \boldsymbol{\beta}_x, \sigma, \mathbf{z}_{xi}) \Pr(g_i = 0 | w_i) q(w_i | \boldsymbol{\beta}_w, \mathbf{z}_{wi}) \\ &\quad \times q(\mathbf{v}_i | \mathbf{z}_i) \Pr(r_i = 1 | \mathbf{z}_i) \pi(\boldsymbol{\theta}) dw_i \\ &\propto \Pr(\tilde{c}_i = c_i | g_i, x_i, \kappa, r_i, \mathbf{v}_i) \int_{-\infty}^{\infty} \Pr(g_i | w_i) q(w_i | \boldsymbol{\beta}_w, \mathbf{z}_{wi}) dw_i \\ &= \begin{cases} \Pr(\tilde{c}_i = c_i | g_i = 0, x_i, \kappa, r_i, \mathbf{v}_i) (1 - \Phi(\mathbf{z}'_{wi} \boldsymbol{\beta}_w)) & \text{if } g_i = 0 \\ \Pr(\tilde{c}_i = c_i | g_i = 1, x_i, \kappa, r_i, \mathbf{v}_i) \Phi(\mathbf{z}'_{wi} \boldsymbol{\beta}_w) & \text{if } g_i = 1. \end{cases} \end{aligned}$$

Hence,

$$\begin{aligned} \Pr(g_i = 1 | x_i, \boldsymbol{\theta}, \mathcal{D}) &= \frac{\Phi(\mathbf{z}'_{wi} \boldsymbol{\beta}_w) \Pr(\tilde{c}_i = c_i | g_i = 1, x_i, \kappa, r_i, \mathbf{v}_i)}{\Phi(\mathbf{z}'_{wi} \boldsymbol{\beta}_w) \Pr(\tilde{c}_i = c_i | g_i = 1, x_i, \kappa, r_i, \mathbf{v}_i) + (1 - \Phi(\mathbf{z}'_{wi} \boldsymbol{\beta}_w)) \Pr(\tilde{c}_i = c_i | g_i = 0, x_i, \kappa, r_i, \mathbf{v}_i)}. \end{aligned}$$

Second, we integrate additionally over the latent times  $x_i$  to obtain (22)

$$\begin{aligned} \Pr(g_i | \boldsymbol{\theta}, \mathcal{D}) &\propto \left[ \int_{-\infty}^{\infty} \Pr(g_i | w_i) q(w_i | \boldsymbol{\beta}_w, \mathbf{z}_{wi}) dw_i \right] \\ &\quad \times \int_0^{\infty} \Pr(\tilde{c}_i = c_i | g_i, x_i, \kappa, r_i, \mathbf{v}_i) f_x(x_i | \boldsymbol{\beta}_x, \sigma, \mathbf{z}_{xi}) dx_i \end{aligned}$$

Hence, if  $g_i = 1$ ,

$$\begin{aligned} \Pr(g_i = 1 | \boldsymbol{\theta}, \mathcal{D}) &\propto \Phi(\mathbf{z}'_{wi} \boldsymbol{\beta}_w) \int_0^\infty \sum_{j=1}^{c_i-1} \kappa^{\rho_i} (1 - \kappa)^{j-1} \mathbb{1}_{\{v_{ic_i-j} < x_i \leq v_{ic_i-j+1}\}} f_x(x_i | \boldsymbol{\beta}_x, \sigma, \mathbf{z}_{xi}) dx_i \\ &= \Phi(\mathbf{z}'_{wi} \boldsymbol{\beta}_w) \sum_{j=1}^{c_i-1} \kappa^{\rho_i} (1 - \kappa)^{j-1} [F_x(v_{ic_i-j+1} | \boldsymbol{\beta}_x, \sigma, \mathbf{z}_{xi}) - F_x(v_{ic_i-j} | \boldsymbol{\beta}_x, \sigma, \mathbf{z}_{xi})] \\ &= \Phi(\mathbf{z}'_{wi} \boldsymbol{\beta}_w) \sum_{j=1}^{c_i-1} \omega_{ij} \end{aligned}$$

and, if  $g_i = 0$ ,

$$\begin{aligned} \Pr(g_i = 0 | \boldsymbol{\theta}, \mathcal{D}) &\propto \left[ 1 - \Phi(\mathbf{z}'_{wi} \boldsymbol{\beta}_w) \right] \int_0^\infty \kappa^{\rho_i} (1 - \kappa)^{c_i-2+r_i} f_x(x_i | \boldsymbol{\beta}_x, \sigma, \mathbf{z}_{xi}) dx_i \\ &= \left[ 1 - \Phi(\mathbf{z}'_{wi} \boldsymbol{\beta}_w) \right] \kappa^{\rho_i} (1 - \kappa)^{c_i-2+r_i} \end{aligned}$$

so that after normalization

$$\Pr(g_i = 1 | \boldsymbol{\theta}, \mathcal{D}) = \frac{\Phi(\mathbf{z}'_{wi} \boldsymbol{\beta}_w) \sum_{j=1}^{c_i-1} \omega_{ij}}{\left[ 1 - \Phi(\mathbf{z}'_{wi} \boldsymbol{\beta}_w) \right] \kappa^{\rho_i} (1 - \kappa)^{c_i-2+r_i} + \Phi(\mathbf{z}'_{wi} \boldsymbol{\beta}_w) \sum_{j=1}^{c_i-1} \omega_{ij}}.$$

#### A.4 Sampling from the posterior predictive CIFs

We draw inference on the conditional CIF of  $x_i$  in the non-prevalent population stratum,  $F_x(x_i | g_i = 0, \boldsymbol{\beta}_x, \sigma, \mathbf{z}_i)$ . To do so after observing the data, we calculate the posterior predictive probability that a newly sampled observation has an event on or before time  $x$  given new covariates  $\tilde{\mathbf{z}}$ ,

$$\Pr(\tilde{x} \leq x | \tilde{g} = 0, \tilde{\mathbf{z}}, \mathcal{D}) = F_x(\tilde{x} | \tilde{g} = 0, \tilde{\mathbf{z}}, \mathcal{D}) = \int_0^\infty \int_{\Theta_x} F_x(\tilde{x} | \tilde{g} = 0, \boldsymbol{\beta}_x, \sigma_x, \tilde{\mathbf{z}}) q(\boldsymbol{\beta}_x, \sigma_x | \mathcal{D}) d\boldsymbol{\beta}_x d\sigma, \quad (\text{S-2})$$

where  $\Theta_x = \{\boldsymbol{\beta}_x \in \mathbb{R}^{p_x}\}$ . This is the posterior predictive CIF, conditional on  $\tilde{\mathbf{z}}$ . To sample from (S-2) we use the MCMC samples  $\boldsymbol{\theta}^{(t)}$  generated by the Gibbs sampler (12)-(17). Specifically, we can use the push forward transform  $F_x(\tilde{x} | \tilde{g} = 0, \boldsymbol{\beta}_x^{(t)}, \sigma^{(t)}, \tilde{\mathbf{z}})$  because  $F_x$  has closed form. Alternatively, we may sample  $\tilde{x}_k^{(t)} \sim f_x(\tilde{x} | \tilde{g} = 0, \boldsymbol{\beta}_x^{(t)}, \sigma^{(t)}, \tilde{\mathbf{z}})$  according to model (1) a large number of times  $K$ .  $F_x(\tilde{x} | \tilde{g} = 0, \boldsymbol{\beta}_x^{(t)}, \sigma^{(t)}, \tilde{\mathbf{z}})$  is then found by the proportion of  $\tilde{x}_1^{(t)}, \dots, \tilde{x}_K^{(t)}$  smaller than  $\tilde{x}$ .

Furthermore, we consider the case where we partially or fully marginalize over the empirical distribution of the covariates  $q_{\mathbf{z}}(\mathbf{z})$  to draw inference on  $F_x(x_i | g_i = 0, \boldsymbol{\beta}_x, \sigma)$ . The marginal posterior predictive CIF is

$$\begin{aligned} \Pr(\tilde{x} \leq x | \tilde{g} = 0, \mathcal{D}) &= F_x(\tilde{x} | \tilde{g} = 0, \mathcal{D}) \\ &= \int_{\Theta_z} \int_0^\infty \int_{\Theta_x} F_x(\tilde{x} | \tilde{g} = 0, \boldsymbol{\beta}_x, \sigma, \mathbf{z}) q(\boldsymbol{\beta}_x, \sigma | \mathcal{D}) q_{\mathbf{z}}(\mathbf{z}) d\boldsymbol{\beta}_x, d\sigma d\mathbf{z}, \end{aligned}$$

where  $\Theta_z$  denotes the support of the covariate space. We use empirical Monte Carlo integration for the integration over  $\mathbf{z}$ . For all  $i = 1, \dots, n$  and given  $\boldsymbol{\theta}^{(t)}$  we sample  $x_i^{(t)} \sim f_x(\tilde{x} | \tilde{g} = 0, \boldsymbol{\beta}_x^{(t)}, \sigma^{(t)}, \mathbf{z}_i)$ . The percentile  $F_x(\tilde{x} | \tilde{g} = 0, \boldsymbol{\beta}_x^{(t)}, \sigma^{(t)})$  is then obtained by the proportion of

$\tilde{x}_1^{(t)}, \dots, \tilde{x}_n^{(t)}$  smaller than  $\tilde{x}$ . Furthermore, often we want to marginalize over a subset  $\mathbf{z}_s$  of  $\mathbf{z}$  while fixing the remaining elements to new values. Specifically, after partitioning  $\mathbf{z} = (\mathbf{z}_s, \mathbf{z}_c)$ , i.e. subset  $\mathbf{z}_s$  and its complement  $\mathbf{z}_c$ , we fix  $\mathbf{z}_c$  at  $\tilde{\mathbf{z}}_c$  while integrating over  $\mathbf{z}_s$ . The Monte Carlo integration is then achieved by sampling  $\tilde{x}_i^{(t)} \sim f_x(\tilde{x}|\tilde{g} = 0, \boldsymbol{\beta}_x^{(t)}, \sigma^{(t)}, \mathbf{z}_{si}, \tilde{\mathbf{z}}_c)$  and obtaining the percentile  $F_x(\tilde{x}|\tilde{g} = 0, \boldsymbol{\beta}_x^{(t)}, \sigma^{(t)}, \tilde{\mathbf{z}}_c)$ , through the proportion of  $\tilde{x}_1^{(t)}, \dots, \tilde{x}_n^{(t)}$  smaller than  $\tilde{x}$ .

In addition, we want to estimate the conditional and marginal CIF of the mixture distribution implied by  $x^*$  defined in (4), i.e.  $F_{x^*}(x^*|\boldsymbol{\beta}, \sigma, \tilde{\mathbf{z}})$  and  $F_{x^*}(x^*|\boldsymbol{\beta}, \sigma)$ . The posterior predictive conditional CIF is

$$\begin{aligned} F_{\tilde{x}^*}(\tilde{x}^*|\tilde{\mathbf{z}}, \mathcal{D}) &= \int_{\Theta_w} \int_0^\infty \int_{\Theta_x} F_{\tilde{x}^*}(\tilde{x}^*|\boldsymbol{\beta}, \sigma, \tilde{\mathbf{z}}, \mathcal{D}) q(\boldsymbol{\beta}, \sigma | \mathcal{D}) d\boldsymbol{\beta} d\sigma d\boldsymbol{\beta}_w \\ &= \int_{\Theta_w} \left[ \Phi(\tilde{\mathbf{z}}' \boldsymbol{\beta}_w) + (1 - \Phi(\tilde{\mathbf{z}}' \boldsymbol{\beta}_w)) F_x(\tilde{x}|\tilde{g} = 0, \tilde{\mathbf{z}}, \mathcal{D}) \right] q(\boldsymbol{\beta}_w | \mathcal{D}) d\boldsymbol{\beta}_w, \end{aligned} \quad (\text{S-3})$$

where  $\Theta_w = \{\boldsymbol{\beta}_w \in \mathbb{R}^{p_w}\}$ . To sample from (S-3) we first draw  $g_k^{(t)} \sim \text{Bernoulli}(\Phi(\tilde{\mathbf{z}}' \boldsymbol{\beta}_w^{(t)}))$ . Subsequently, we set  $\tilde{x}_k^{*(t)} = 0$  if  $g_k^{(t)} = 1$  or we draw  $\tilde{x}_k^{*(t)} \sim f_x(\tilde{x}|\tilde{g} = 0, \boldsymbol{\beta}_x^{(t)}, \sigma^{(t)}, \tilde{\mathbf{z}})$  if  $g_k^{(t)} = 0$ . As before, we repeat for a large number of times  $K$  and find  $F_{\tilde{x}^*}(\tilde{x}^*|\boldsymbol{\beta}^{(t)}, \sigma^{(t)}, \tilde{\mathbf{z}}, \mathcal{D})$  by the proportion of  $\tilde{x}_1^{*(t)}, \dots, \tilde{x}_K^{*(t)}$  smaller than  $\tilde{x}^*$ . Finally, we use again empirical Monte Carlo integration over  $\mathbf{z}$ , as explained above, to obtain the marginal posterior predictive mixture CIF

$$F_{\tilde{x}^*}(\tilde{x}^*|\mathcal{D}) = \int_{\Theta_z} F_{\tilde{x}^*}(\tilde{x}^*|\tilde{\mathbf{z}}, \mathcal{D}) q_{\mathbf{z}}(\mathbf{z}) d\mathbf{z}.$$

## B Additional results from simulation 1

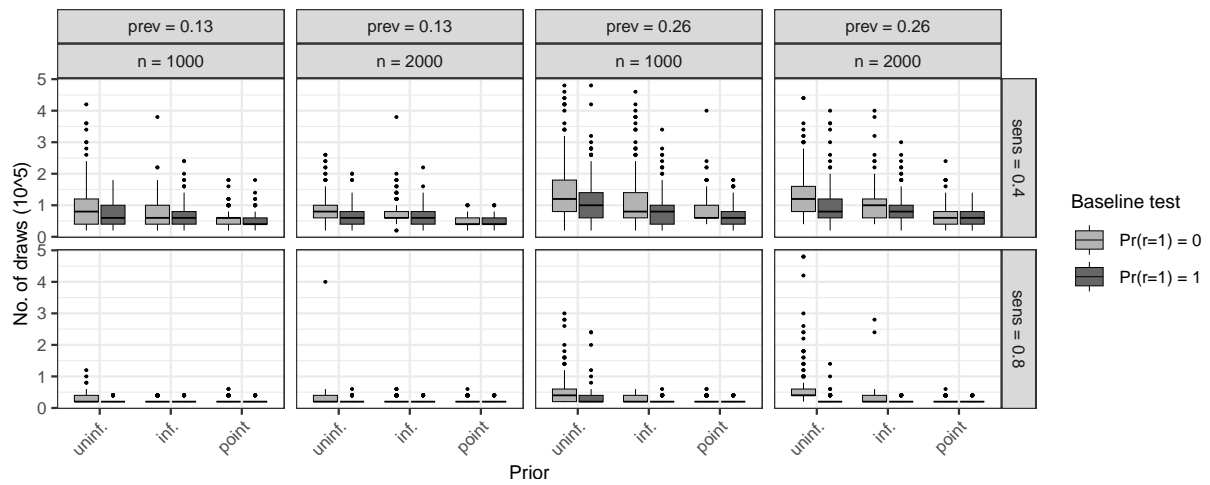


**Figure B.1:** Number of posterior draws until convergence including burn-in (scaled by  $10^5$ ) by simulation conditions. Convergence was evaluated every  $2 \times 10^5$  draws. Abbreviations *prev* and *sens* denote, respectively, the prevalence probability  $\Pr(g_i = 1)$  and the test sensitivity  $\kappa$ . The priors on the test sensitivity  $\kappa$  are either uninformative (*uninf.*), informative (*inf.*) or fixed at the true value (*point*).

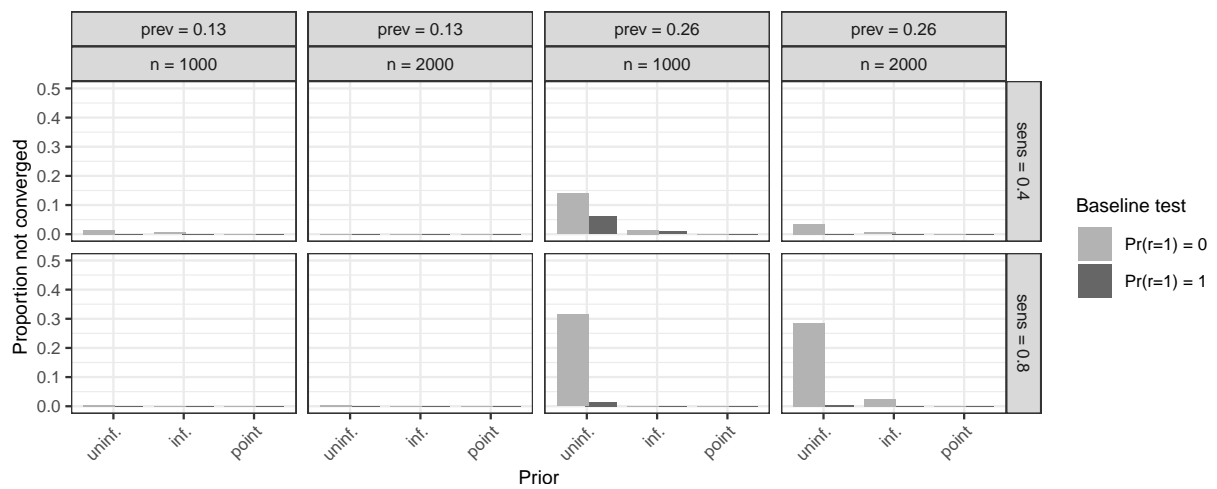


**Figure B.2:** Proportion of runs that did not converge per simulation condition. Convergence was evaluated every  $2 \times 10^5$  draws. Abbreviations *prev* and *sens* denote, respectively, the prevalence probability  $\Pr(g_i = 1)$  and the test sensitivity  $\kappa$ . The priors on the test sensitivity  $\kappa$  are either uninformative (*uninf.*), informative (*inf.*) or fixed at the true value (*point*).

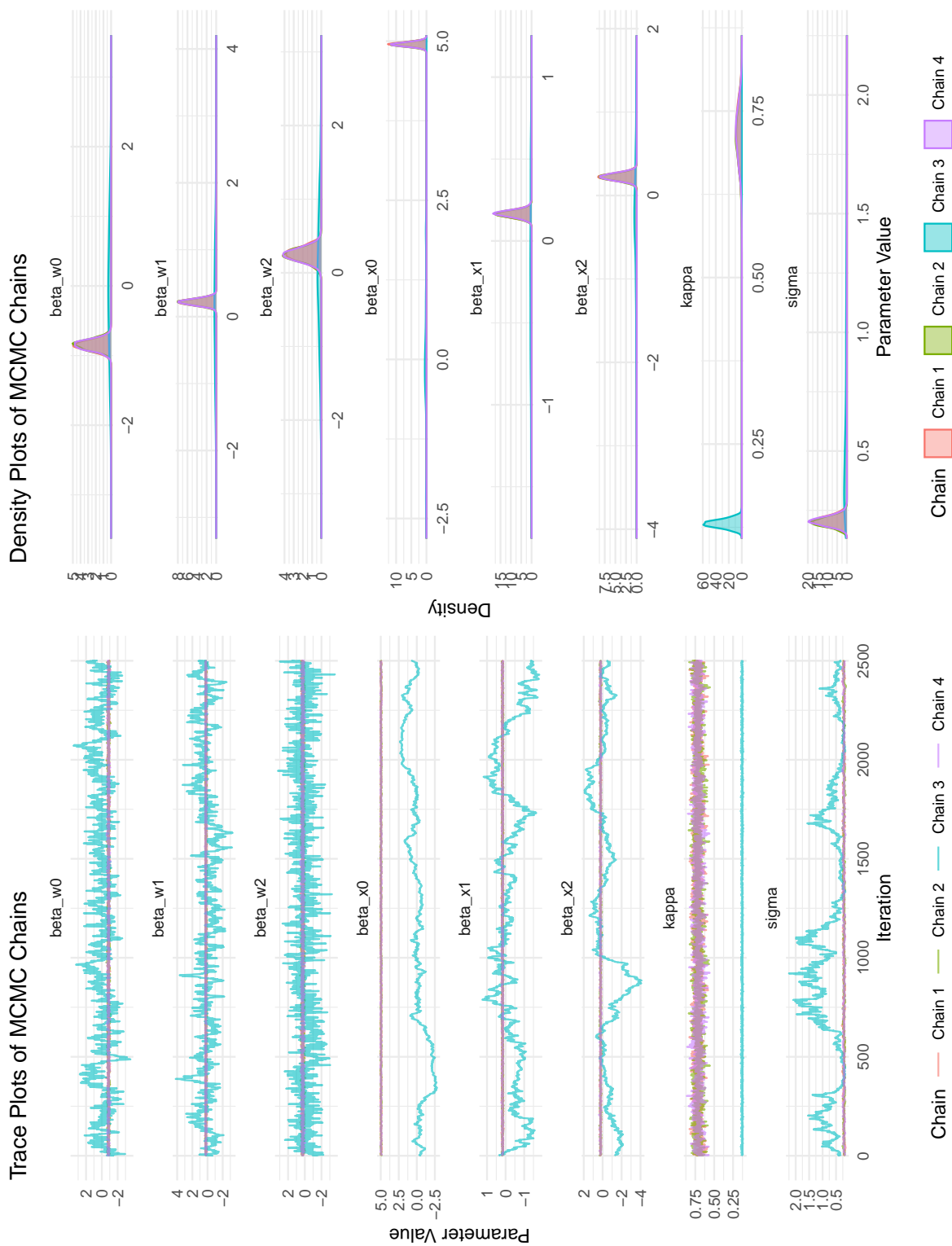


**Figure B.3:** Example of the MCMC chains resulting from a non-convergent run on a data set from simulation 1 ( $n = 1000$ ,  $\Pr(r_i = 1) = 1$ ,  $\text{prev.} = .26$ ,  $\kappa = .80$ , uninformative prior on  $\kappa$ ). The Gibbs sampler finds a local posterior mode in chain 2 centered around an incorrect, very low  $\kappa$  estimate. Chains are thinned with an interlace rate of 200 between draws ( $5 \times 10^5$  draws in total, of which half are discarded for burn-in).



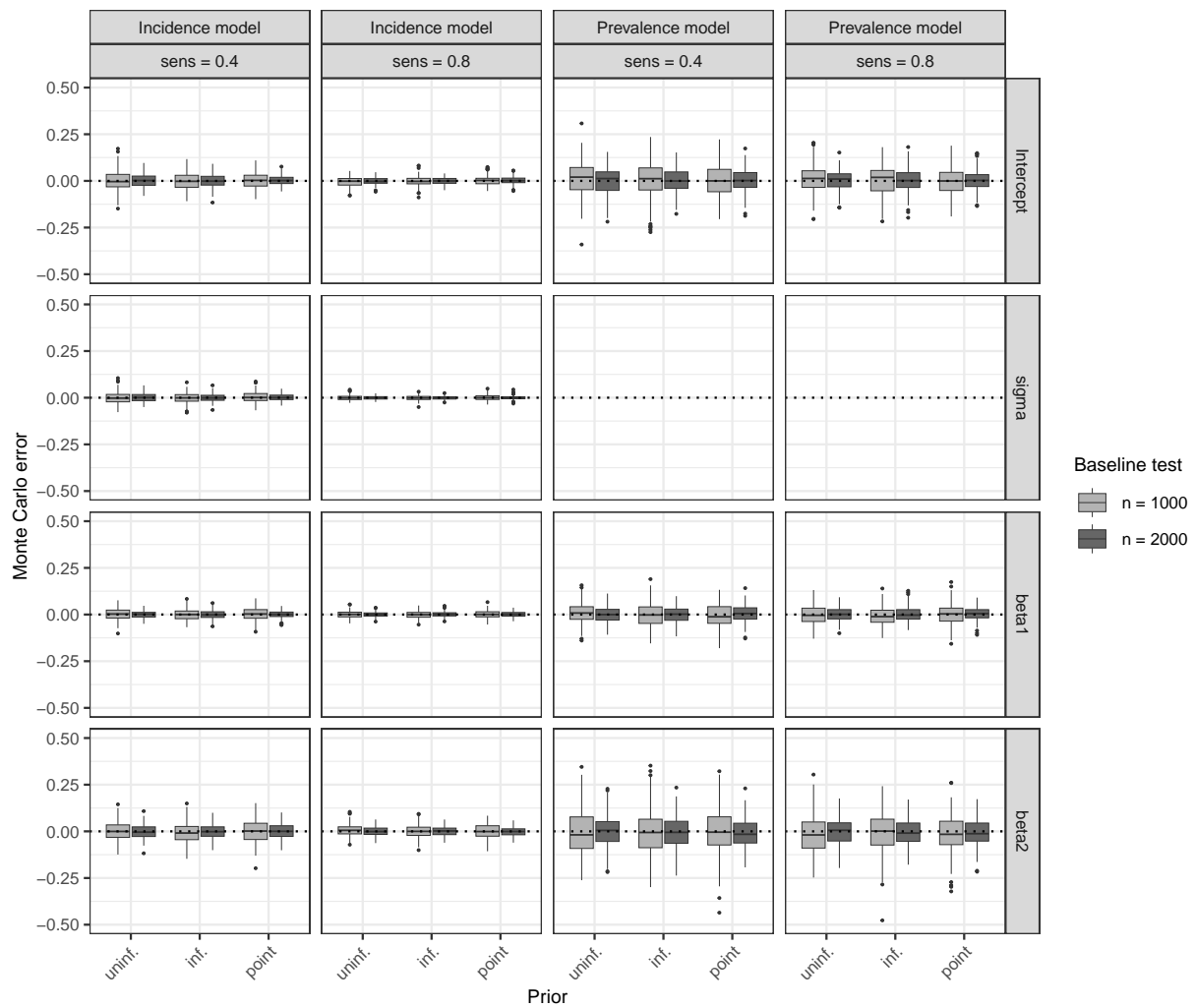


**Figure B.4:** Monte Carlo error of the model parameters, as indicated on the right, for both the incidence model (1) and the prevalence model (2) in the simulation condition:  $\Pr(g_i = 1) = 0.13$ ,  $\Pr(r_i = 1) = 1$ . Note that there is no  $\sigma$  parameter in the prevalence model and hence the corresponding panels are left blank. Abbreviations prev and sens denote, respectively, the prevalence probability  $\Pr(g_i = 1)$  and the test sensitivity  $\kappa$ . The priors on the test sensitivity  $\kappa$  are either uninformative (uninf.), informative (inf.) or fixed at the true value (point).

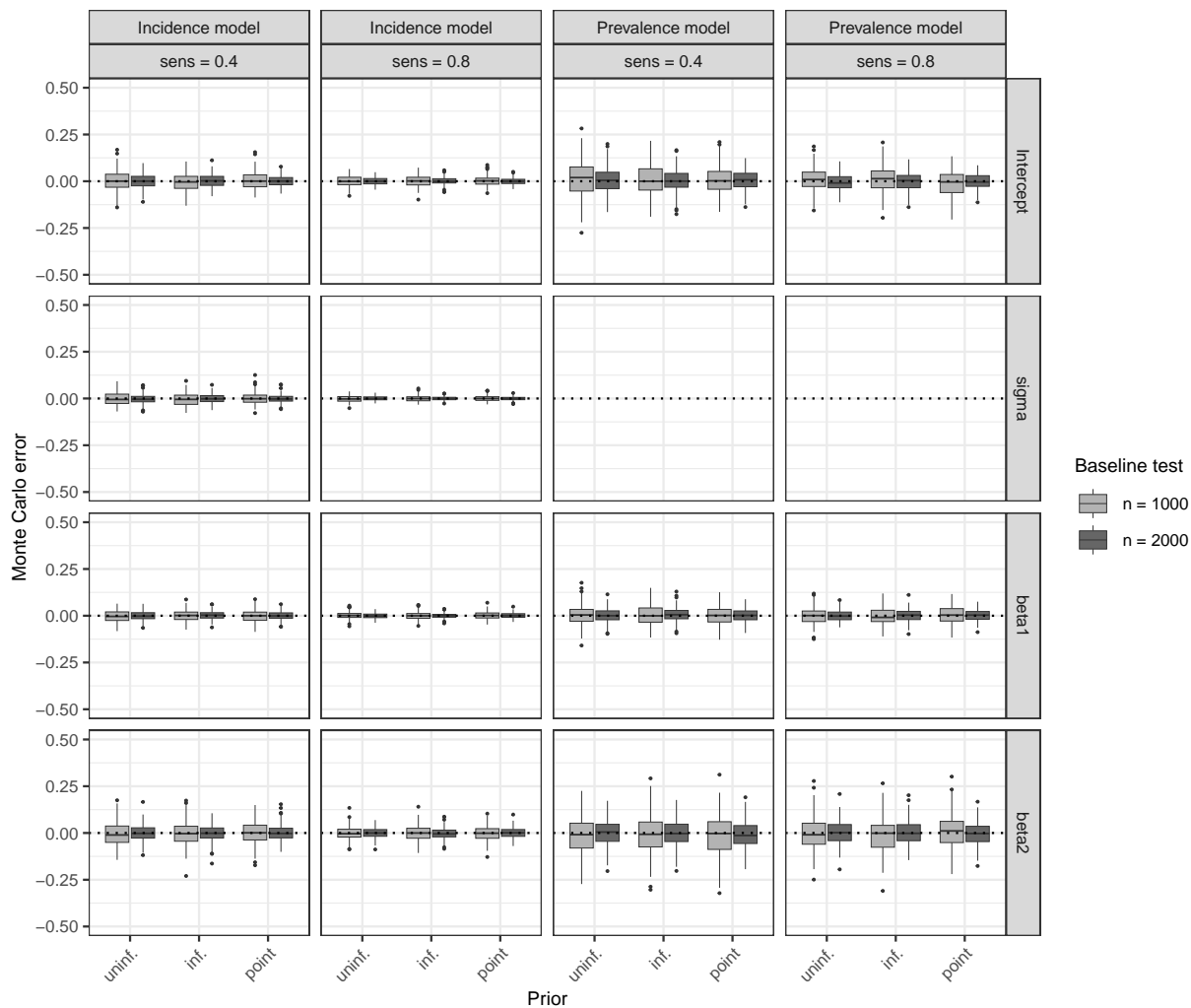


**Figure B.5:** Monte Carlo error of the model parameters, as indicated on the right, for both the incidence model (1) and the prevalence model (2) in the simulation condition:  $\Pr(g_i = 1) = 0.26$ ,  $\Pr(r_i = 1) = 1$ . Note that there is no  $\sigma$  parameter in the prevalence model and hence the corresponding panels are left blank. Abbreviations prev and sens denote, respectively, the prevalence probability  $\Pr(g_i = 1)$  and the test sensitivity  $\kappa$ . The priors on the test sensitivity  $\kappa$  are either uninformative (uninf.), informative (inf.) or fixed at the true value (point).

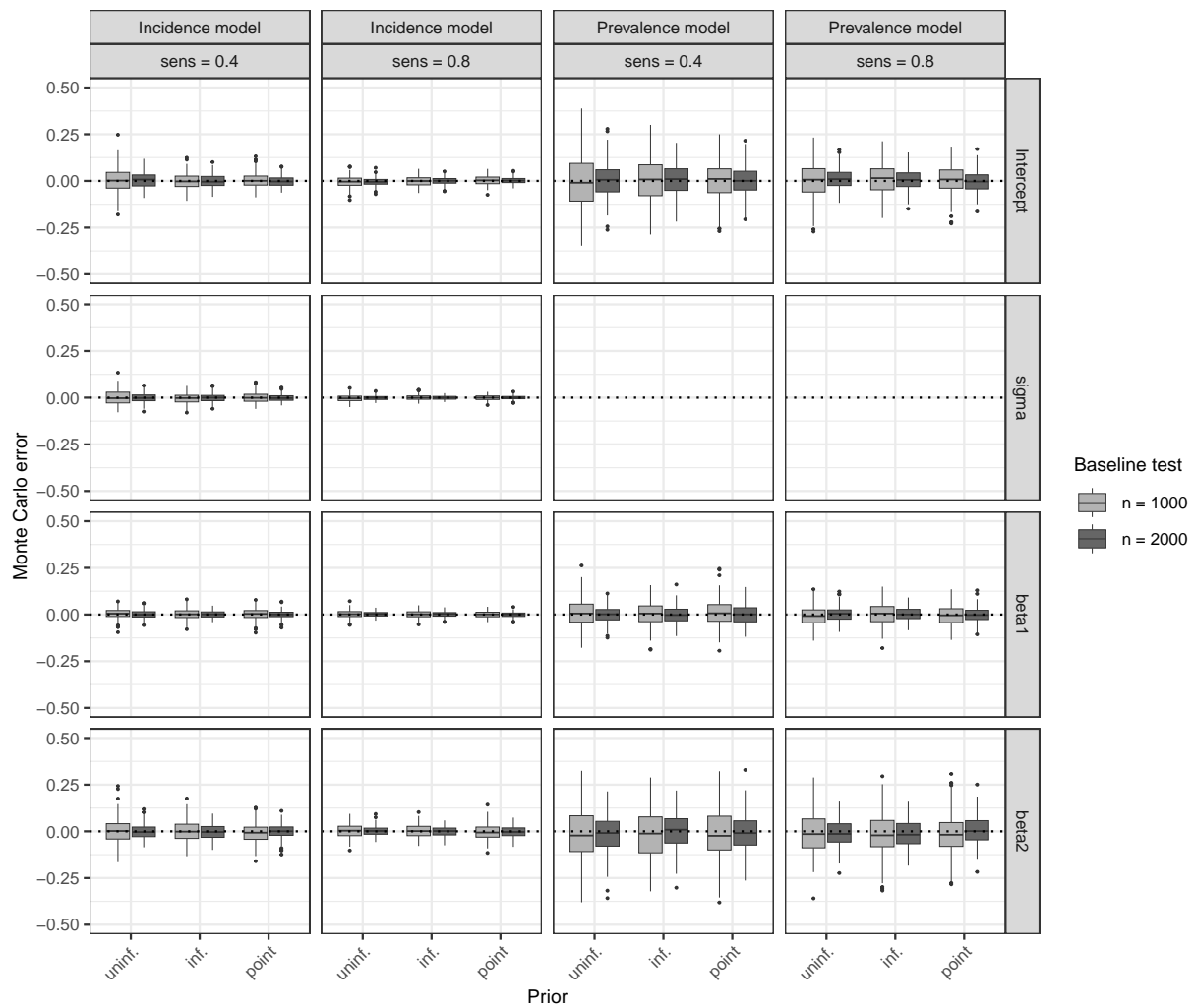


**Figure B.6:** Monte Carlo error of the model parameters, as indicated on the right, for both the incidence model (1) and the prevalence model (2) in the simulation condition:  $\Pr(g_i = 1) = 0.13$ ,  $\Pr(r_i = 1) = 0$ . Note that there is no  $\sigma$  parameter in the prevalence model and hence the corresponding panels are left blank. Abbreviations prev and sens denote, respectively, the prevalence probability  $\Pr(g_i = 1)$  and the test sensitivity  $\kappa$ . The priors on the test sensitivity  $\kappa$  are either uninformative (uninf.), informative (inf.) or fixed at the true value (point).

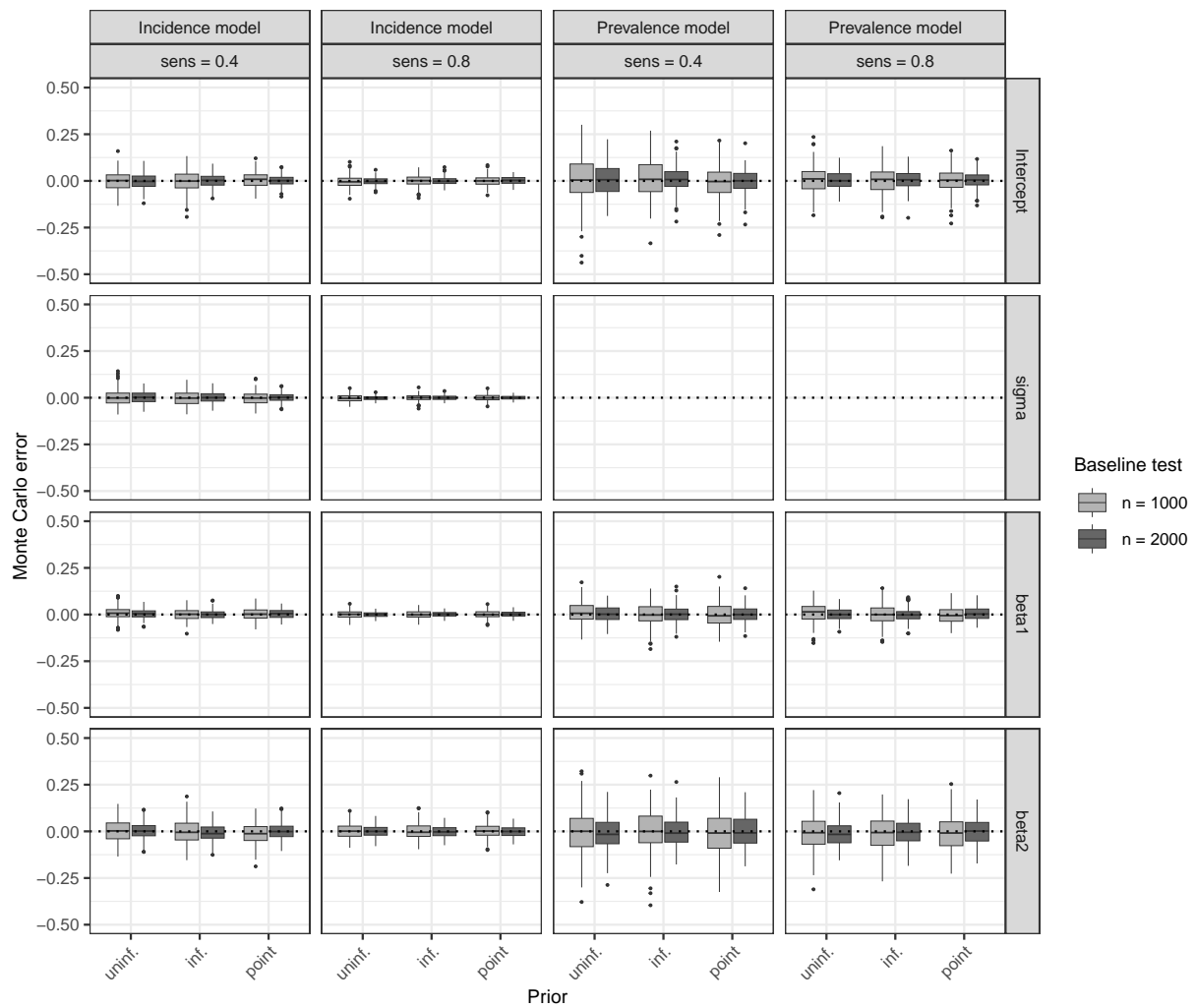


**Figure B.7:** Monte Carlo error of the model parameters, as indicated on the right, for both the incidence model (1) and the prevalence model (2) in the simulation condition:  $\Pr(g_i = 1) = 0.26$ ,  $\Pr(r_i = 1) = 0$ . Note that there is no  $\sigma$  parameter in the prevalence model and hence the corresponding panels are left blank. Abbreviations prev and sens denote, respectively, the prevalence probability  $\Pr(g_i = 1)$  and the test sensitivity  $\kappa$ . The priors on the test sensitivity  $\kappa$  are either uninformative (uninf.), informative (inf.) or fixed at the true value (point).

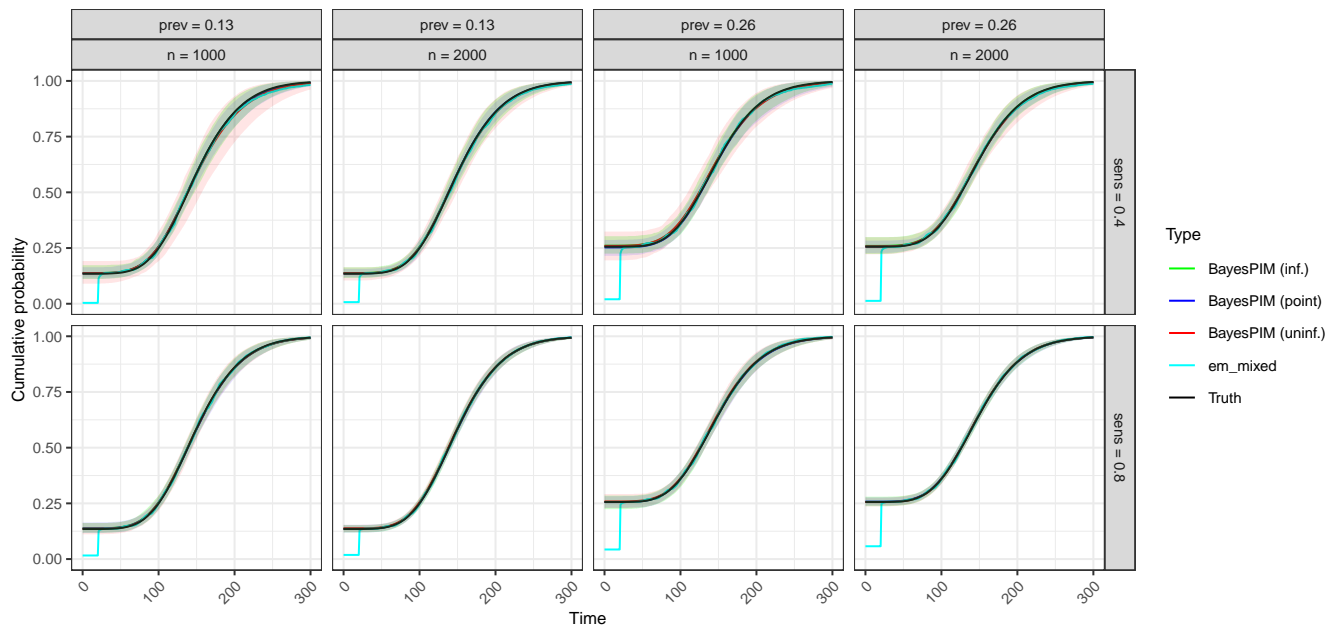


**Figure B.8:** Posterior median marginal mixture CIFs (27), point-wise averaged over 200 Monte Carlo simulation runs with 95% quantiles shown as shaded regions. The condition  $\Pr(r_i = 1) = 0$  is shown.

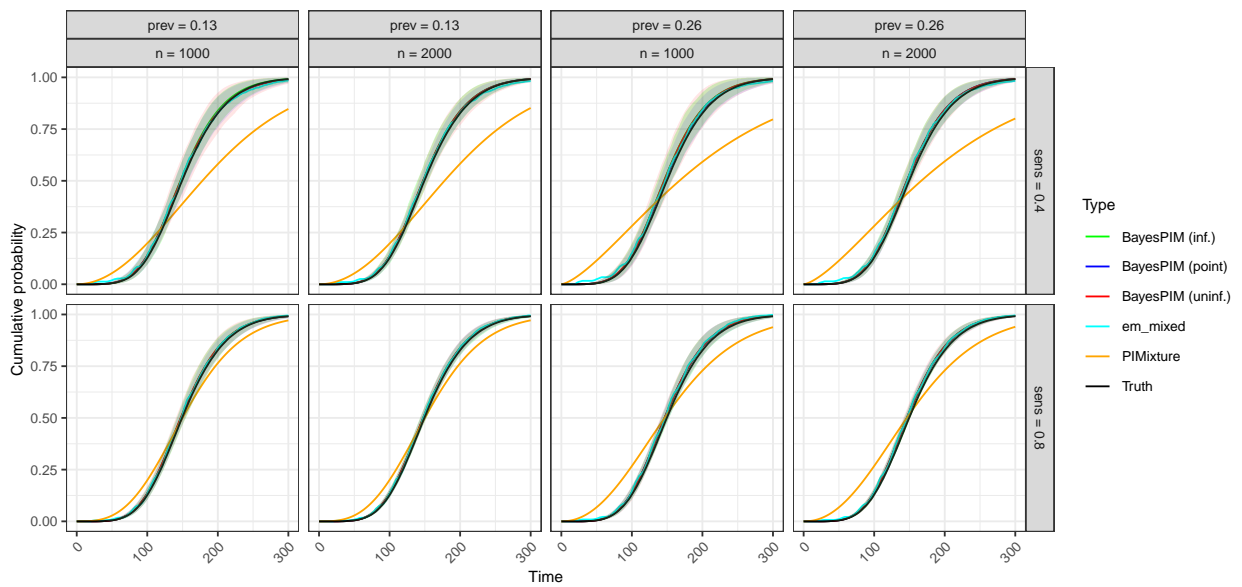


**Figure B.9:** Posterior median marginal CIFs for non-prevalent cases (25), point-wise averaged over 200 Monte Carlo simulation runs with 95% quantiles shown as shaded regions. The condition  $\Pr(r_i = 1) = 1$  is shown.

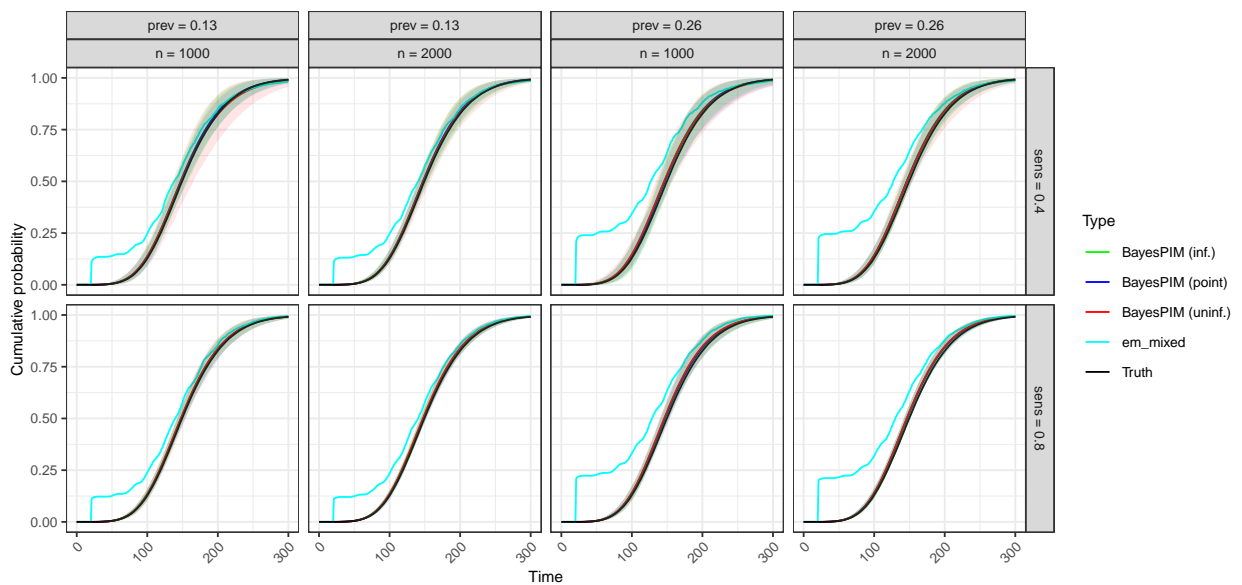


**Figure B.10:** Posterior median marginal CIFs for non-prevalent cases (25), point-wise averaged over 200 Monte Carlo simulation runs with 95% quantiles shown as shaded regions. The condition  $\Pr(r_i = 1) = 0$  is shown.

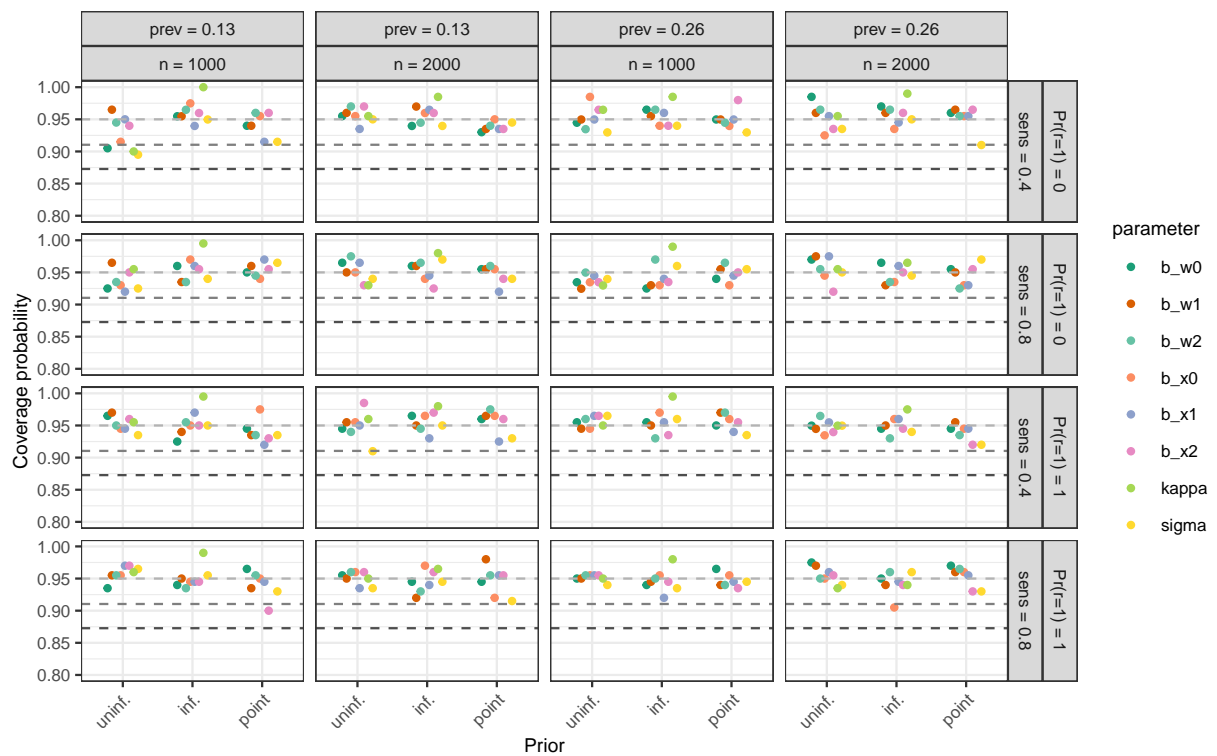


**Figure B.11:** Frequentist coverage probability of the Bayesian 95% posterior credible intervals for the 48 simulation conditions (estimated from 200 Monte Carlo data sets per condition by the proportion of intervals covering the true parameter value). The gray dotted lines in each panel denote, from top to bottom: (a) the nominal 95% level, (b) the value of a point estimate whose 95% confidence upper bound is equal to 95%, (c) the value of a point estimate whose 95% confidence upper bound is equal to 95% with a Bonferroni adjustment for 48 repeated tests.



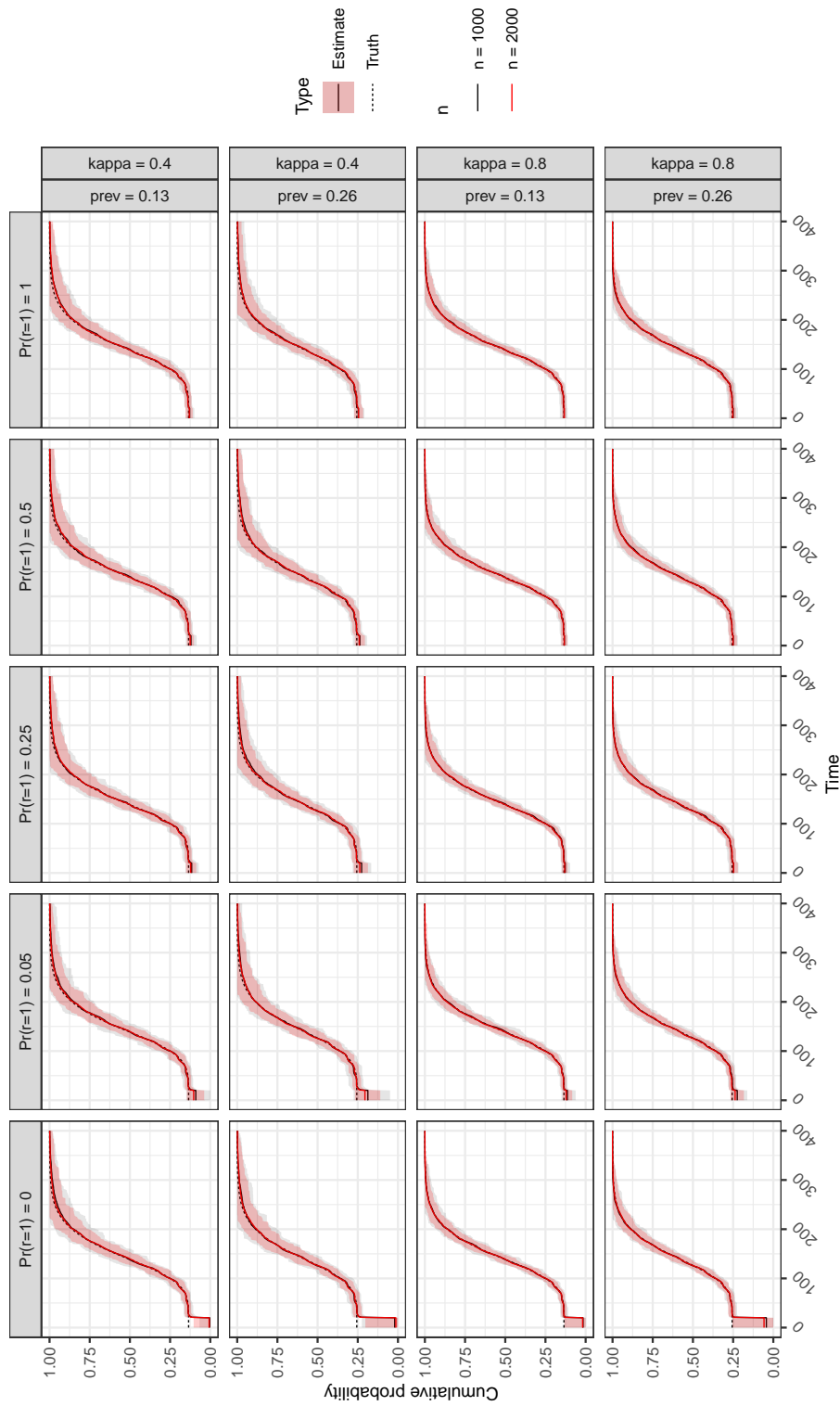


**Figure B.12:** Additional results on the `em_mixed` estimator. The same simulation conditions as in simulation 1 are used, but a wider range of baseline test probabilities  $\Pr(r_i = 1) \in \{0, 0.05, 0.25, 0.5, 1\}$  is reported. The results demonstrate that `em_mixed` was only approximately unbiased in the  $\Pr(r_i = 1) = 1$  but the bias was negligible when a moderate number of tests was available (e.g.  $\Pr(r_i = 1) = 0.5$ ).

## C Additional results from the CRC application

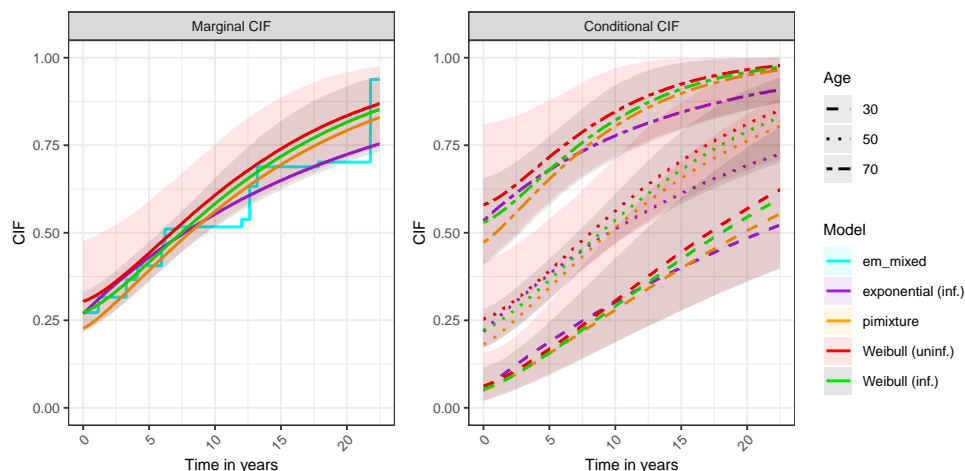


**Figure C.1:** Marginal and conditional mixture cumulative incidence functions (CIF), (27) and (26), for Weibull BayesPIM with uninformative (uninf.) prior and informative (inf.) priors. For comparison, CIF from the Weibull PIMixture model, the exponential BayesPIM model (inf.), and `em_mixed` are given. The lines represent posterior median estimates and the shaded regions indicates the 95% credible interval of the Weibull (inf. in gray) and Weibull (uninf. in red) models.

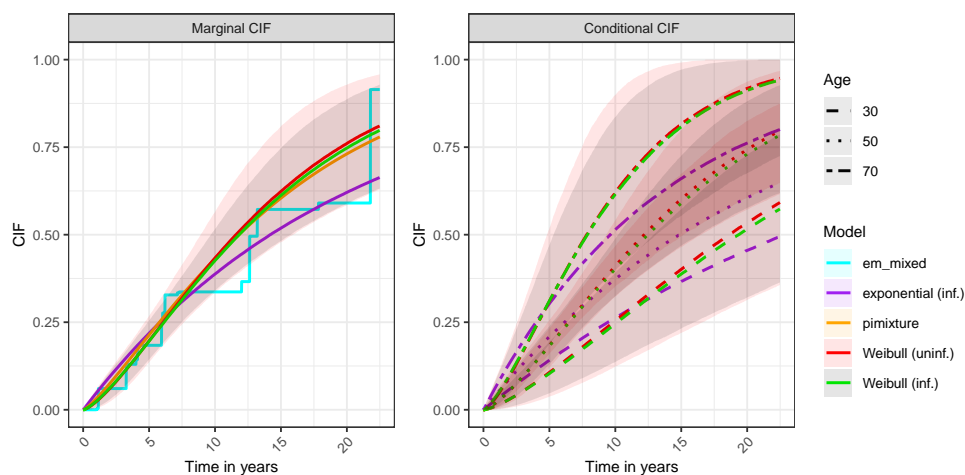


**Figure C.2:** Marginal and conditional cumulative incidence functions (CIF) for the non-prevalent population, (25) and (24), for Weibull BayesPIM with uninformative (uninf.) prior and informative (inf.) priors. For comparison, CIF from the Weibull PIMixture model, the exponential BayesPIM model (inf.), and `em_mixed` are given. The lines represent posterior median estimates and the shaded regions indicates the 95% credible interval of the Weibull (inf. in gray) and Weibull (uninf. in red) models.

## D Additional details about simulation 2

### D.1 Generation of screening times

Here we give details on the process used to sample new screening times  $\tilde{v}_{kj}$  from the observed screening times distribution  $\hat{q}(v_{ij}|\bar{v}_{ij}, \mathbf{z}_i)$ . Specifically, for each newly generated unit  $k$  we obtained by resampling a vector of screening times until right censoring  $\tilde{\mathbf{v}}_k$  as described in the following. The observed screening times distribution was compared through resampling with the observed screening times distribution on a number of benchmark statistics to assure that the simulated data resembled the CRC EHR (see Figure D.1).

For each  $k$ , we sequentially sampled:

1.  $\tilde{\mathbf{z}}_k \sim \hat{q}(\mathbf{z})$
2.  $\tilde{\epsilon}_k \sim q(\epsilon_k)$
3.  $\tilde{x}_k = \tilde{\mathbf{z}}_k' \boldsymbol{\beta}_x + \sigma \tilde{\epsilon}_k$
4.  $\tilde{\phi}_k \sim N(0, 1)$
5.  $\tilde{w}_k = \tilde{\mathbf{z}}_k' \boldsymbol{\beta}_w + \tilde{\phi}_k$
6.  $\tilde{g}_k = \mathbb{1}_{\{w_k > 0\}}$ ,

Then iterative for  $j = 1, 2, \dots, c_k$  screening moments we

7. Proposed a new  $\tilde{v}_{kj} \sim \hat{q}(v_{ij}|\bar{v}_{ij}, \tilde{\mathbf{z}}_k)$  for  $j > 1$
8. Evaluated stopping  $\tilde{s}_{kj}$  with probability (6)

To sample  $\tilde{\mathbf{z}}_k \sim \hat{q}(\mathbf{z})$  in step 1, we selected one  $i$  randomly from  $i = 1, \dots, n$  and set  $\mathbf{z}_k := \mathbf{z}_i$ . Then, in step 7, we used the associated observed vector of screening times  $\mathbf{v}_i = (v_{i1}, v_{i2}, \dots, v_{ic_i})$  of unit  $i$  as a donor vector for new  $\tilde{v}_{kj}$  through the following step-wise procedure:

- Set  $\tilde{v}_{k1} := v_{i1}$
- Draw  $s_{k1}$  with stopping probability (6)
- Set  $\tilde{v}_{k2} := v_{i2}$
- Draw  $s_{k2}$  with stopping probability (6)
- ...
- Set  $\tilde{v}_{kc_i-1} := v_{ic_i-1}$
- Draw  $s_{kc_i-1}$  with stopping probability (6)

At any step, the procedure was stopped if  $s_{kj} = 1$  such that  $\tilde{\mathbf{v}}_k = (\tilde{v}_{k1}, \dots, \tilde{v}_{kj})$ . If the process was not stopped until  $\tilde{v}_{kc_i-1}$ , its continuation depended on  $\rho_i$  indicating whether  $i$  was not right censored at  $v_{ic_i-1}$ . If  $\rho_i = 0$ ,  $i$  was right censored, we set  $\tilde{v}_{kc_i} := v_{ic_i} = \infty$ , to indicate that also  $\tilde{\mathbf{v}}_k$  was right censored. However, when  $\rho_i = 1$ ,  $\mathbf{v}_i$  was not right censored because an event was observed and screening stopped at  $v_{ic_i} < \infty$  due to (6). As a consequence, no further screening times beyond  $v_{ic_i}$  were available as donors.

To generate new times after  $v_{ic_i}$  (if  $\rho_i = 1$ ) we therefore had to devise a procedure to approximate the unobserved distribution of screening times that would have occurred if, counter to the fact,

after the first  $\mathbf{v}_i$  times the series had not been stopped due to an observed event. We accomplished this through resampling time difference scores  $\tilde{d}$  from the empirical distribution  $\hat{q}(d|\rho_i = 1)$  of difference scores  $d_{ij} = v_{ij} - v_{ij-1}$  in the non-right censored part of the sample. Samples from this distribution are obtained by calculating  $d_{ij}$  for all  $i$  and  $j$  in the data for which  $\rho_i = 1$  and then randomly selecting, with replacement, one  $\tilde{d}$  from the pool of all  $d_{ij}$ . Then the procedure for generating screening times is continued as follows:

- Set  $\tilde{v}_{kc_i} = \tilde{v}_{ic_i}$
- Draw  $s_{kc_i}$  with stopping probability (6)
- Set  $\tilde{v}_{kc_i+1} := \tilde{v}_{kc_i} + \tilde{d}$ , where  $\tilde{d} \sim \hat{q}(d|\rho_i = 1)$
- Draw  $s_{kc_i+1}$  with stopping probability (6)
- Set  $\tilde{v}_{kc_i+2} := \tilde{v}_{kc_i+1} + \tilde{d}$ , where  $\tilde{d} \sim \hat{q}(d|\rho_i = 1)$
- Draw  $s_{kc_i+2}$  with stopping probability (6)
- ...

This process is continued until stopping or  $\tilde{v}_{kc_i+j} > \tilde{v}_{kr}$ , the time of right censoring. We explain below how we obtained right censoring time  $\tilde{v}_{kr}$  from the empirical distribution  $\hat{q}(v_{ir})$ .

Our imputation procedure was based on assumptions that we, here, make explicit. We assumed (a) that the observed time differences  $d_{ij} = v_{ij} - v_{ij-1}$  between the observed screening visits  $v_{ij}$  were exchangeable with those between the unobserved screening times (i.e. the screening process would have continued as it was observed into the future), (b) that the difference scores  $d_{ij}$  were exchangeable between units  $i$  and (c) the ordering implied by index  $j$  did not matter for future screening moments. Assumption (b) was needed to avoid very similar distances between successive screening moments (e.g., if  $\mathbf{v}$  is short such as  $\mathbf{v} = (0, 3)$  using only the observed difference  $d_i = 3$  to impute subsequent screening times would not have appropriately represented the empirically observed variation in timely distance between screening moments on other units).

We now return to the question of how to sample the time of right censoring  $\tilde{v}_{kr}$  from the empirical right censoring distribution  $\hat{q}(v_{ir})$ . We start by noting that  $v_{ir}$  is unobserved in all cases and should not be confused with  $v_{ic_i}$ . Time  $v_{ic_i}$  is the finite time point at which the event occurred if  $\rho_i = 1$  and  $v_{ic_i} = \infty$  in case of right censoring ( $\rho_i = 0$ ). Then (if  $\rho_i = 0$ )  $v_{ic_i-1} < v_{ir}$  denotes the last follow-up moment (without event), but not the time of right censoring. Hence, the last screening moment is a lower bound for  $v_{ir}$ . Now we note that right censoring is defined to occur if the time of right censoring  $v_{ir}$  is before the time of the next screening moment. Therefore, if  $\rho_i = 0$ , right censoring occurs when  $v_{ic_i-1} < v_{ir} \leq v_{ic_i-1} + \Delta_i$ , where  $\Delta_i$  denotes the unknown time until the next screening moment. Through this realization an upper bound for  $v_{ir}$  is found, namely  $v_{ic_i-1} + \Delta_i$ . Therefore, if  $\Delta_i$  was known, which it is not, the distribution of  $v_{ir}$  could be estimated by treating the time as interval censored between the last observed time  $v_{ic_i-1}$  and the missing  $v_{ic_i-1} + \Delta_i$  in the right-censored group with  $\rho_i = 0$ . Our strategy for estimating the distribution of  $v_{ir}$  therefore was defined as follows. For all  $i : \rho_i = 0$ , set

1.  $l_i := v_{ic_i-1}$
2.  $r_i := l_i + \Delta_i$  where  $\Delta_i \sim \hat{q}(d|\rho_i = 0)$

Subsequently, we estimate  $\hat{F}_b(v_{ir})$ , the empirical CDF of  $v_{ir}$ , through interval censored nonparametric maximum likelihood using the Turnbull estimator (Turnbull, 1976), where the intervals

were given by  $(l_i, r_i]$ . This procedure was repeated  $b = 1, \dots, 1000$  times on bootstrapped samples to reflect the uncertainty in the Turnbull estimator as well as the repeated imputations  $\Delta_i$  (Figure D.1). To draw one  $\tilde{v}_{kr}$  from this approximated distribution, we first randomly selected one  $\hat{F}_b$  and subsequently used the inverse sampling method to obtain  $\tilde{v}_{kr}$  under the constraint that  $\tilde{v}_{kr} > \tilde{v}_{kc_i}$ .

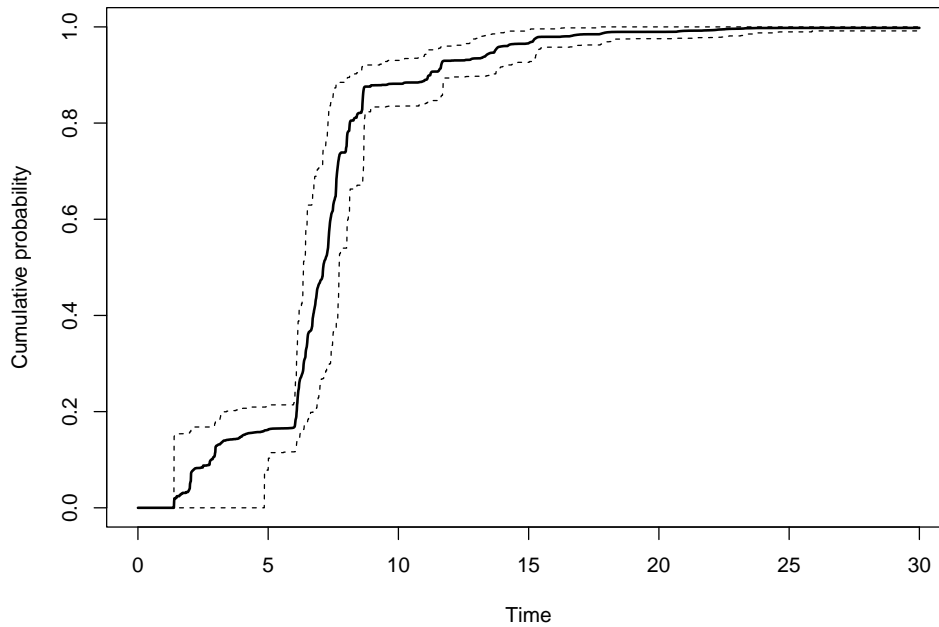


**Figure D.1:** Bootstrapped approximated empirical CDF of  $v_{ir}$  in the CRC EHR, the time of right censoring in the data. Solid line represents point-wise averages across bootstrapped samples with the interval representing point-wise 95% confidence intervals.

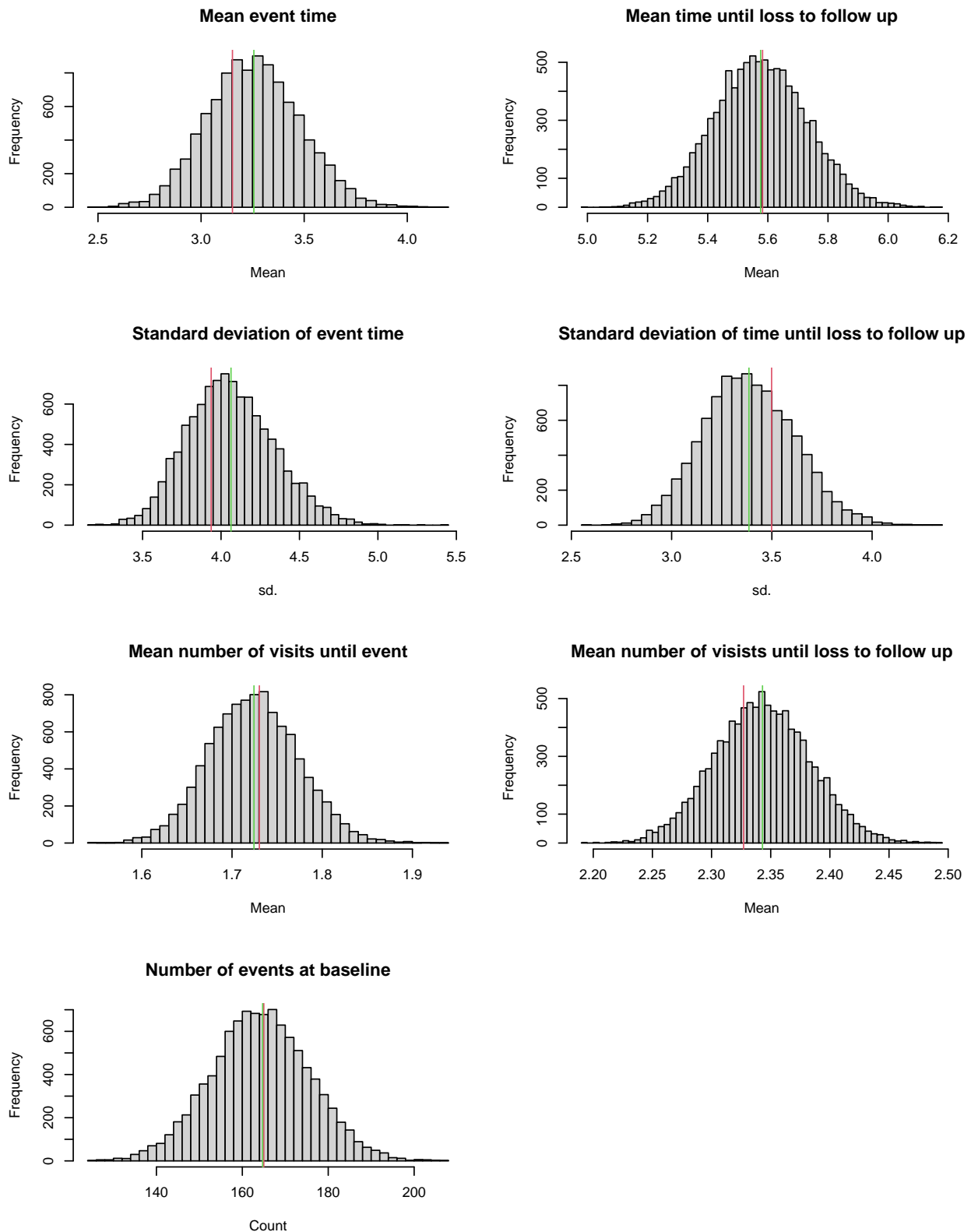


**Figure D.2:** Sampling distributions (simulation 2) of statistics calculated on 10,000 samples of censoring times ( $\tilde{\mathbf{v}}_1, \dots, \tilde{\mathbf{v}}_n$ ) where  $n = 810$  (sample size of the CRC EHR data). Green shows the mean of the sampling distribution, red shows the observed value calculated on  $(\mathbf{v}_1, \dots, \mathbf{v}_n)$  from the CRC EHR. These comparisons demonstrate that the simulated screening times distribution was similar to the observed screening times distribution in the CRC EHR.

## D.2 Generation of screening times under extended right censoring

We considered two right censoring distributions in this simulation. First,  $q(v_{ir})$  approximated by  $\hat{F}_b(v_{ir})$ , as described in section D.1, called the observed right censoring distribution. Second, an extended right censoring distribution that we obtained through adding an offset to any sampled time of right censoring  $\tilde{v}_{kr}$ . Specifically, if  $\tilde{v}_{kr}^{(ext)}$  is the extended time of right censoring we added an offset  $\omega$  by specifying

$$\tilde{v}_{kr}^{(ext)} := \tilde{v}_{kr} + \omega,$$

where  $\omega = 10$  years. This procedure generally leads to longer follow up and more screening moments for any  $k$ . However, the extension slightly changed the generation of screening times described in section D.1. In particular, for any individuals  $i : \rho_i = 1$  (right censored event), and hence their  $\mathbf{v}_i = (v_{i1}, v_{i2}, \dots, v_{ic_i})$  with  $v_{ic_i} = \infty$  their unobserved time of right censoring  $v_{ir}$  was too early as it should have been  $v_{ir} + \omega$  under the extended right censoring scheme. Therefore, the follow-up would have needed to continue with additional times  $v_{ic_i+1}, v_{ic_i+2} \dots$  until right censoring at the extended time  $v_{ir} + \omega$ . These times are augmented using a similar approach as in section D.1 for the individuals  $i : \rho_i = 0$ .

Specifically, for any  $i : \rho_i = 1$  (observed event) the sampling procedure remains unchanged. However, for any  $i : \rho_i = 0$  the procedure is slightly amended. As before, we use their  $\mathbf{v}_i$  as donors for new  $\tilde{v}_{kj}$  generated through the stepwise procedure:

- Set  $\tilde{v}_{k1} := v_{i1}$
- Draw  $s_{k1}$  with stopping probability (6)
- Set  $\tilde{v}_{k2} := v_{i2}$
- Draw  $s_{k2}$  with stopping probability (6)
- ...
- Set  $\tilde{v}_{kc_i-1} := v_{ic_i-1}$

However, now, if the process was not stopped until  $\tilde{v}_{kc_i-1} := v_{ic_i-1}$ , we generated additional times through the augmentation process

- Set  $\tilde{v}_{kc_i} := \tilde{v}_{kc_i-1} + \tilde{d}$ , where  $\tilde{d} \sim \hat{q}(d|\rho_i = 0)$
- Draw  $s_{kc_i}$  with stopping probability (6)
- Set  $\tilde{v}_{kc_i+1} := \tilde{v}_{kc_i} + \tilde{d}$ , where  $\tilde{d} \sim \hat{q}(d|\rho_i = 0)$
- Draw  $s_{kc_i+1}$  with stopping probability (6)
- ...

That is, we augment by the difference score from the distribution of difference scores observed in individuals  $i : \rho_i = 0$  until stopping or right censoring when  $\tilde{v}_{kc_i+j} > \tilde{v}_{kr}^{(ext)}$ .



## E Additional results from simulation 2 (CRC EHR)

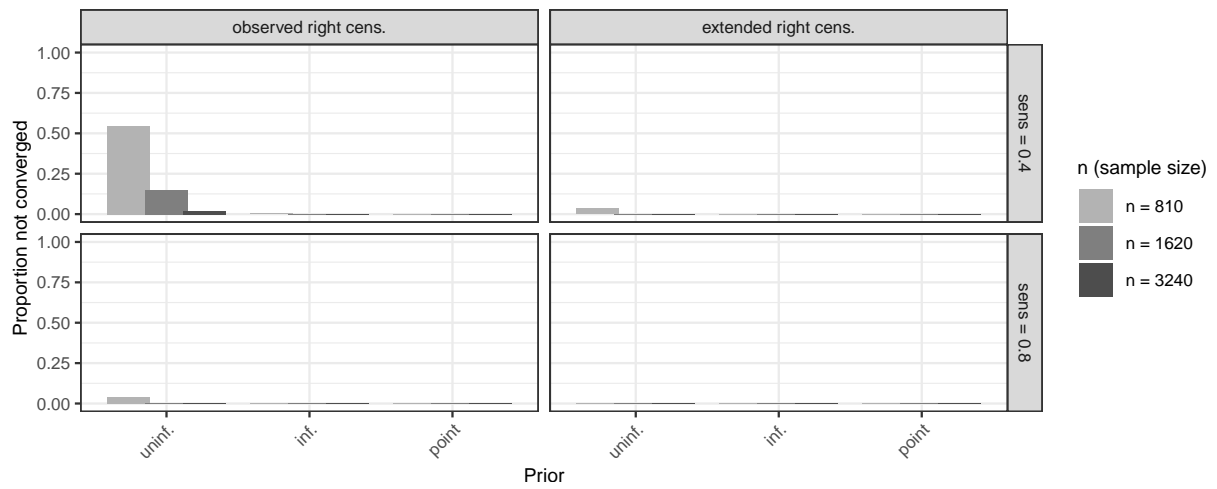


**Figure E.1:** Proportion of runs that did not converge per simulation condition. Convergence was evaluated every  $2 \times 10^5$  draws. Abbreviations prev and sens denote, respectively, the prevalence probability  $\Pr(g_i = 1)$  and the test sensitivity  $\kappa$ . The priors on the test sensitivity  $\kappa$  are either uninformative (uninf.), informative (inf.) or fixed at the true value (point).

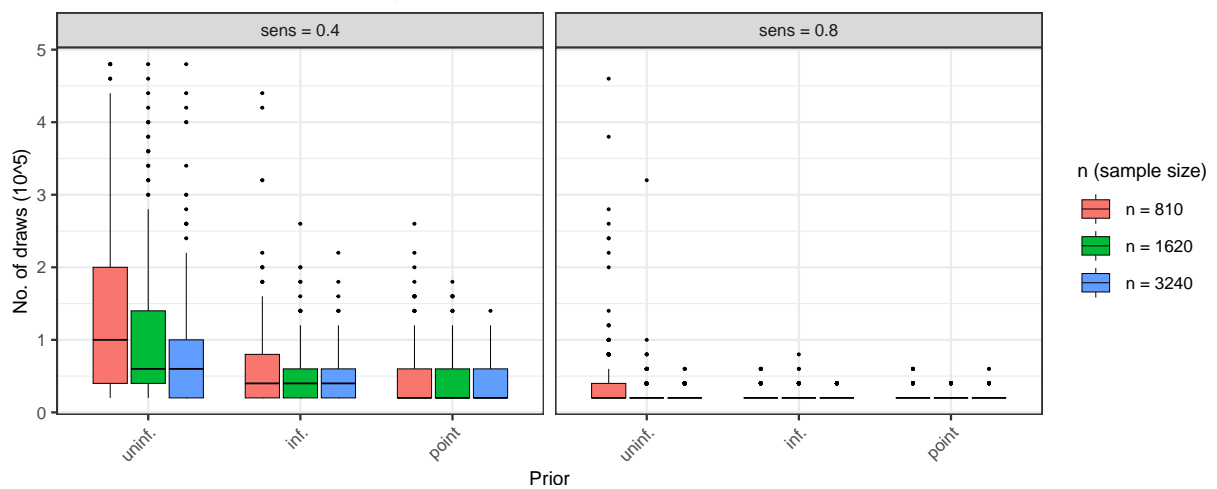


**Figure E.2:** Number of posterior draws until convergence including burn-in (scaled by  $10^5$ ) by simulation conditions. Convergence was evaluated every  $2 \times 10^5$  draws. Abbreviation sens denotes the test sensitivity  $\kappa$ . The priors on the test sensitivity  $\kappa$  are either uninformative (uninf.), informative (inf.) or fixed at the true value (point).

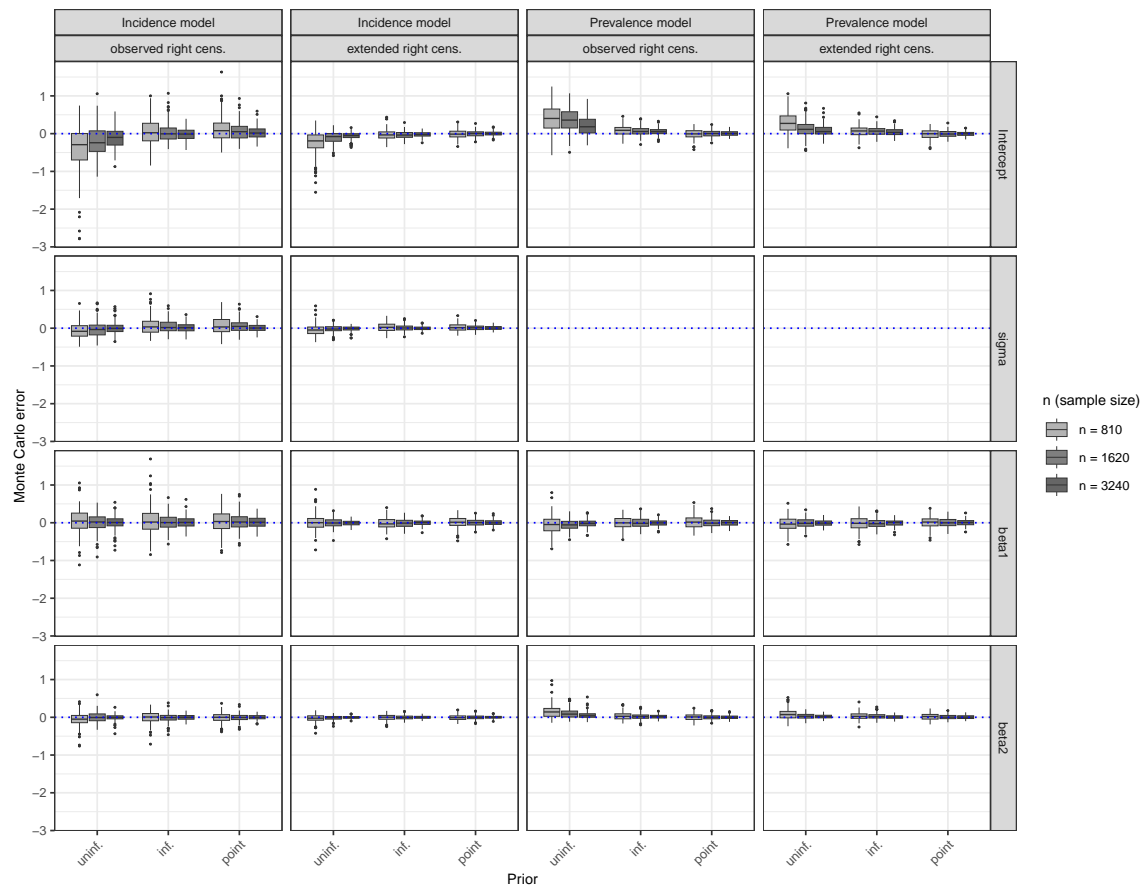


**Figure E.3:** Monte Carlo error of the model parameters (simulation 2), as indicated on the right, for both the incidence model (1) and the prevalence model (2) in the simulation condition:  $\kappa = 0.4$ . Note that there is no  $\sigma$  parameter in the prevalence model and hence the corresponding panels are left blank. Abbreviation sens denotes the test sensitivity  $\kappa$ . The priors on the test sensitivity  $\kappa$  are either uninformative (uninf.), informative (inf.) or fixed at the true value (point).

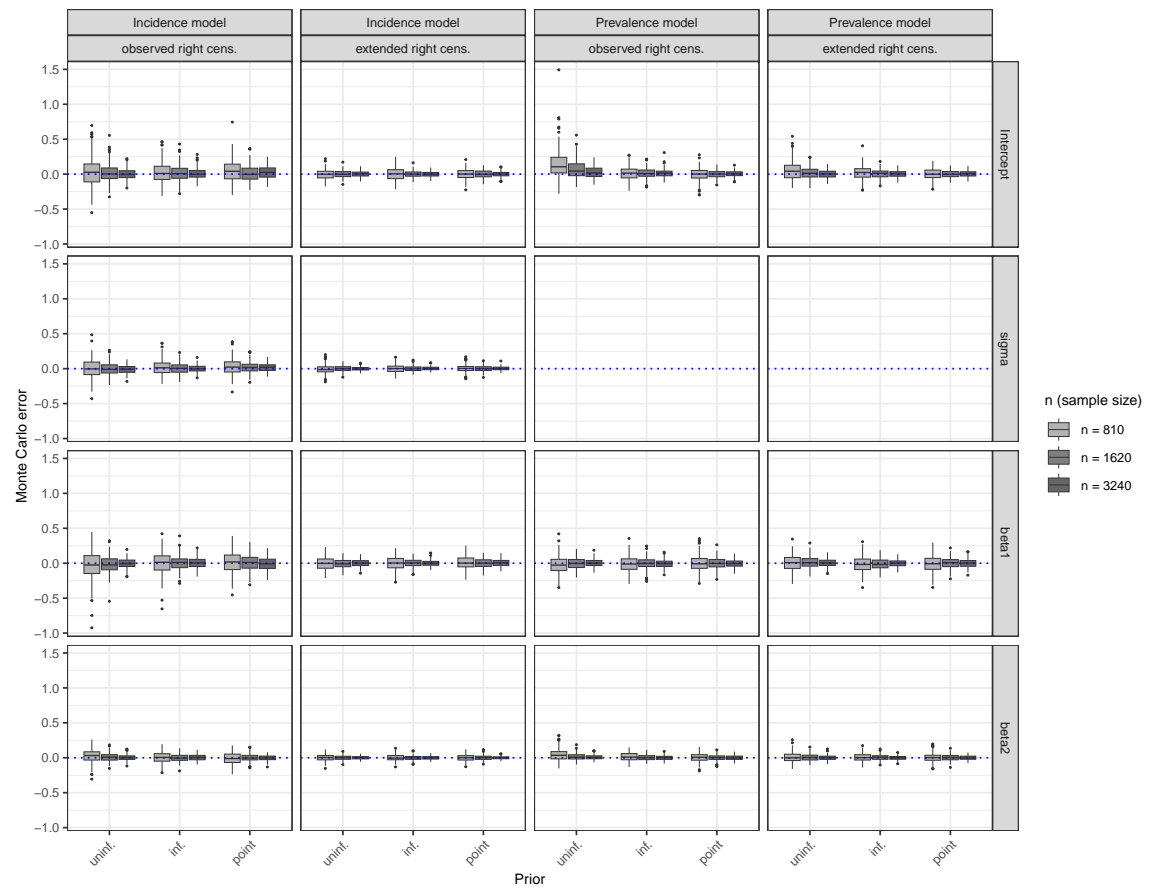


**Figure E.4:** Monte Carlo error of the model parameters (simulation 2), as indicated on the right, for both the incidence model (1) and the prevalence model (2) in the simulation condition:  $\kappa = 0.8$ . Note that there is no  $\sigma$  parameter in the prevalence model and hence the corresponding panels are left blank. Abbreviation sens denotes the test sensitivity  $\kappa$ . The priors on the test sensitivity  $\kappa$  are either uninformative (uninf.), informative (inf.) or fixed at the true value (point).

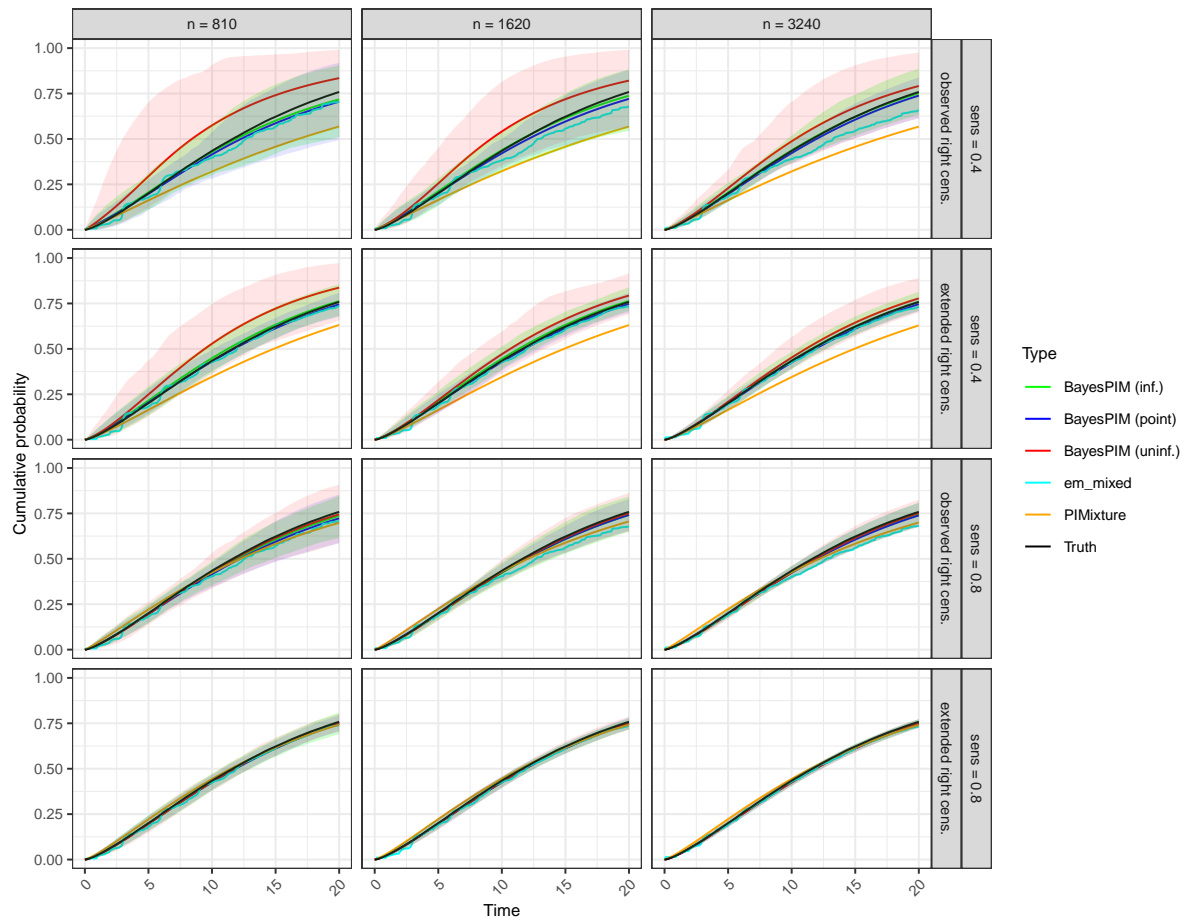


**Figure E.5:** Marginal CIFs (25) for the non-prevalent population, point-wise averaged over 200 Monte Carlo simulation runs with 95% quantiles shown as shaded regions. For BayesPIM the posterior median of the posterior predictive CIF (25) is used. For Pimixture and em\_mixed the corresponding maximum likelihood estimates are used, rescaled to the non-prevalent population.

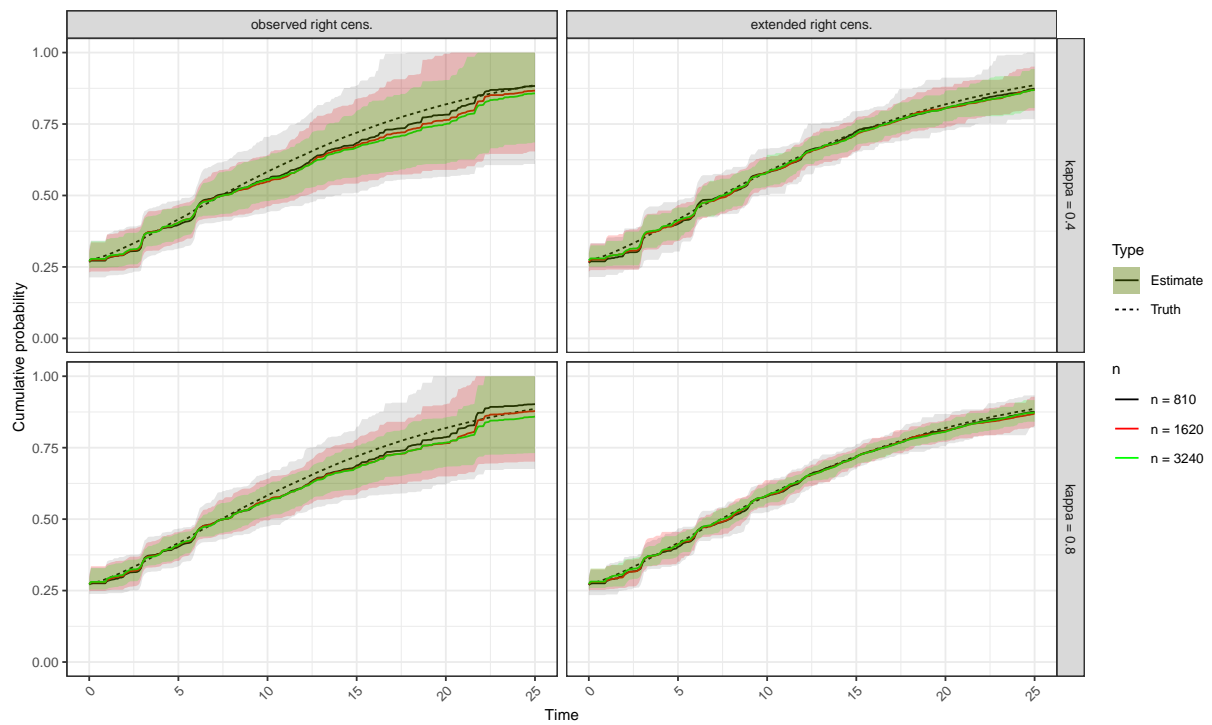


**Figure E.6:** Marginal mixture CIFs (27), estimated by `em_mixed`, point-wise averaged over 200 Monte Carlo simulation runs with 95% quantiles shown as shaded regions.

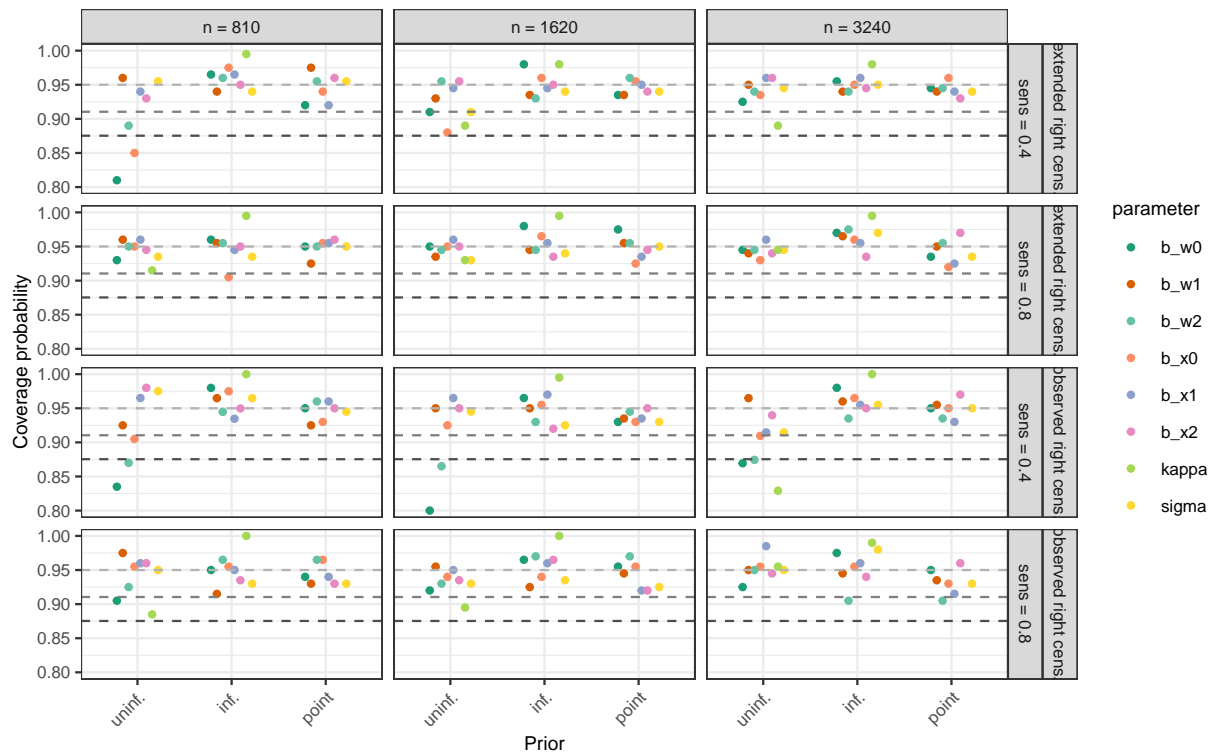


**Figure E.7:** Frequentist coverage probability of the Bayesian 95% posterior credible intervals for the 36 simulation conditions in simulation 2 (estimated from 200 Monte Carlo data sets per condition by the proportion of intervals covering the true parameter value). The gray dotted lines in each panel denote, from top to bottom: (a) the nominal 95% level, (b) the value of a point estimate whose 95% confidence upper bound is equal to 95%, (c) the value of a point estimate whose 95% confidence upper bound is equal to 95% with a Bonferroni adjustment for 36 repeated tests.